2018 Fall

Advanced Solidification

11.27.2018

Eun Soo Park

Office: 33-313
Telephone: 880-7221
Email: espark@snu.ac.kr
Office hours: by appointment

Chapter 6 Polyphase solidification

6.1. Evolution of a Gas during solidification

(a) Gas-metal equilibria

A typical solubility diagram

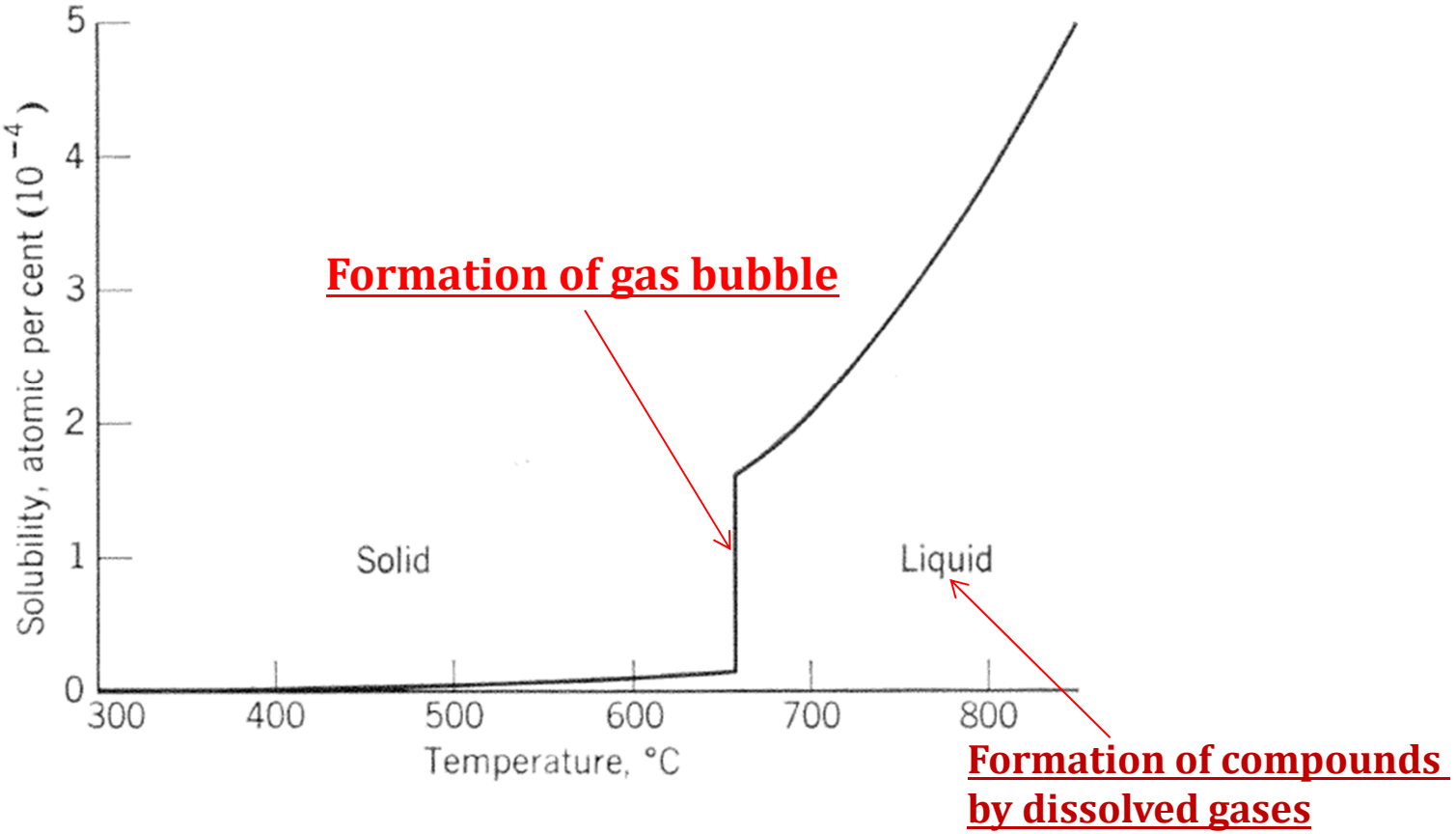

Fig. 6.2. Solubility of hydrogen in aluminum.

But , a solid-liquid interface should not be an effective nucleant for a bubble;

Equilibrium corresponds to Θ < 180 °,

$$\sigma_{SL} = \sigma_{SG} + \sigma_{LG} \cos\theta$$

$$\cos\theta = \frac{\sigma_{SL} - \sigma_{SG}}{\sigma_{LG}}$$

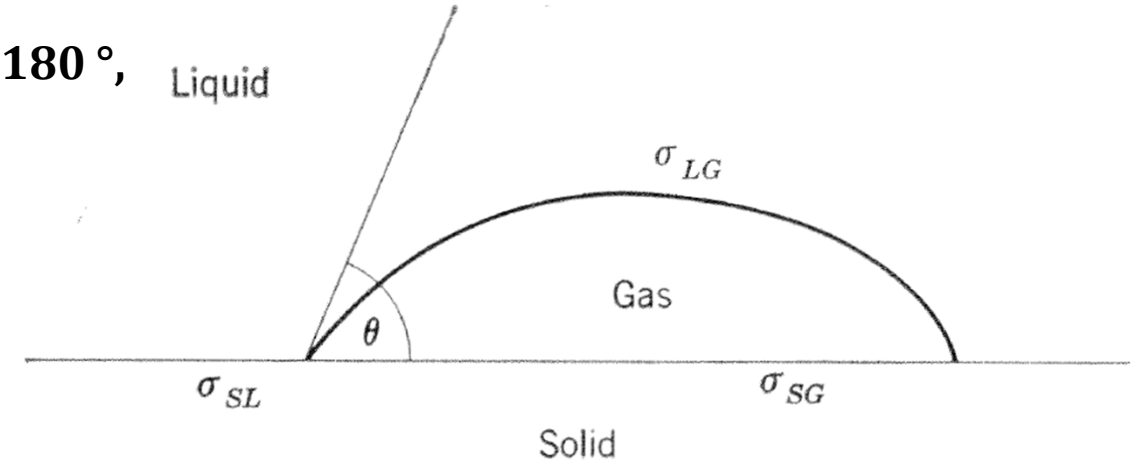

Fig. 6.4. Solid-liquid as nucleant for a gas bubble.

$\sigma_{SG} >> \sigma_{SL}$ & $\sigma_{SG} > \sigma_{LG}$

$\therefore \cos\theta < -1$

→ Surface E of the bubble is increased by contact with the solid-liquid interface.

However, gas bubbles are formed at solid-liquid interfaces.

This location is in part due to the fact that the gas concentration would be highest there during solidification; but it may also be due to the fact that any re-entrant in the interface, such as a cell wall, grain boundary, or inter-dendritic space, would have an even higher gas content because of lateral segregation, as shown in Fig. 6.5.

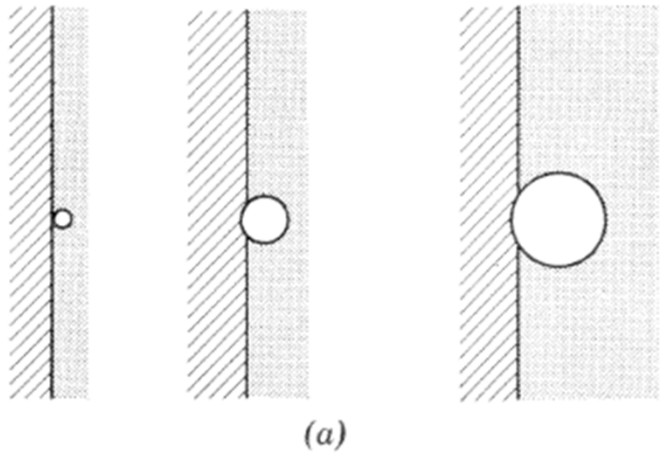

* Growth rate of bubble > Advanced speed of interface

→ increase of bubble diameter

The diameter of the bubble is maintained in the longitudinal direction

* Growth rate of bubble ~ Advanced speed of interface

→ Bubble growth progresses in the longitudinal direction while maintaining bubble diameter

* Growth rate of bubble < Advanced speed of interface

→ bubble are trapped in the solid.

Fig. 6.6. Effect of speed of growth of a bubble on its shape and size. (a) Slow growth, (b) intermediate speed, (c) fast growth.

Q: Thermodynamics and Kinetics of eutectic solidification ($L \rightarrow \alpha + \beta$) ?

Undercooling ΔT_0

$$\Delta T_0 = \Delta T_r + \Delta T_D$$

Curvature Composition gradient

$$\Delta G_{total} = \Delta G_r + \Delta G_D$$

$$v = k_2 D \frac{\Delta T_0}{\lambda}\left(1 - \frac{\lambda^*}{\lambda}\right)$$

$$\Delta G_r = \frac{2\gamma_{\alpha\gamma} V_m}{\lambda}$$

→ *free energy dissipated in forming α/β interfaces*

$\Delta G_D \rightarrow$ *free energy dissipated in diffusion*

By varying the interface undercooling (ΔT_0), it is possible to vary the growth rate (v) and spacing (λ) independently.

Therefore, it is impossible to predict the spacing (λ) that will be observed for a given growth rate (v). However, controlled growth experiments show that a specific value of λ is always associated with a given growth rate (v).

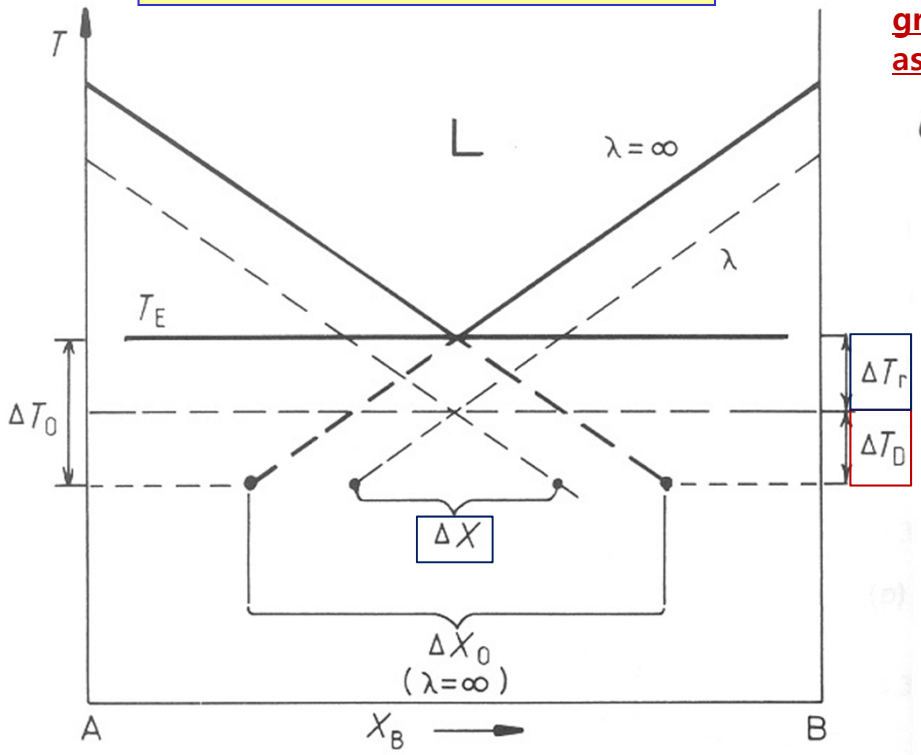

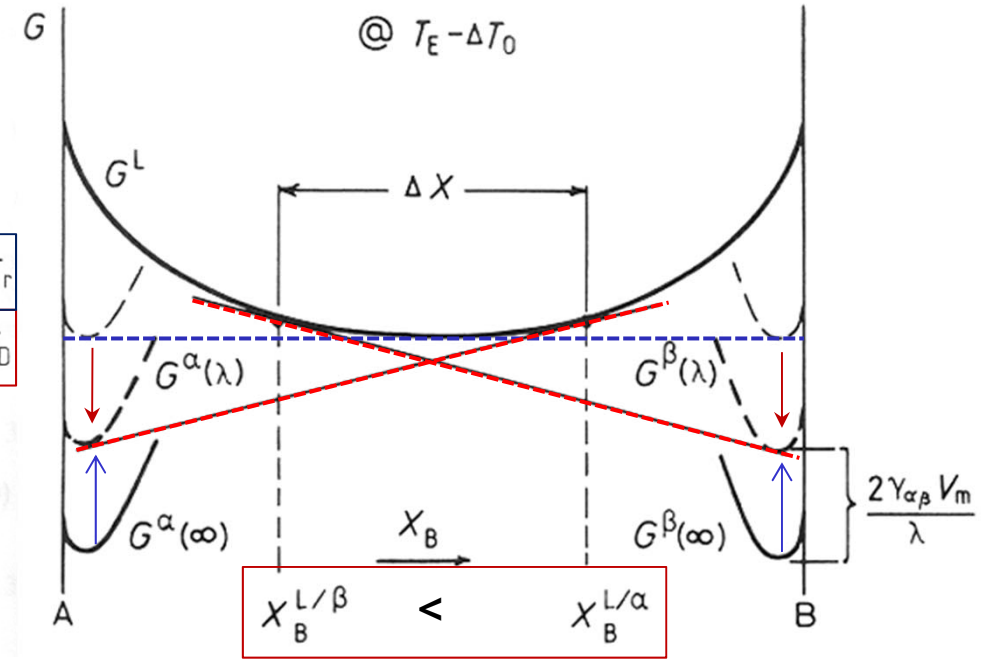

Fig. 4.34 Eutectic phase diagram showing the relationship between ΔX and ΔX_0 (exaggerated for clarity)

Undercooling ΔT_0

$$\Delta T_0 = \Delta T_r + \Delta T_D$$

Curvature Composition gradient

$$\Delta G_{total} = \Delta G_r + \Delta G_D$$

$$v = k_2 D \frac{\Delta T_0}{\lambda}\left(1 - \frac{\lambda^*}{\lambda}\right)$$

By varying the interface undercooling (ΔT_0), it is possible to vary the growth rate (v) and spacing (λ) independently.

$$\Delta G_r = \frac{2\gamma_{\alpha\gamma} V_m}{\lambda}$$

→ *free energy dissipated in forming α/β interfaces*

$\Delta G_D \rightarrow$ *free energy dissipated in diffusion*

Therefore, it is impossible to predict the spacing (λ) that will be observed for a given growth rate (v). However, controlled growth experiments show that a specific value of λ is always associated with a given growth rate (v).

* For example,

Maximum growth rate at a fixed $\Delta T_0 \rightarrow \lambda_0 = 2\lambda^*$

(4) $v = k_2 D \frac{\Delta T_0}{\lambda}\left(1 - \frac{\lambda^*}{\lambda}\right)$ → $v_0 = k_2 D \Delta T_0 / 4\lambda^*$ **(5)**

From Eq. 4.39 $\lambda^* = +\frac{2T_E \gamma V_m}{\Delta H \Delta T_0}$ → $\Delta T_0 \propto 1/\lambda^*$ **(6)**

So that the following relationships are predicted:

(5) + (6) →

$$v_0 \lambda_0^2 = k_3 \text{ (constant)}$$

$$\frac{v_0}{(\Delta T_0)^2} = k_4$$

Ex) Lamellar eutectic in the Pb-Sn system

$k_3 \sim 33\ \mu m^3/s$ and $k_4 \sim 1\ \mu m/s \cdot K^2$

→ v = 1 μm/s, λ_0 = 5 μm and ΔT_0 = 1 K

* Total Undercooling

$$\Delta T_0 = \Delta T_r + \Delta T_D$$

Undercooling required to overcome the interfacial curvature effects

Undercooling required to give a sufficient composition difference to drive the diffusion

Strictly speaking,

ΔT_i term should be added but, negligible for high mobility interfaces

Driving force for atom migration across the interfaces

$\Delta T_D \rightarrow$ Vary continuously from the middle of the α to the middle of the β lamellae

$\Delta T_0 = const$ ← Interface is essentially isothermal.

$\Delta T_D \rightarrow \Delta T_r$ The interface curvature will change across the interface.

Should be compensated

* A planar eutectic front is not always stable.

Binary eutectic alloys contains impurities or other alloying elements ➡ "Form a cellular morphology"

analogous to single phase solidification

restrict in a sufficiently high temp. gradient.

➡ The solidification direction changes as the cell walls are approached and the lamellar or rod structure fans out and may even change to an irregular structure.

➡ Impurity elements (here, mainly copper) concentrate at the cell walls.

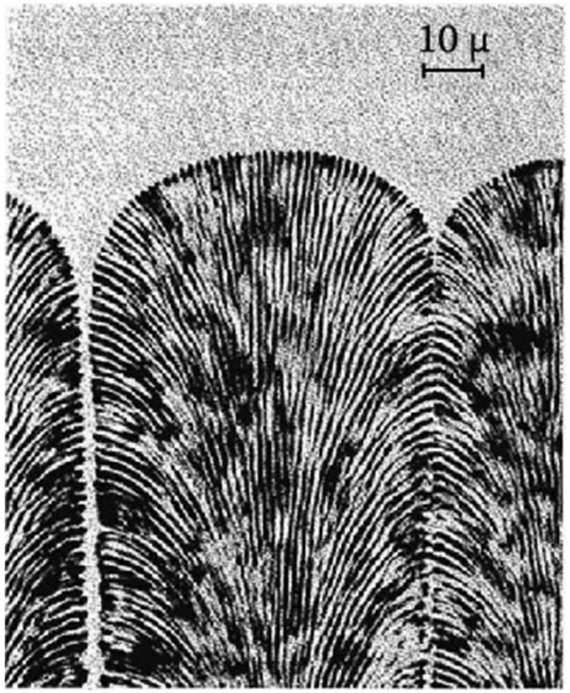

A planar eutectic front is not always stable.

Binary eutectic alloys contains impurities or other alloying elements

➡ "Form a cellular morphology"

analogous to single phase solidification

restrict in a sufficiently high temp. gradient.

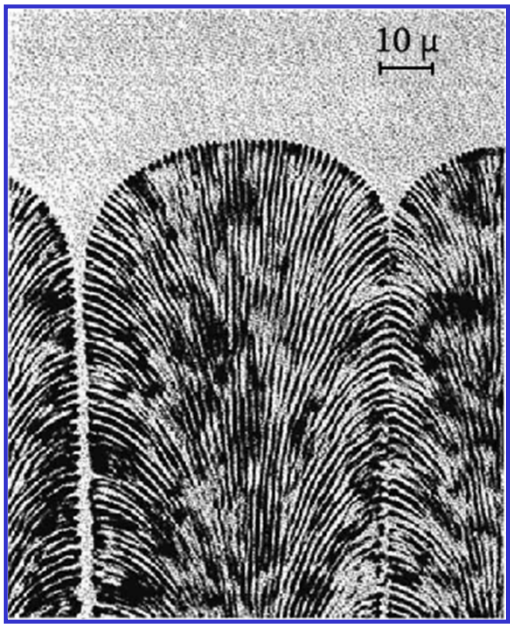

➡ The solidification direction changes as the cell walls are approached and the lamellar or rod structure fans out and may even change to an irregular structure.

➡ Impurity elements (here, mainly copper) concentrate at the cell walls.

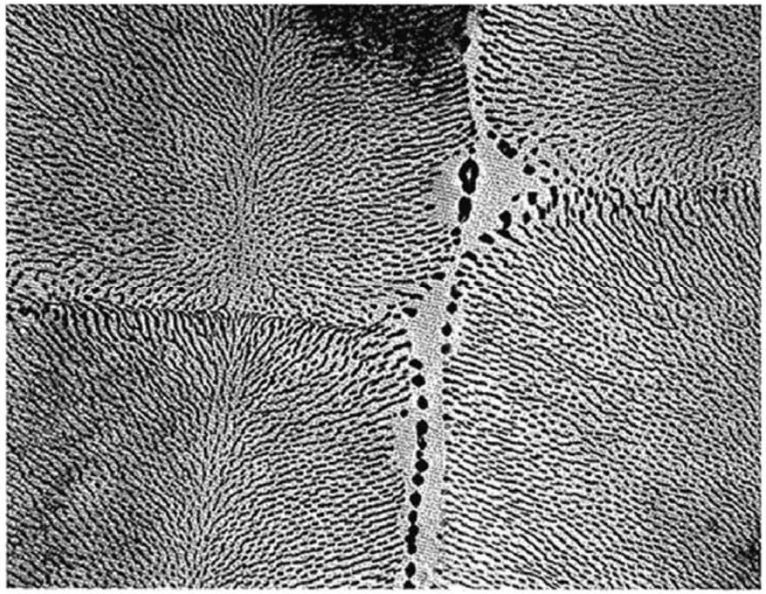

Fig. 4.35 Transverse section through the cellular structure of an Al-Al_6Fe rod eutectic (x3500).

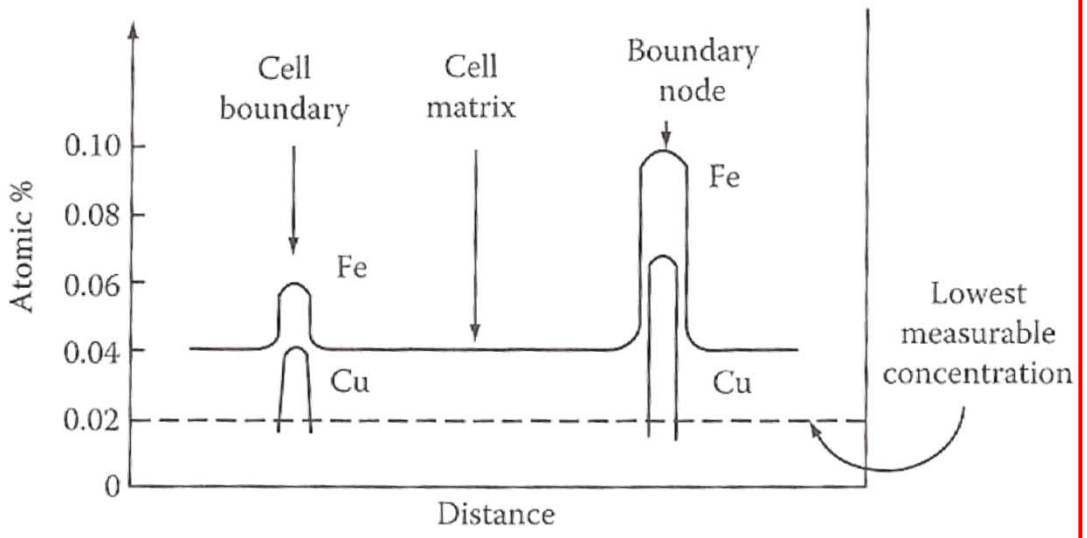

Fig. 4.36 Composition profiles across the cells in Fig. 4.35b.

An alternative approach for lamellar growth by Jackson and Chalmers,

Terminating layer T
by change of speed of growth

The stability of the tip T is the criterion for the stable lamellar width, λ.

Assumption:

1) interface ~ isothermal
2) Total supercooling of interfaces
   ~ sum of the supercooling due to curvature
3) the enrichment of the liquid in contact with the interface by rejection of the solute

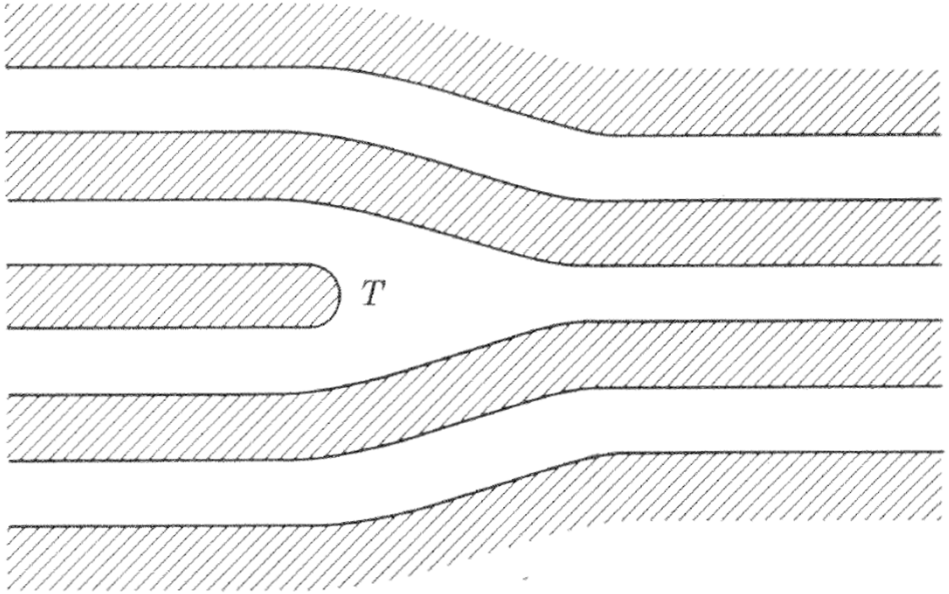

Fig. 6.16. Termination of lamellar (schematic)

The supercooling is calculated 1) at the intersection of a termination with the interface, and 2) at a position remote from terminations.

Assumptions: 1) Width of two lamellar ~ equal

2) Curvature ~ uniform and equal

3) Surface free energies of the two phases (α and β) ~ equal

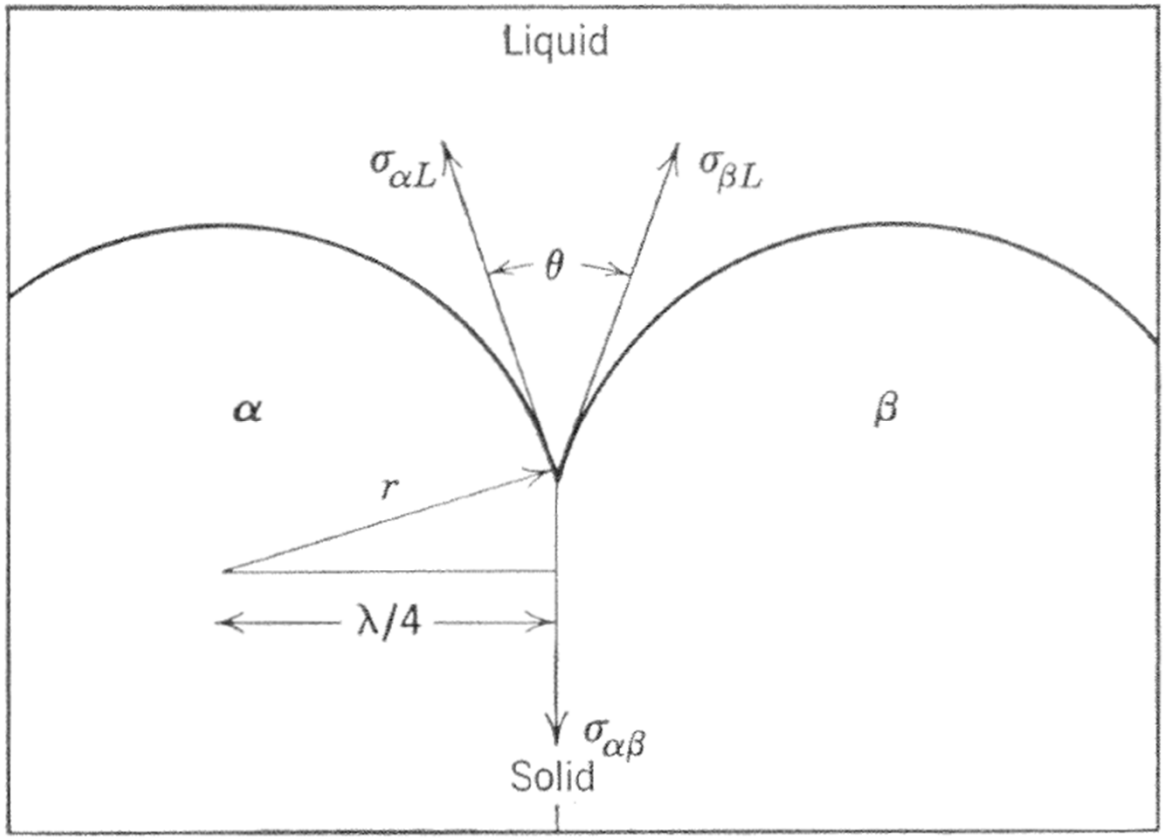

$$2\sigma_{\alpha L}\cos\frac{\theta}{2} = \sigma_{\alpha\beta}$$

$$\frac{\lambda}{4} = r\cos\frac{\theta}{2}$$

$$\cos\frac{\theta}{2} = \frac{\sigma_{\alpha\beta}}{2\sigma_{\alpha L}} = \frac{\lambda}{4r}$$

$$\frac{\sigma_{\alpha L}}{r} = \frac{2\sigma_{\alpha\beta}}{\lambda}$$

Fig. 6.17. Region of interface near the junction of two lamellae.

Diffusion of solute ahead of the interface

$$(C_\alpha{}^L - C_E) = [(1 - k_\alpha)C_E R\lambda]/8D$$

$$\Delta T_c = [(1 - k_\alpha)C_E R\lambda m_\alpha]/8D$$

m : slope of liquidus line

Supercooling at curvature center

$$\Delta T_r = \frac{\sigma_{\alpha L} T_E}{Lr} \quad \text{but} \quad \frac{\sigma_{\alpha L}}{r} = \frac{2\sigma_{\alpha\beta} T_E}{L\lambda}$$

and therefore

$$\Delta T_r = \frac{2\sigma_{\alpha\beta} T_E}{L\lambda}$$

At termination point T, Curvature change (cylindrical → Spherical)

$$\Delta T_r = 4\sigma_{\alpha\beta} T_E / L\lambda$$

Amount of solute rejected by the half cylinder of the termination (assumed to be stable),

$$(1 - k_\alpha) C_E R (\pi/2) (\lambda^2/16)$$ **per unit time**

Amount of solute diffuses across the semicircular interphase boundary

$$(1 - k_\alpha) C_E R \frac{\pi}{2} \frac{\lambda^2}{16} = \frac{D(C_\alpha{}^L - C_E)\lambda/2}{\lambda/4} \pi \frac{\lambda}{4}$$

or

$$C_\alpha{}^L - C_E = \frac{(1 - k_\alpha) C_E R \lambda}{16D}$$

from which

$$\Delta T_c = \frac{m_\alpha (1 - k_\alpha) C_E R \lambda}{16D}$$

The sums of the two supercoolings are equated, giving

$$\lambda^2 R = \frac{32\sigma_{\alpha\beta} T_E D}{m_\alpha (1 - k_\alpha) C_E L}$$

from which $\lambda^2 R$ is a constant, or, $\lambda \propto R^{-1/2}$.

5) Lamellar growth: experimental

Al-Zn, Al-Cu, Al-Zn, Pb-Sn, Pb-Cd
good agreement

$$v_0 \lambda_0^2 = k_3 \text{ (constant)}$$

$$\frac{v_0}{(\Delta T_0)^2} = k_4$$

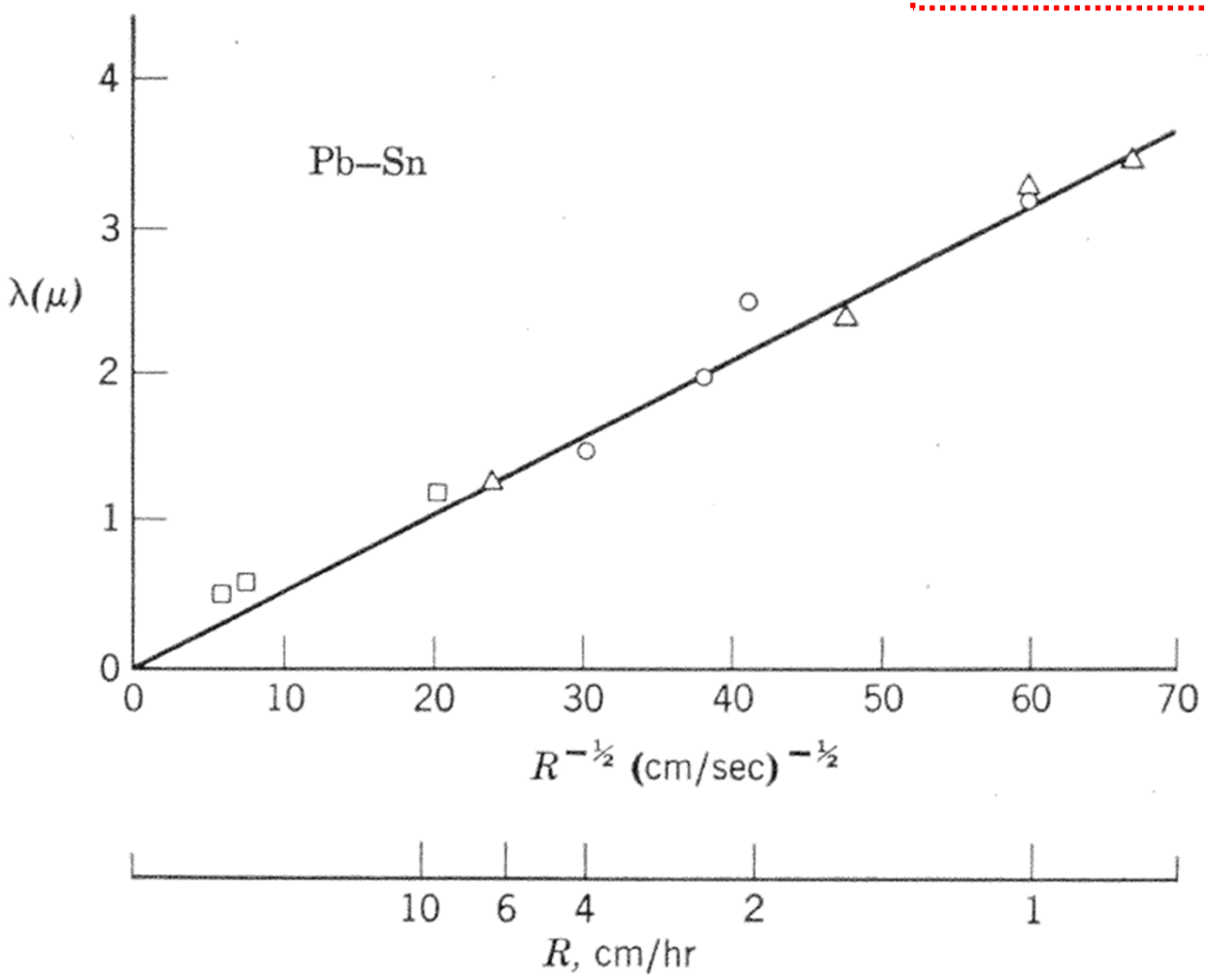

Fig. 6.18. Relationship between interlamellar spacing and growth rate for the lead-tin eutectic.

5) Lamellar growth: experimental

Al-Zn, Al-Cu, Al-Zn, Pb-Sn, Pb-Cd
good agreement

$$v_0 \lambda_0^2 = k_3 \quad \text{(constant)}$$

$$\frac{v_0}{(\Delta T_0)^2} = k_4$$

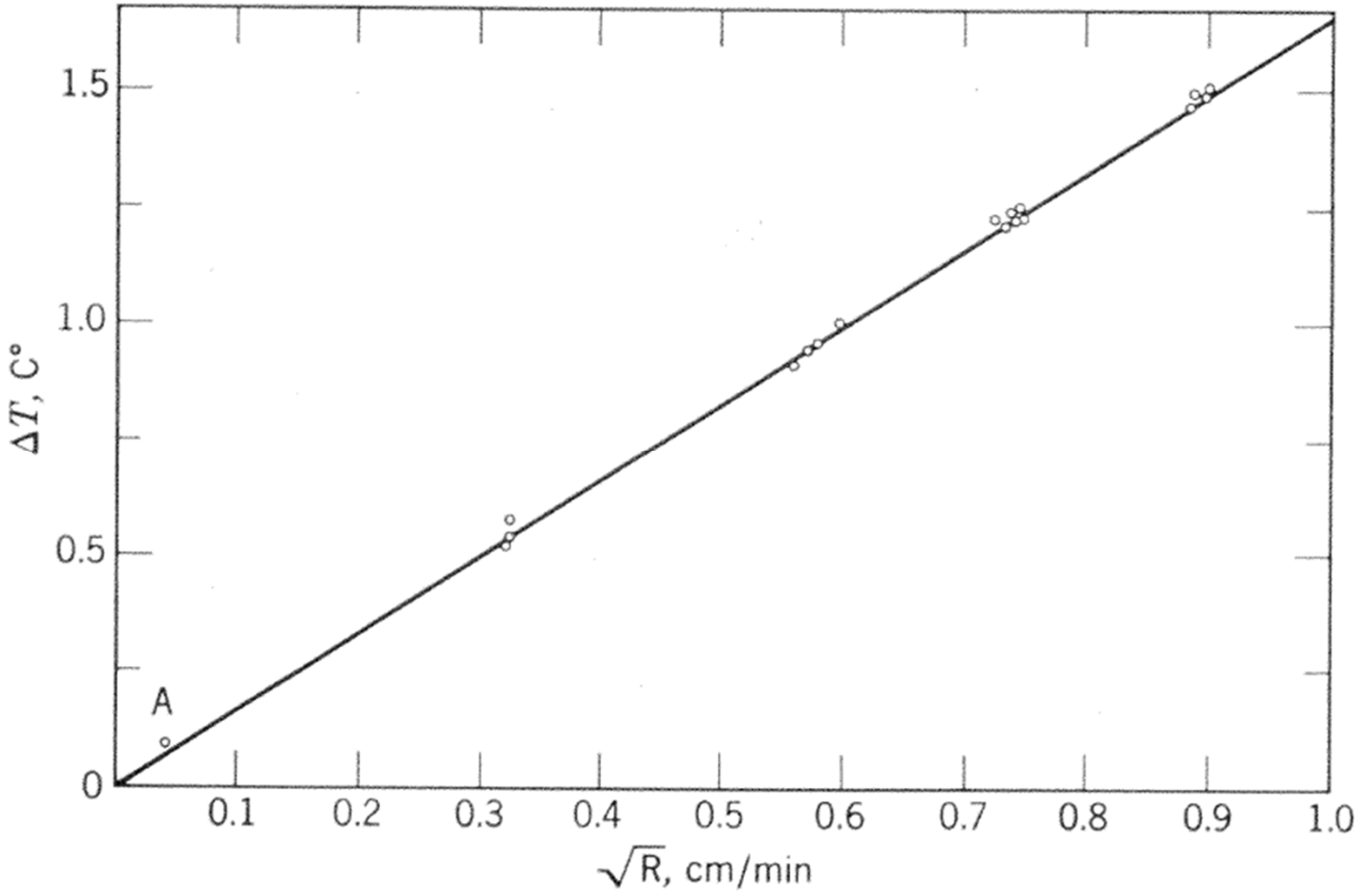

Fig. 6.19. Supercooling of eutectic interface as a function of growth rate (lead-tin).

6) Degenerate eutectic structure

Pure eutectic (lamellar type) ~ a very wide range of solidification rate

→ structure degenerate at very slow rates of solidification (less than 1cm/hr)

*** Degenerate structure:**
resemble the beginning of the spheroidization process that occurs during prolonged annealing

→ But, the degenerate structure is formed during, and not after, solidification.

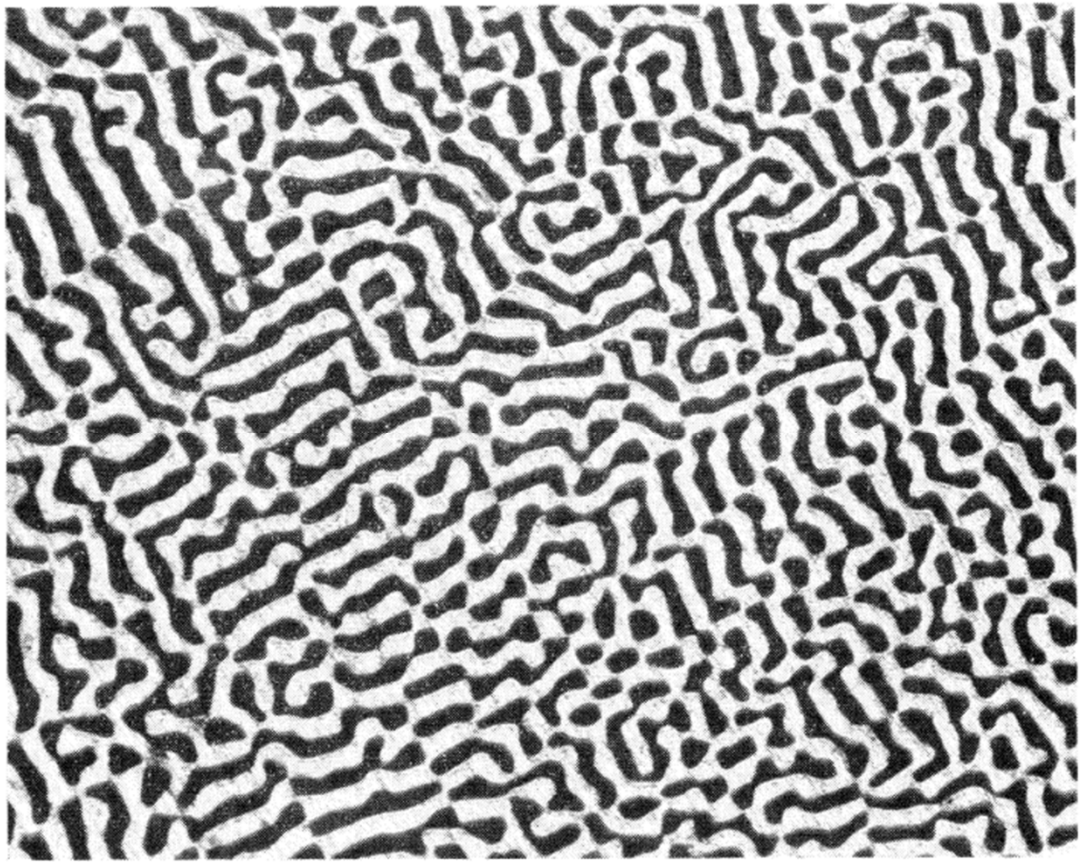

Fig. 6.20. Degenerate eutectic structure in CuAl2-Al eutectic at 0.8 cm/hr (X500).

7) Modification of Eutectics

Two degenerate forms of the lamellar structure by impurities

→ (a) Colony structure and (b) Rod structure

(a) Colony structure
: a cellular structure superimposed on the lamellar eutectic structure

*** An impurity or an excess of one constituent, would diffuse much farther ahead of the interface than would be required for transverse interlamellar diffusion**

→ The long range diffusion sets up constitutional supercooling → Cell formation and the resulting transverse diffusion of the impurity

→ if purity of the eutectic were sufficiently high, the colony structure are eliminated (regular lamellar structure is produced)

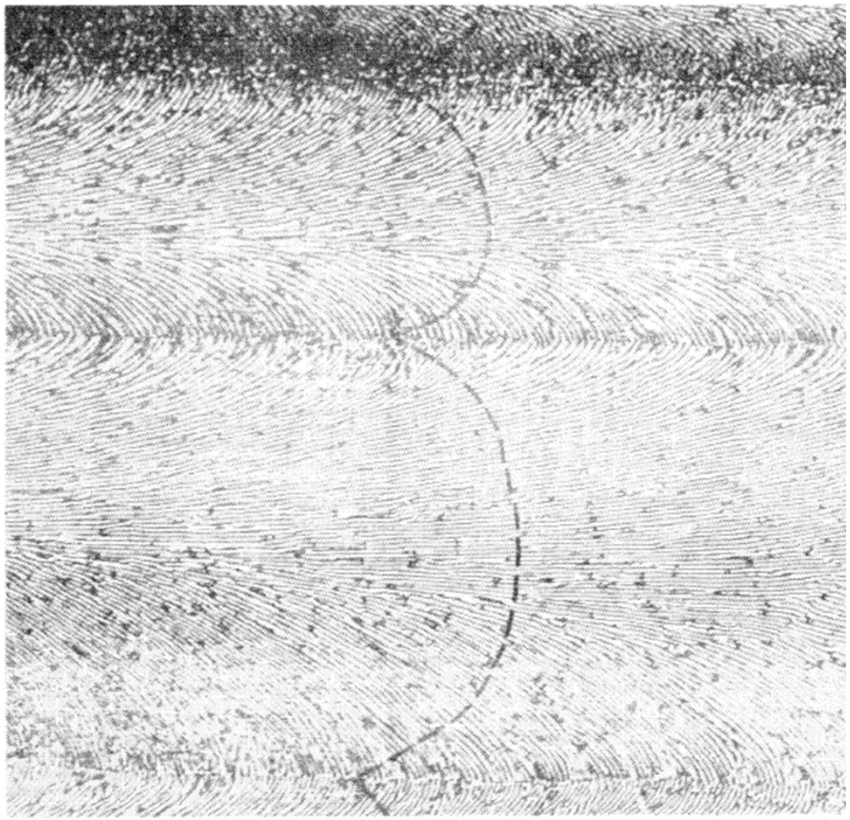

Fig. 6.21. Longitudinal section of impure $CuAl_2$-Al eutectic alloy. Broken line indicates shape of interface during growth.

A planar eutectic front is not always stable.

Binary eutectic alloys contains impurities or other alloying elements ➡ **Form a cellular morphology**
analogous to single phase solidification
Restrict in a sufficiently high temp. gradient.

➡ The solidification direction changes as the cell walls are approached and the lamellar or rod structure fans out and may even change to an irregular structure.

➡ Impurity elements (here, mainly copper) concentrate at the cell walls.

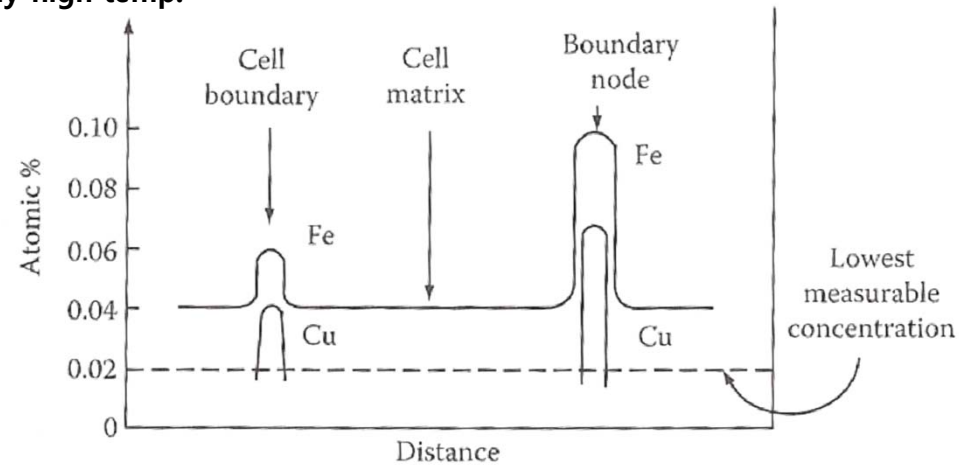

Fig. Composition profiles across the cells

* Total Undercooling $\Delta T_0 = \Delta T_r + \Delta T_D$

Undercooling required to overcome the interfacial curvature effects

Undercooling required to give a sufficient composition difference to drive the diffusion

Strictly speaking,

ΔT_i term should be added but, negligible for high mobility interfaces

Driving force for atom migration across the interfaces

$\Delta T_D \rightarrow$ Vary continuously from the middle of the α to the middle of the β lamellae

$\Delta T_0 = const$ ← Interface is essentially isothermal.

$\Delta T_D \rightarrow \Delta T_r$ The interface curvature will change across the interface.

Should be compensated

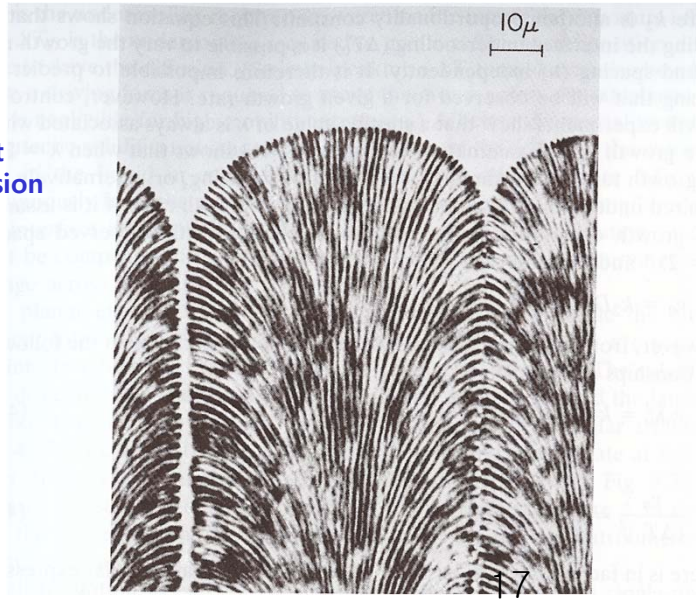

17

(b) Rod structure

: Impurity has sufficiently different distribution coefficients for the two solid phases

*** <u>When the two distribution coefficient are very different</u>, the lamellae of one phase should grow into the liquid ahead of the other, and the lamellae of the lagging phase then break up into very small cells, separated by the other phase.**

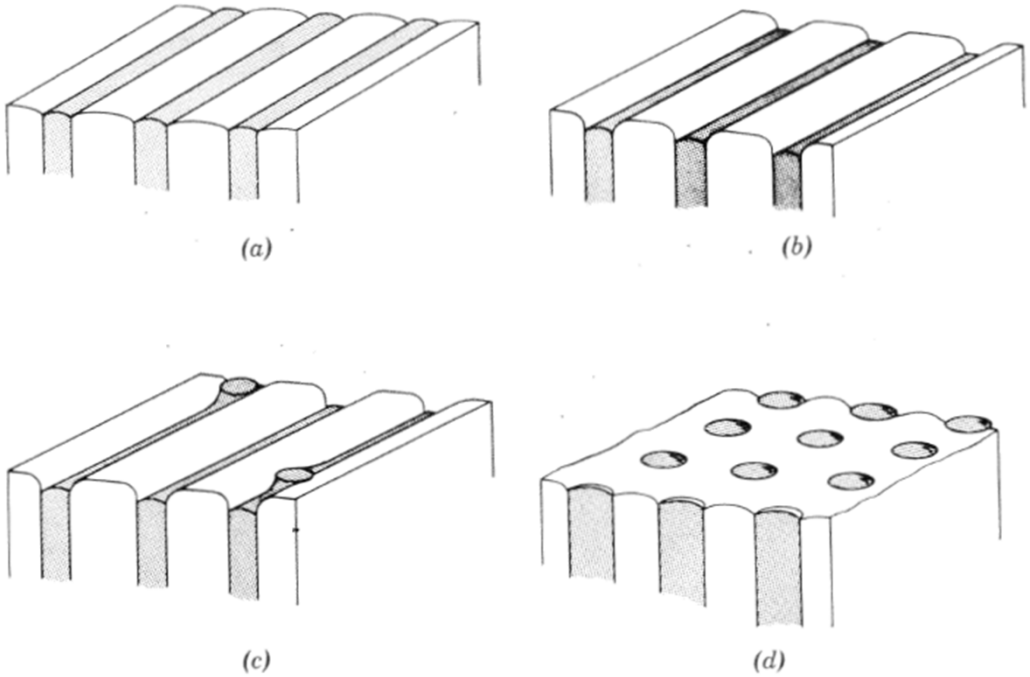

Fig. 6.22. Origin of "rod-type" eutectic structure (schematic).

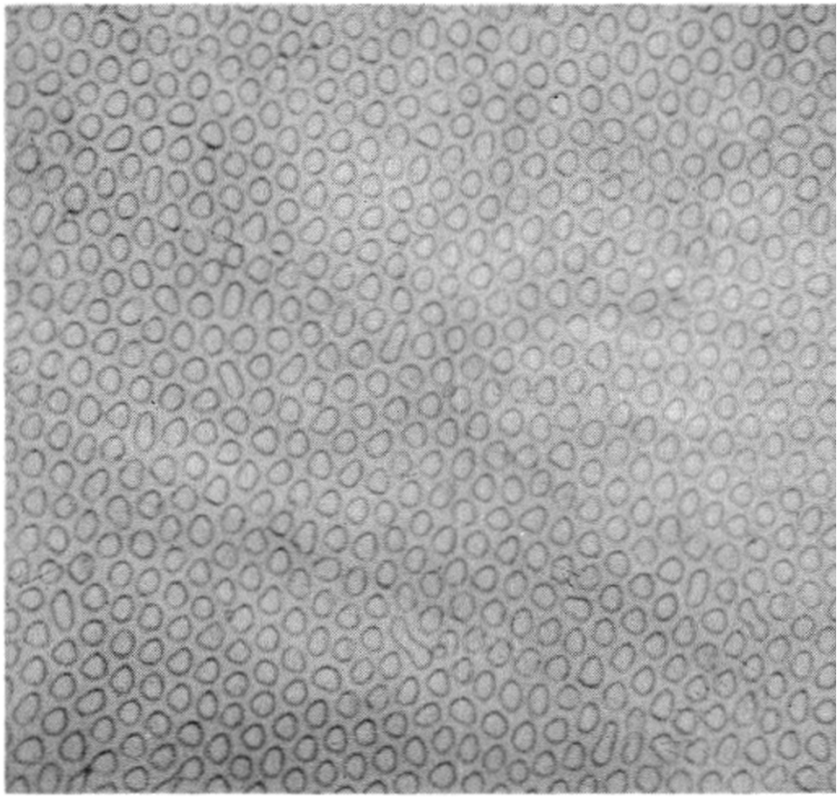

Fig. 6.23. Cross section of "rod-type" eutectic structure.

(C) Intermediate structure: Middle= lamellar structure/ edge = rod-type colony

: This is caused by an impurity which when present at a low concentration, has nearly equal distribution coefficient for the two solid phases, but which has increasingly differing distribution coefficients as its concentration increases.

*** Middle part of Cell**

: relatively low concentration of impurity & similar distribution coefficients

→ Lamellar structure

*** Edge of cell (near wall)**

: relatively high concentration of impurity & increasing differing distribution coefficients

→ Rod-type structure

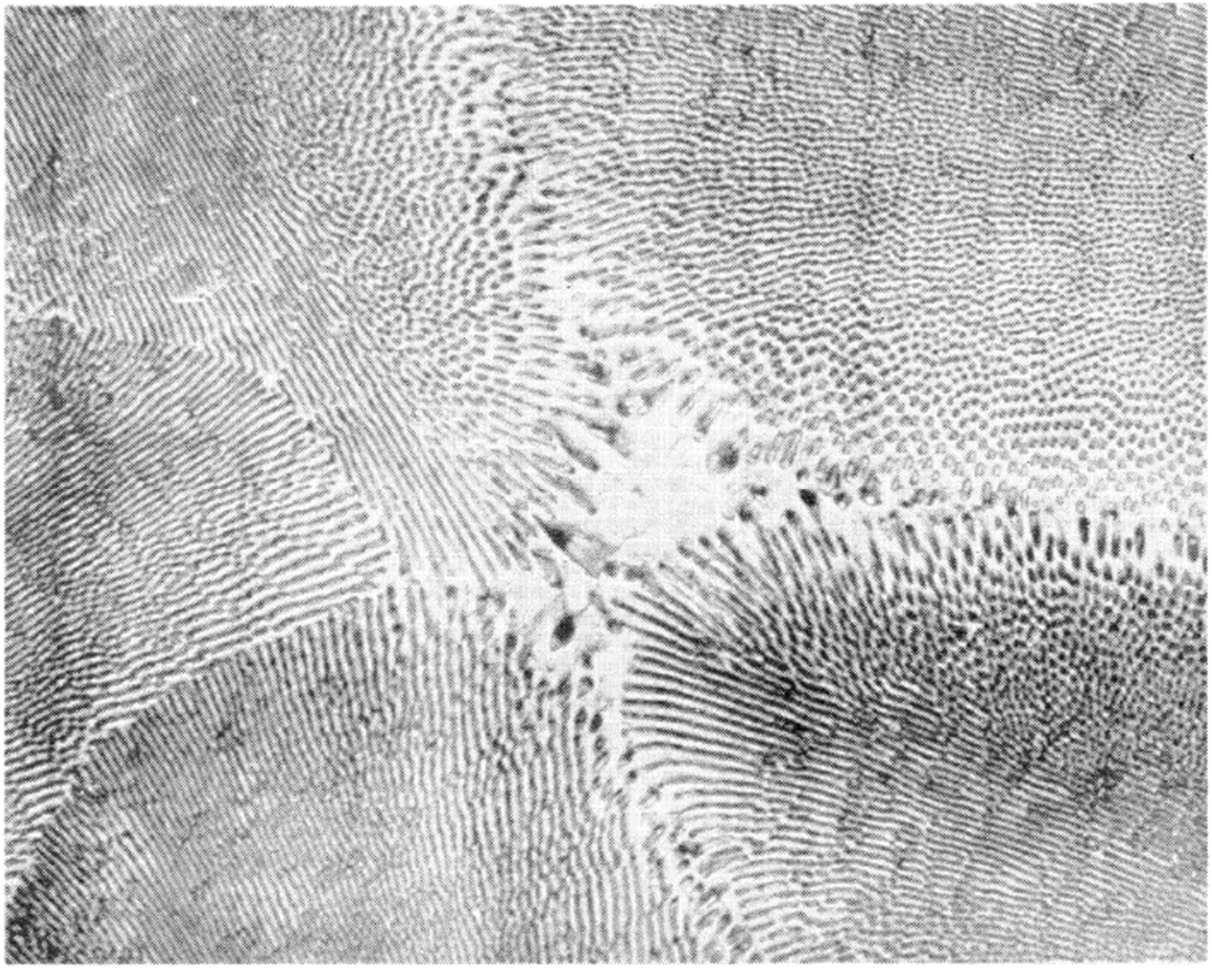

Fig. 6.24. "Mixed lamellar and rod structure" (Pb-Cd eutectic alloy with 0.1% Sn)

(d) Discontinuous eutectic structure

In lamellar type & degenerate form, each phase grows continuously
→ does not required repeated nucleation.

"Discontinuous eutectic" : required renucleate repeatedly due to "strong anisotropy" of growth characteristics of one of the phases

a) Case I: both phases renucleate repeatedly due to the termination of growth of crystals

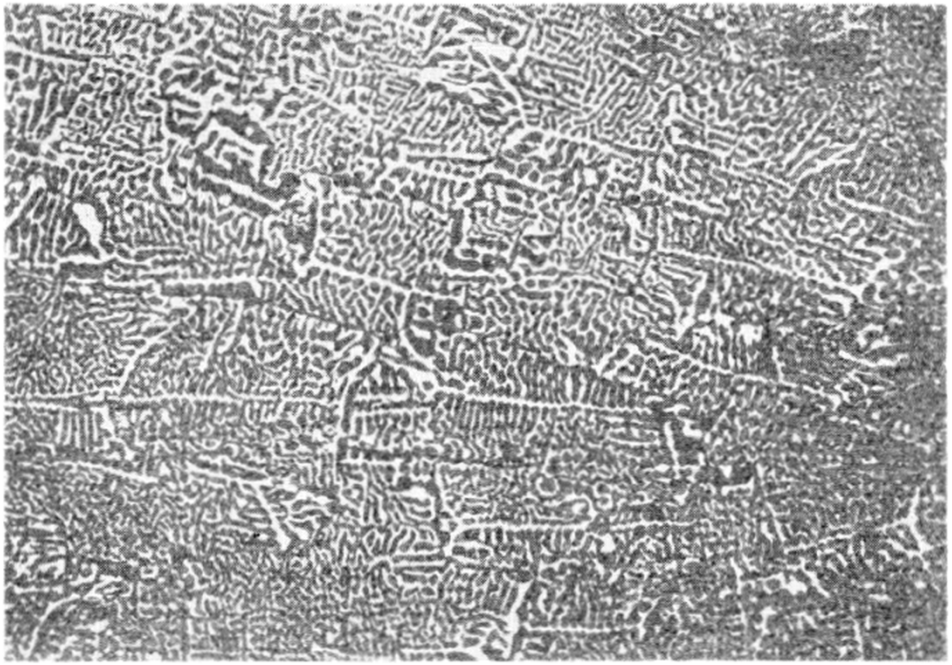

Fig. 6.25. "Chinese script" structure in Bi-Sn eutectic alloy

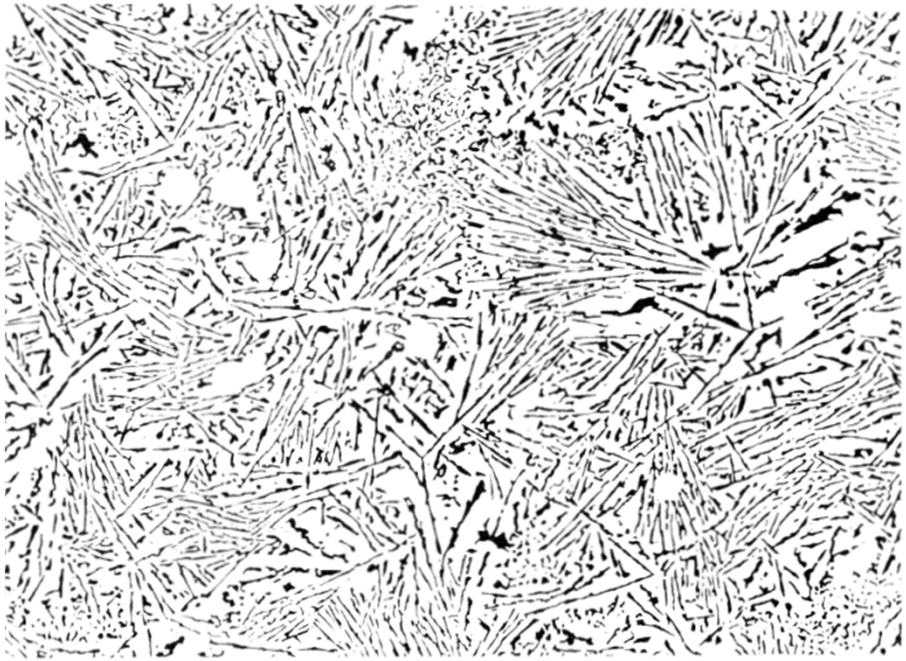

Fig. 6.26. Microstructure of Al-Si eutectic alloy.

(d) Discontinuous eutectic structure

: required renucleate repeatedly due to "strong anisotropy" of growth characteristics

a) Case I: both phases renucleate repeatedly due to the termination of growth of crystals

*** Typical discontinuous eutectic type growth mechanism (Figure 6.26)**

-Random nucleation and growth independent with growth interface

- I_1: three Si phases (A, B, C) growth
B= block of growth of C
A & B distance increase
I_2 : Nucleation and growth of D

- Chinese script (Fig. 6.25) type has not been investigated sufficiently.

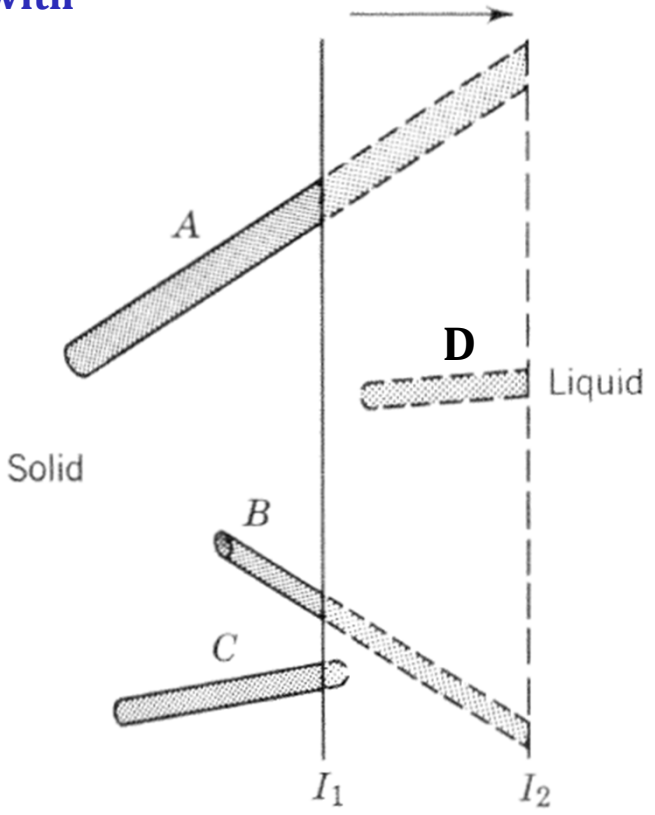

Fig. 6.27. Growth of a discontinuous eutectic (schematic), showing two positions of the interface (I_1 and I_2).

(d) Discontinuous eutectic structure

b) "Spiral type의 discontinuous eutectic" **- Al-Th & Zn-Mg alloys**

: one or both of the phases → anisotropic in growth rate

→ α phase grows faster than the β phase in one direction and more slowly in the other (unusual structure in Fig. 6.30).

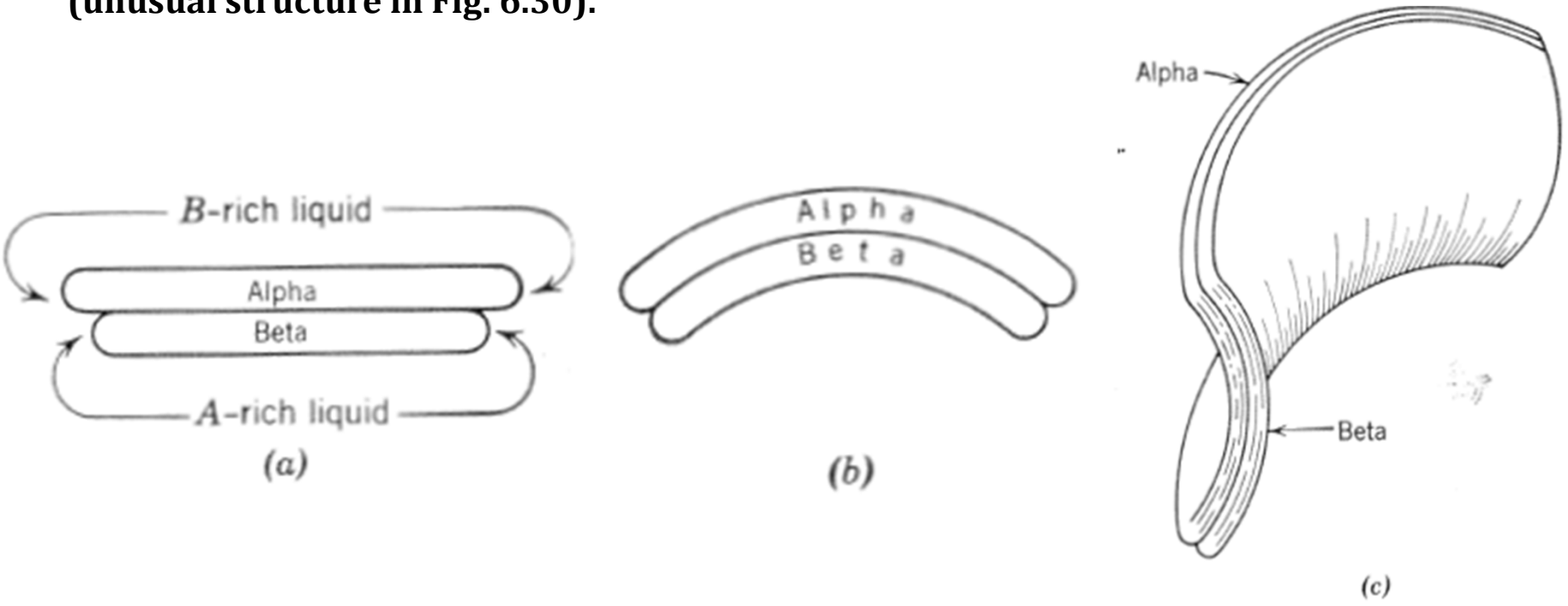

Fig. 6.30. Origin of spiral eutectic (schematic).

(d) Discontinuous eutectic structure

b) "Spiral type의 discontinuous eutectic" - Al-Th & Zn-Mg alloys

: one or both of the phases → anisotropic in growth rate

*** If the two edges of the β phase do not form a closed ring, but overlap, then a spiral will be formed in that plane, and the complete structure will develop into a double conical spiral as shown in Fig. 6.29.**

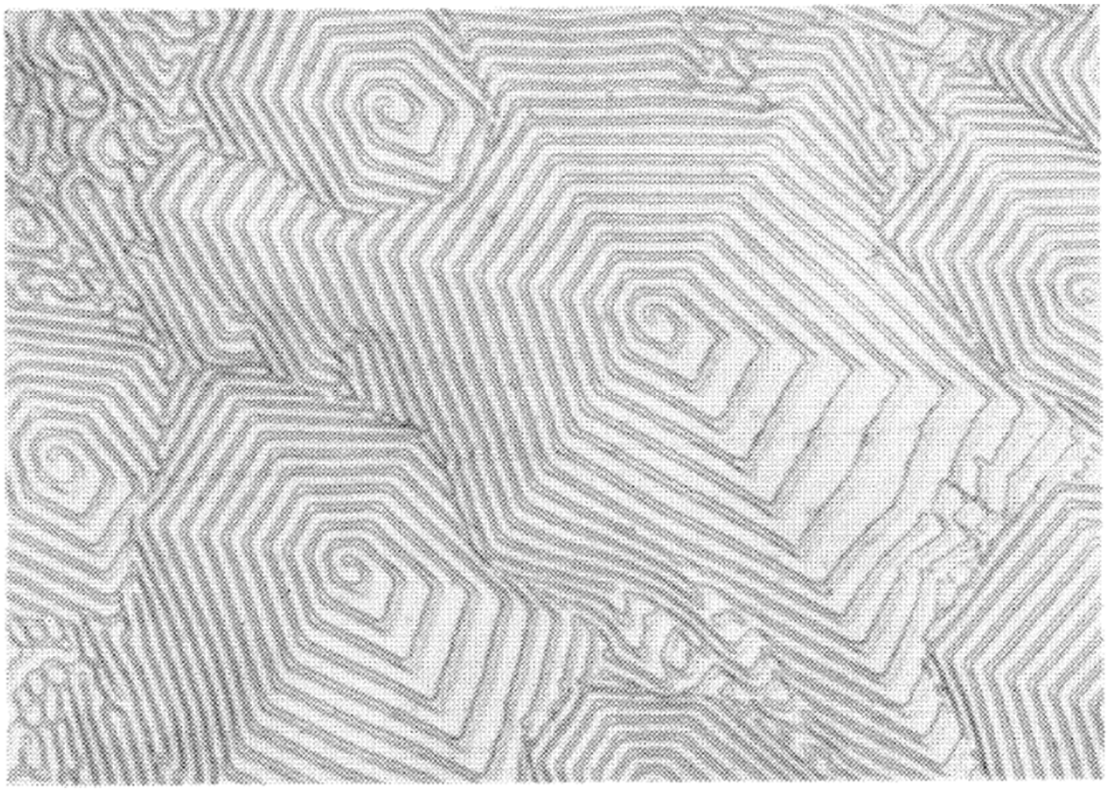

Fig. 6.28. Spiral eutectic structure in Zn-Mg alloy.

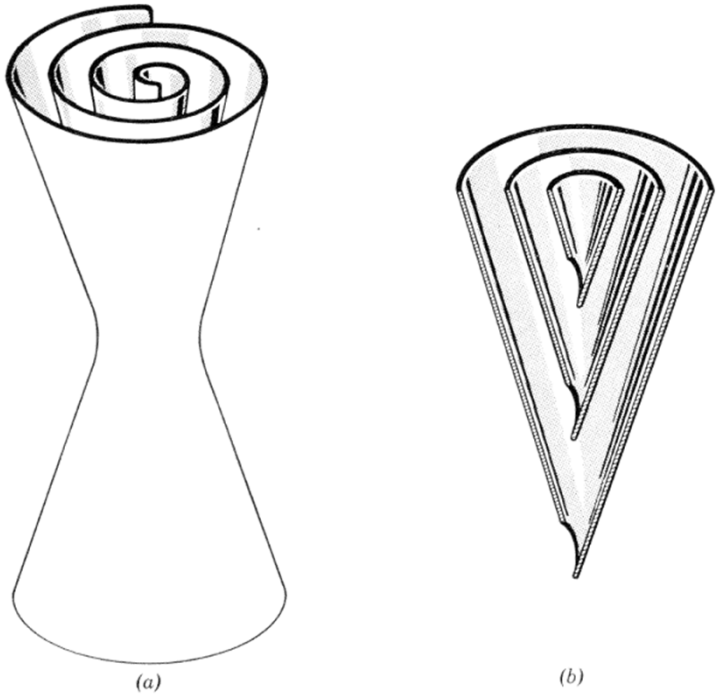

Fig. 6.29. Detailed structure of the spiral eutectic (schematic).

(e) Special cases of the modification of eutectics

Ex) Microstructure of Al-Si eutectic could be modified by the minor addition of solutes:

① Addition of 0.01 % Sodium

Needle or plate type Si morphology → very smaller, more spherical Si particles

② Rapid Cooling → very smaller, more spherical Si particles

*** An explanation for these phenomena**

→ the modified structure is formed at a temp. a few degrees below the normal T_e.

① <u>Modifier changes the surface tension relationships</u> (due to lower latent heat and higher thermal conductivity of Al) → very smaller, more spherical Si particles

② Rapid quenching →

due to thermal difference로

→ Large supercooling

a. decrease of Si precipitation (follows EA line)

b. decrease of r* of Si and constantly renucleating Si

→ very smaller, more spherical Si particles

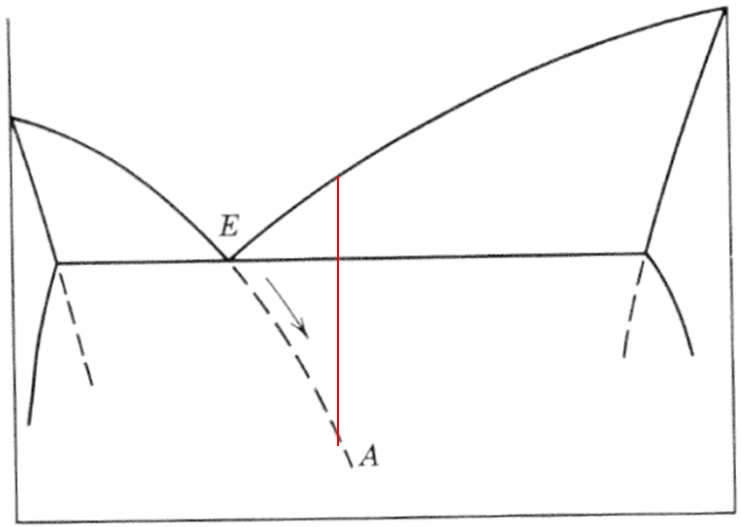

Fig. 6.31. Supercooling of eutectic in the absence of the second phase.

8) Non-eutectic composition

Solidification of C_0 liquid

① complete mixing: Primary α $C_s \rightarrow C_T$

Liquid 조성 $C_0 \rightarrow E$

② less complete mixing: primary solidification

Depending on undercooling: Cellular →

Cellular-dendritic → New crystal nuclei

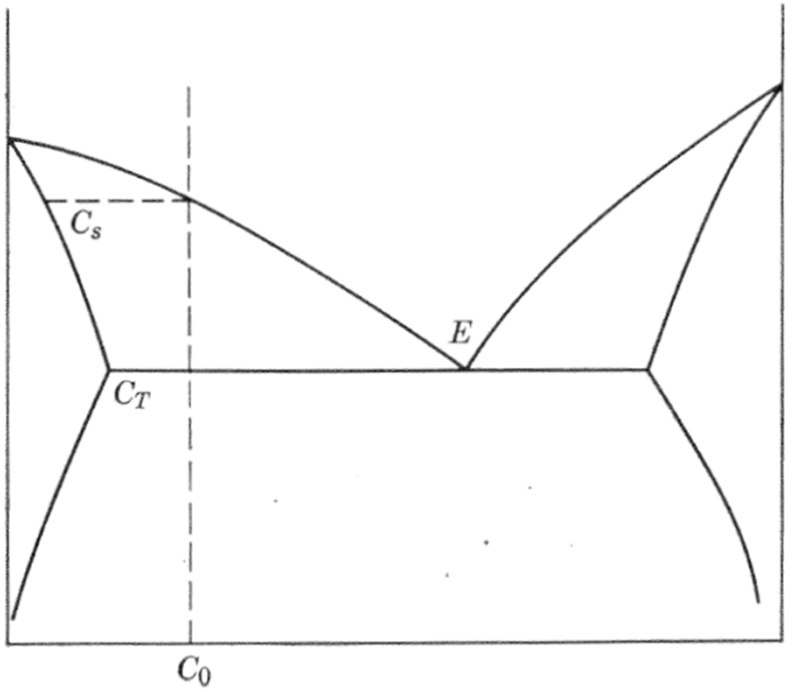

Fig. 6.32. Soldification of a eutectic system at a non-eutectic composition.

In real cases, the terminal transient liquid is far richer in solute than would be predicted from the equilibrium diagram, and it is therefore difficult to avoid the formation of some eutectic if the relevant liquid line terminates at a eutectic point.

* Off-eutectic Solidification

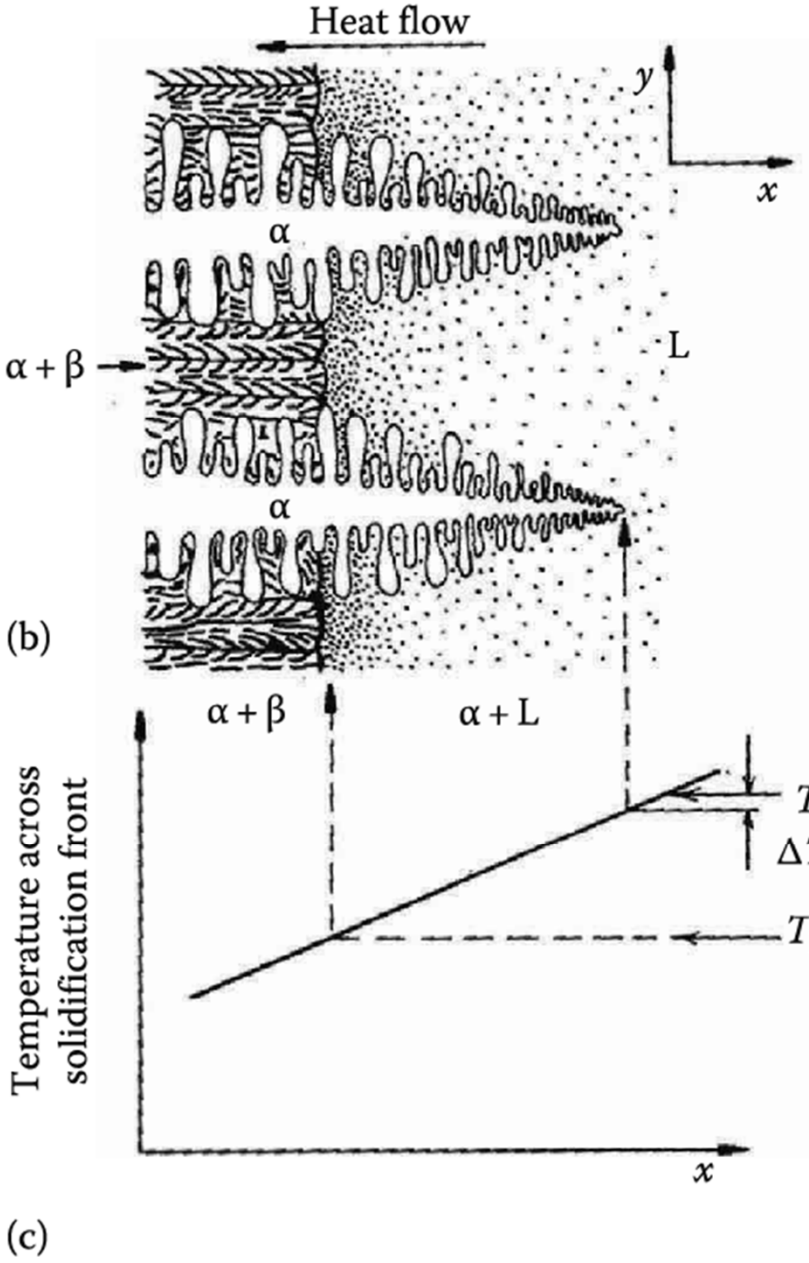

primary α + eutectic lamellar

- Primary α dendrites form at T_1. Rejected solute increases X_L to X_E; eutectic solidification follows.
- Coring : primary α (low solute) at T_1 and the eutectic (high solute) at T_E.

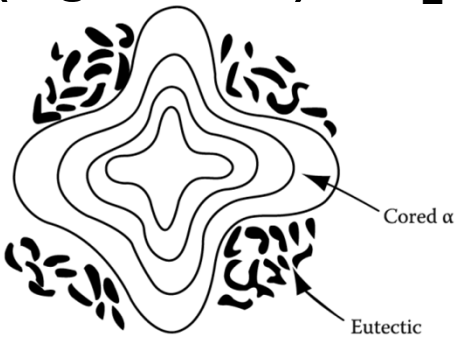

→ **in-situ composite materials**

→ The alloy solidifies as 100% 'eutectic' with an overall composition X_0 instead of X_E.

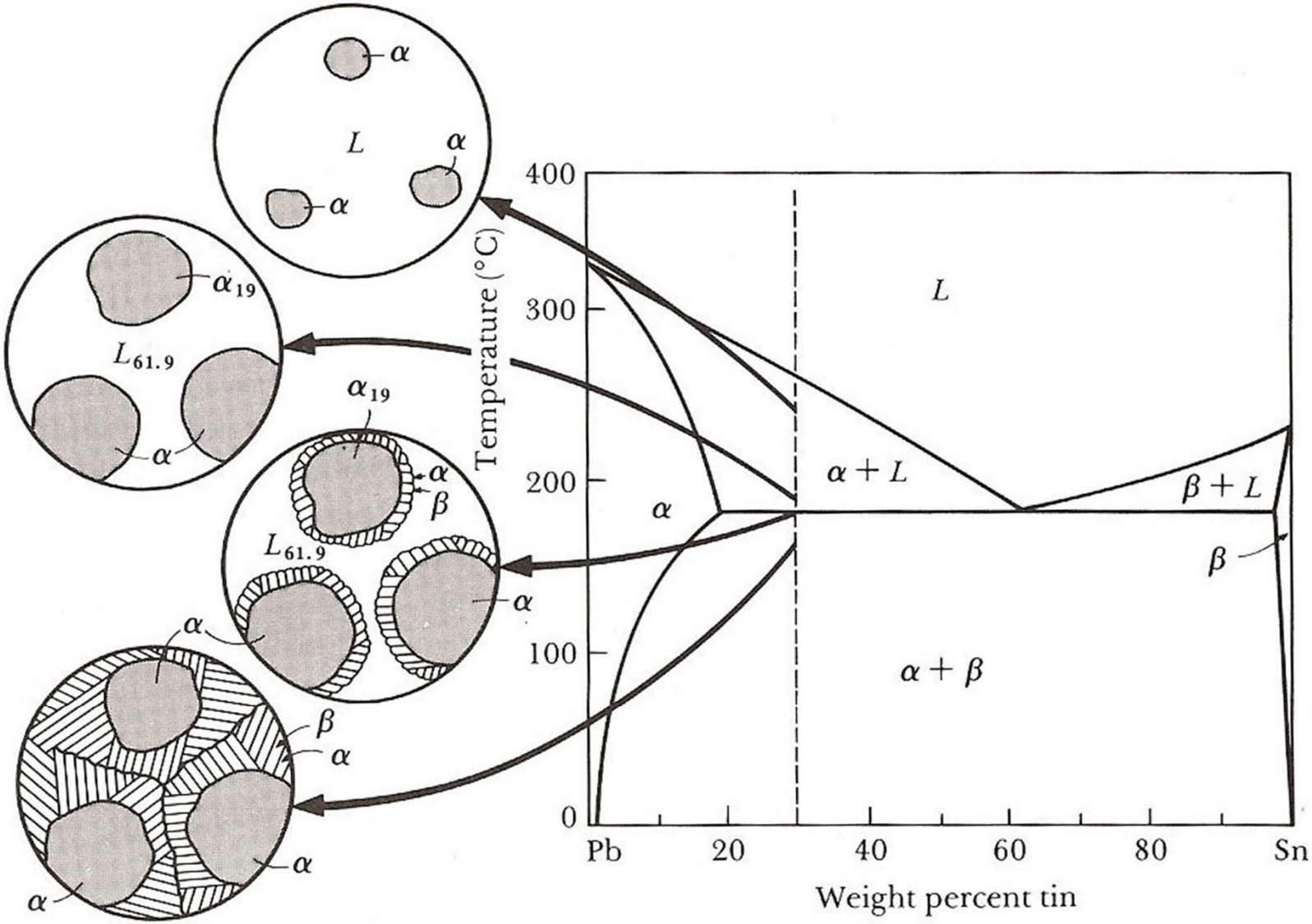

FIGURE 10-12 The solidification and microstructure of a hypoeutectic alloy (Pb-30% Sn).

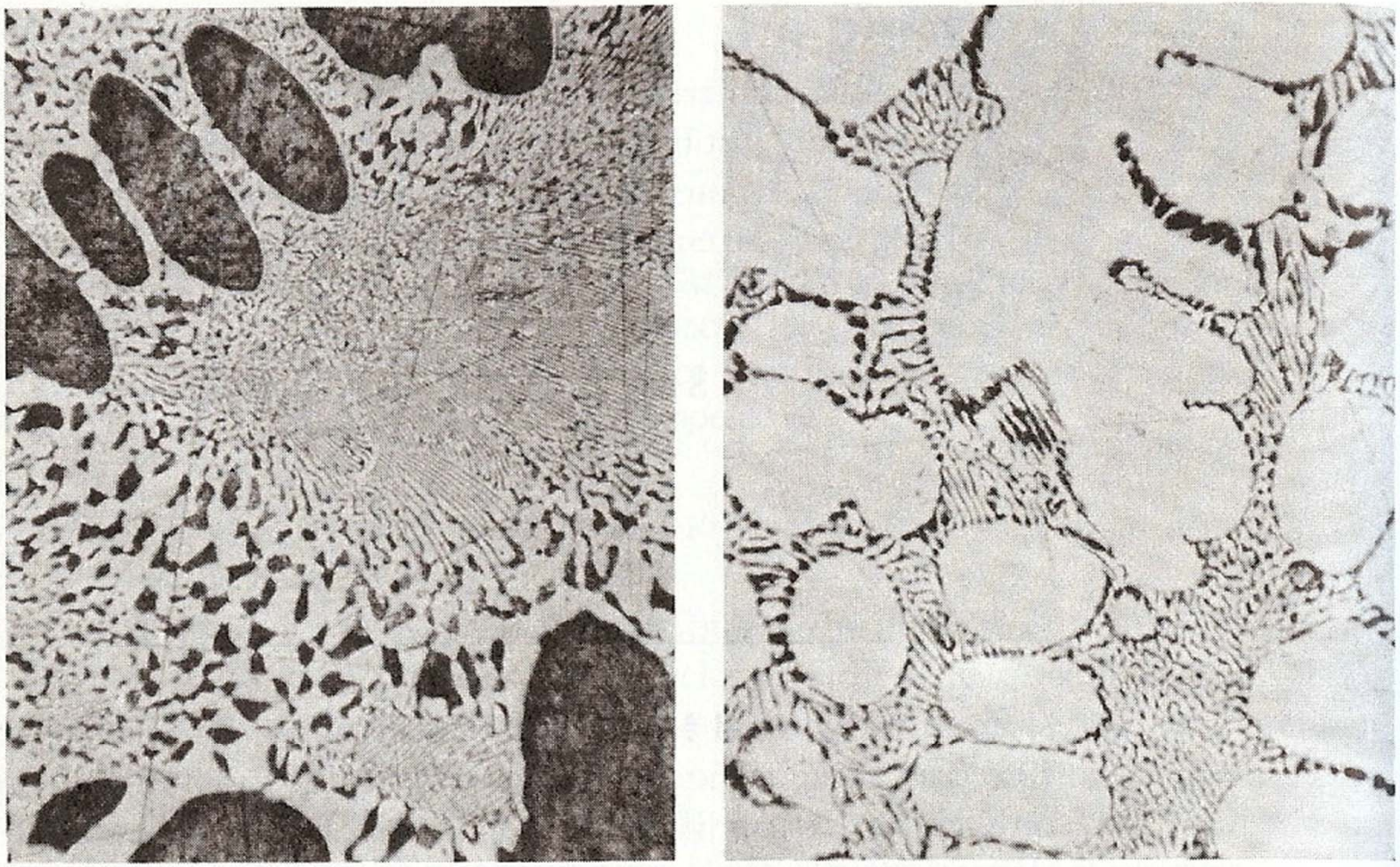

(a) (b)

FIGURE 10-13 *(a) A hypoeutectic lead-tin alloy. (b) A hypereutectic lead-tin alloy. The dark constituent is the lead-rich solid α, the light constituent is the tin-rich solid β, and the fine plate structure is the eutectic (× 400).*

9) Gravity segregation of eutectic

*** Uranium-Al eutectic region: "Cycled" up and down of T_E**

→ marked segregation: crucible bottom_U concentration↑/ top: Al concentration↑

→ Degree of Segregation : depending on # of Cycles

Ex) Al-13.3 wt% U → 168 cycles → bottom 45.4%/ top only 2.2%

: The segregation is in fact a result of the motion of the liquid enriched with solute during solidification and of the purer liquid formed by melting the separated phases during melting part of the cycle.

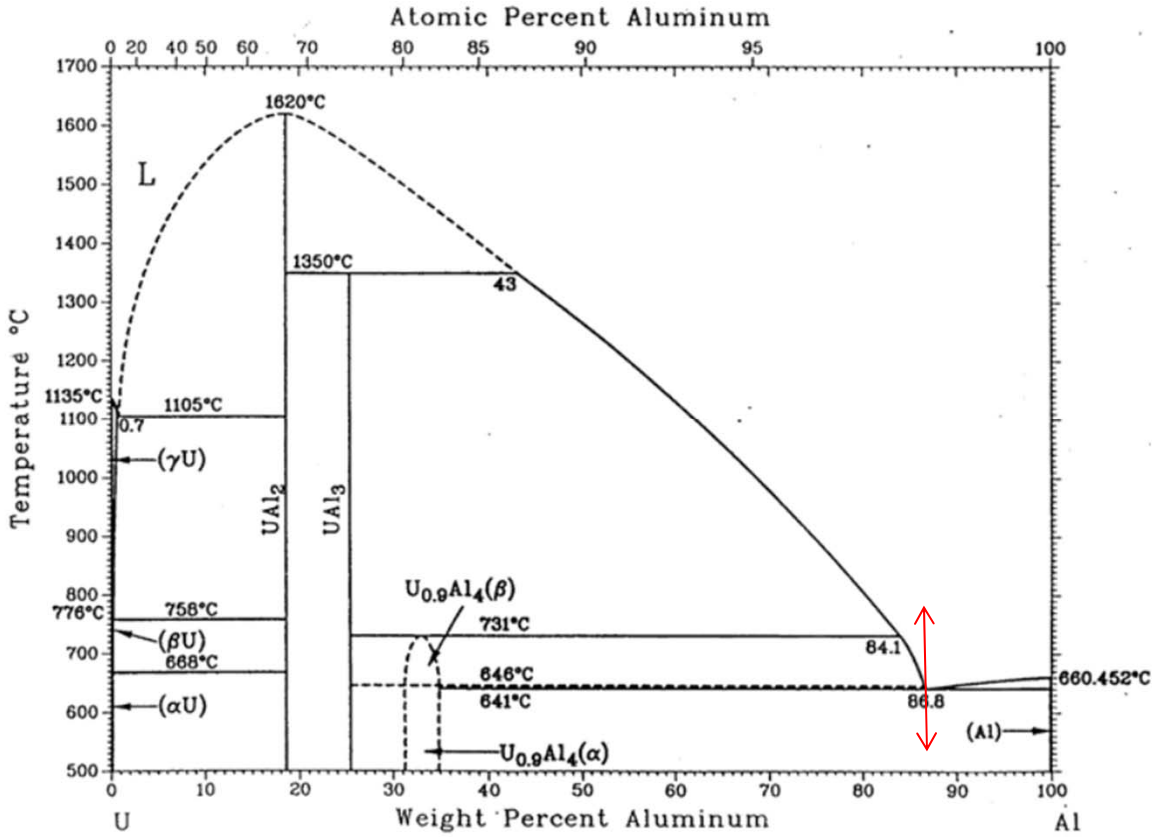

10) Divorced eutectic

- The primary phase continues to solidify past the eutectic point (along the line EA) of Fig. 6.31 until either the whole of the liqud has solidified or the other phase nucleated and forms a layer, which is some times dendritic, separating the two layers of the primary phase.

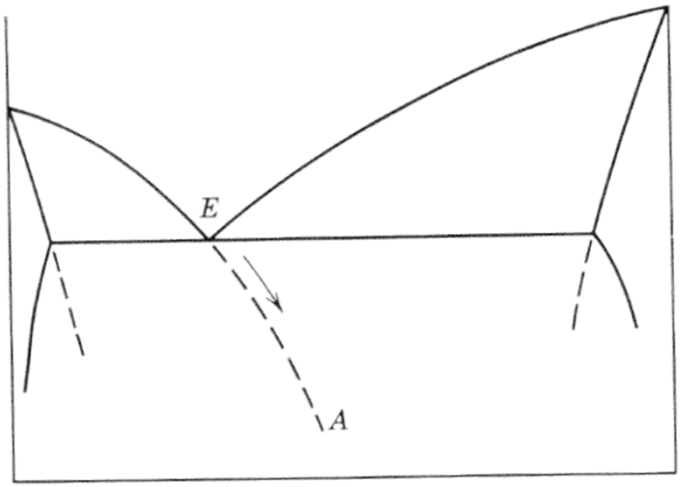

Fig. 6.31. Supercooling of eutectic in the absence of the second phase.

- One of the phases requires considerable supercooling for nucleation.

- "Divorced eutectic" is used to denote eutectic structures in which one phase is either absent or present in massive form.

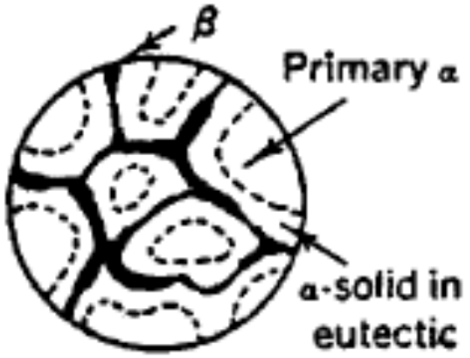

- **Massive Transformation**

: The original phase decomposes into one or more new phases which have the same composition as the parent phase, but different crystal structures.

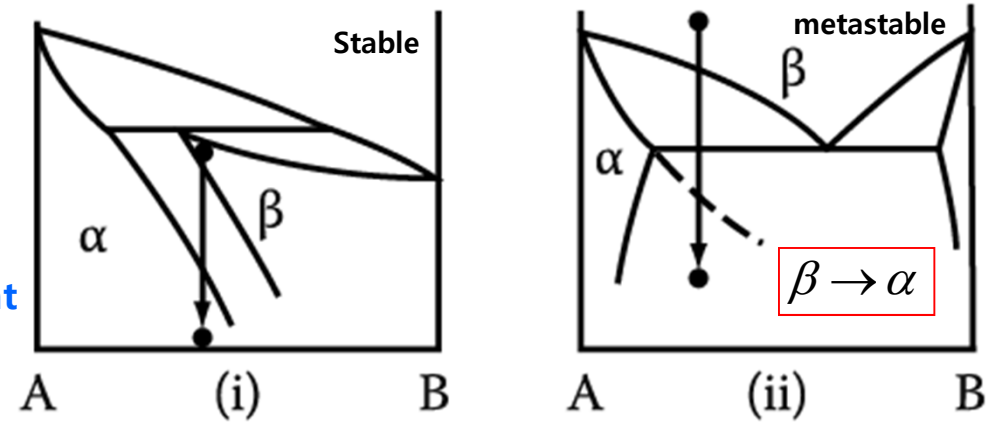

11) Ternary eutectic: very little work has been reported

* lamellar form, alternating three phases in ternary eutectic of Pb-Sn-Cd

: This arrangement is the one which would provide the shortest possible diffusion path for a given total area of interphase boundary, since each phase is adjacent to both of the other two phases.

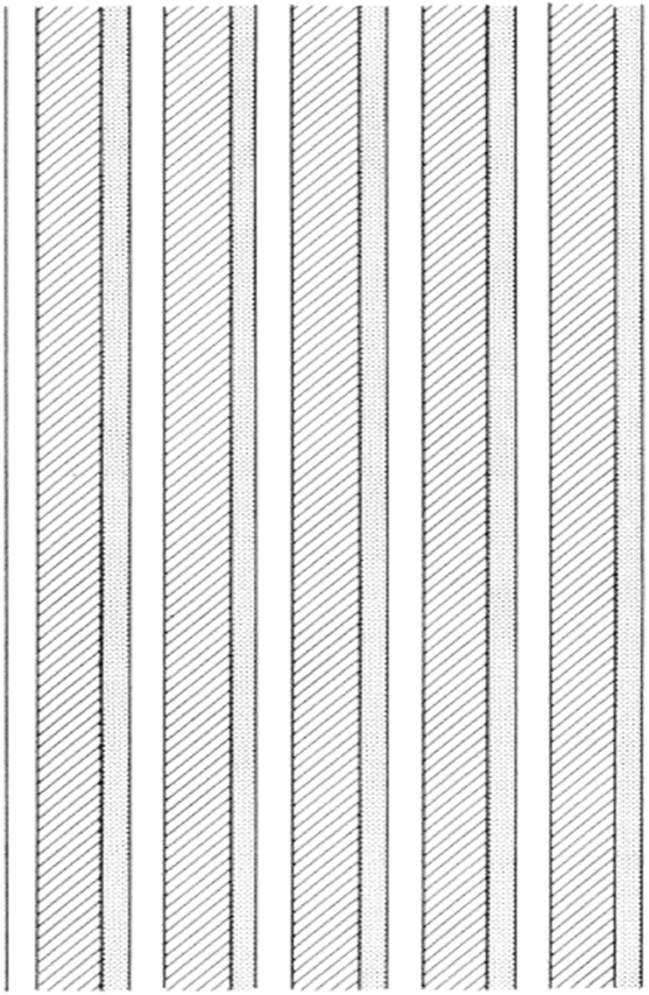

Fig. 6.34. Lamellar ternary eutectic.

- **IH _ Summary of recently reported paper for Quar-ternary or higher eutectic (within 3 pages of PPT)**

12) Cast Iron: Fe-C alloy (1.7 ≦ c ≦ 4.5%)

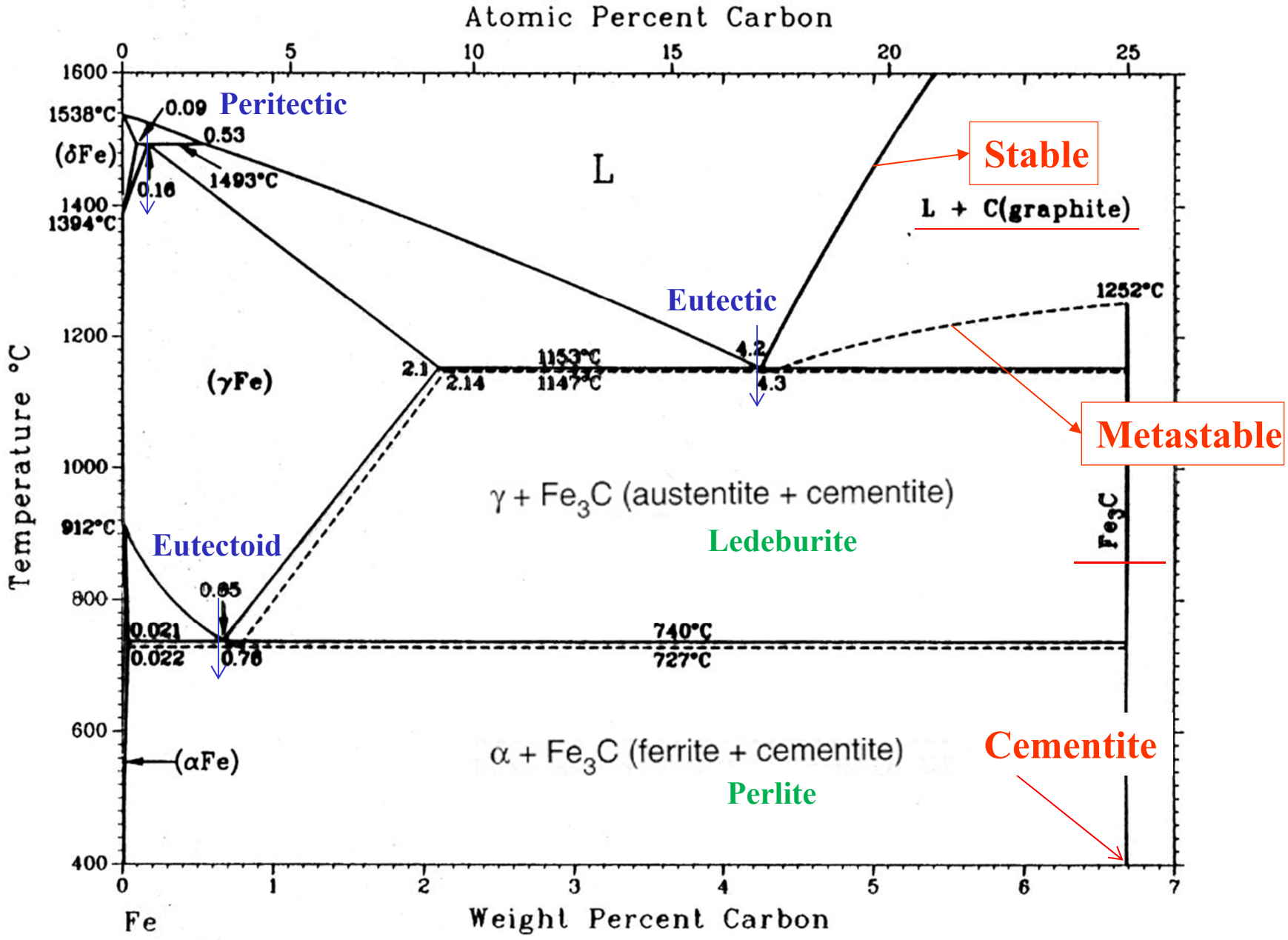

* Two eutectic system: Fe-graphite & Fe-Fe_3C

: If there is no other additive element, the Fe-graphite system is stable
& Fe-Fe_3C (cementite) eutectic is formed by rapid cooling of liquid phase

* Classification of Cast Iron is possible depending on the type of Carbon.

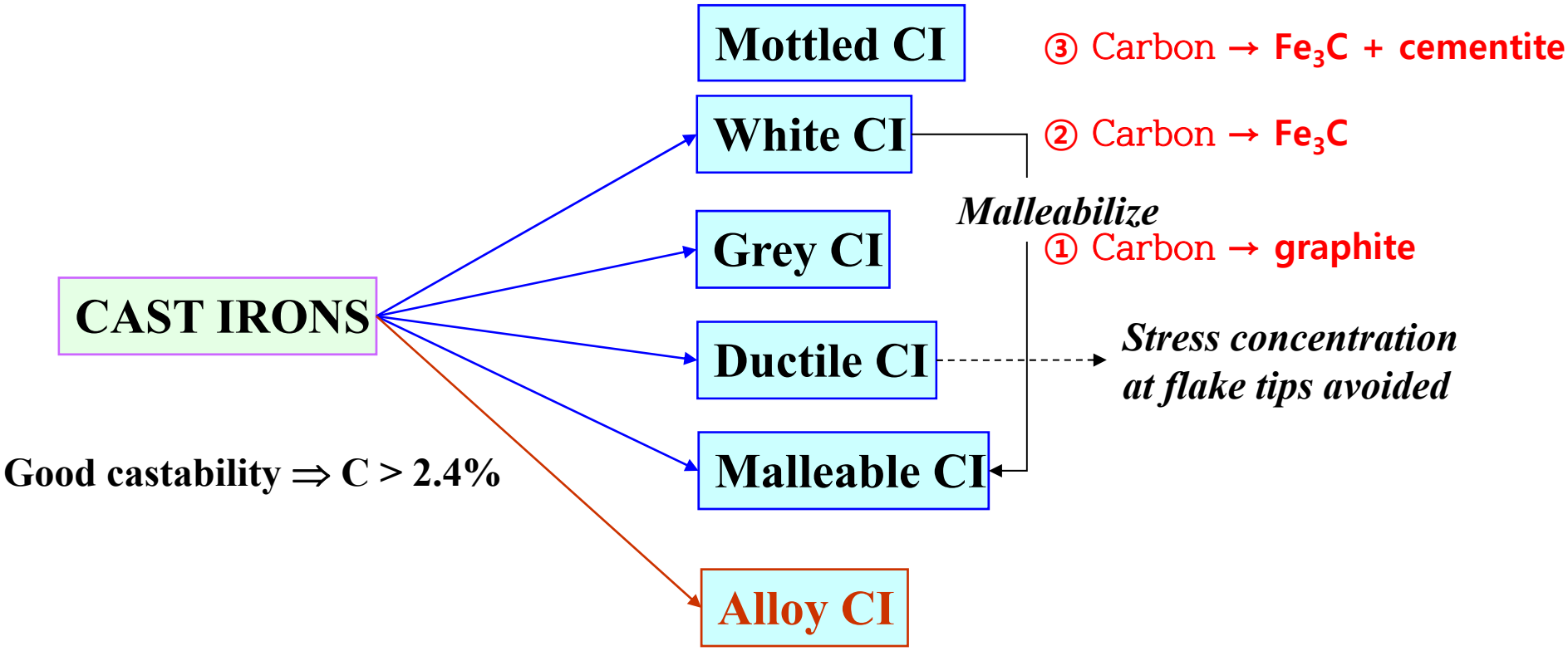

* Fe-Fe_3C eutectic temp < Fe-graphite eutectic temp. (6°C)

* If solidification proceeds at interface temperature above the cementite eutectic temperature,
Graphite eutectic formation

→ Gray cast Iron

* If the solidification proceed below Cementite eutectic temperature due to lower the liquidus temperature through fast quenching and a suitable nucleation agent to form an over-solute layer,

→ White cast Iron

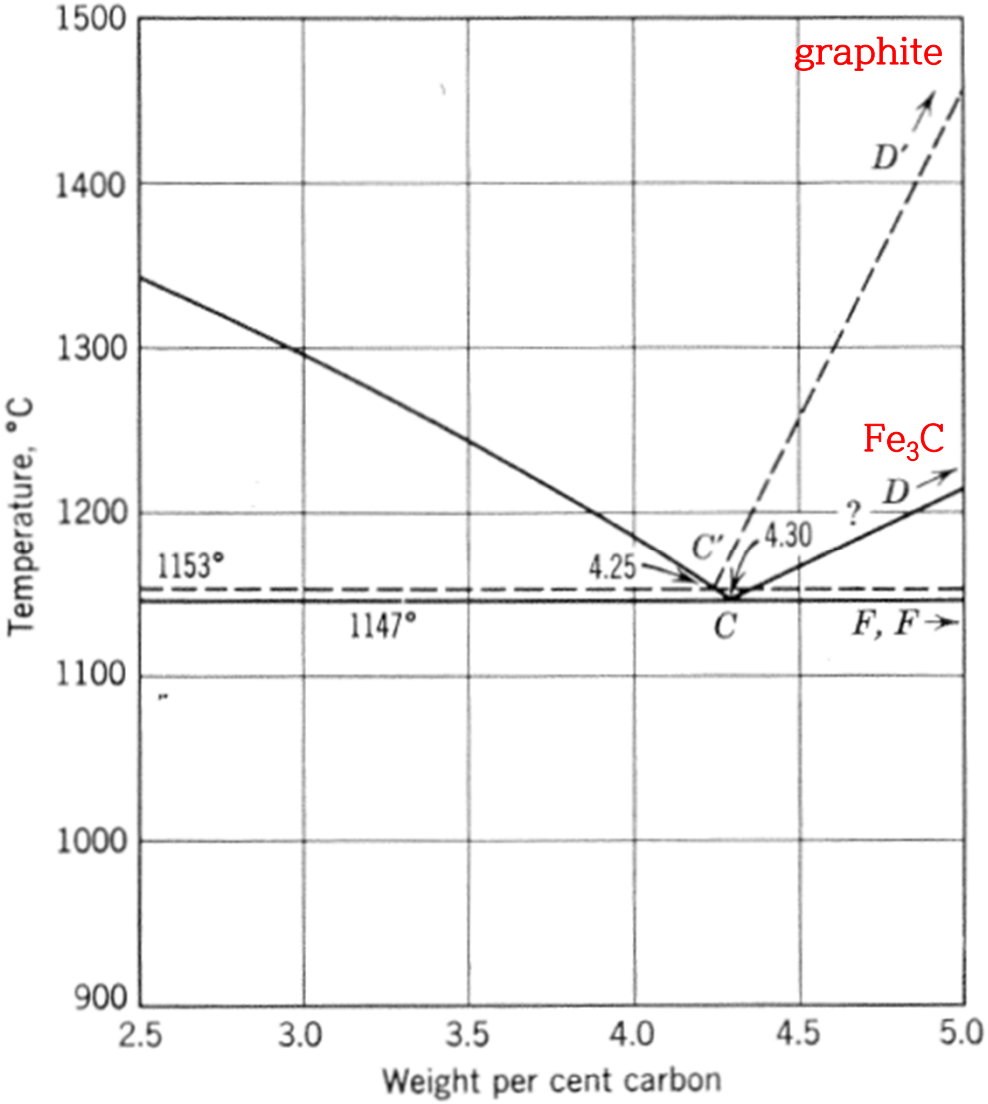

Fig. 6.35. Eutectic region of the iron carbon system.

* Addition effects of other elements

① Si → $T_E^{graphite}$ ↑ / $T_E^{Cementite}$ ↓

② Cr: decreasing the temperature rage where graphite is formed

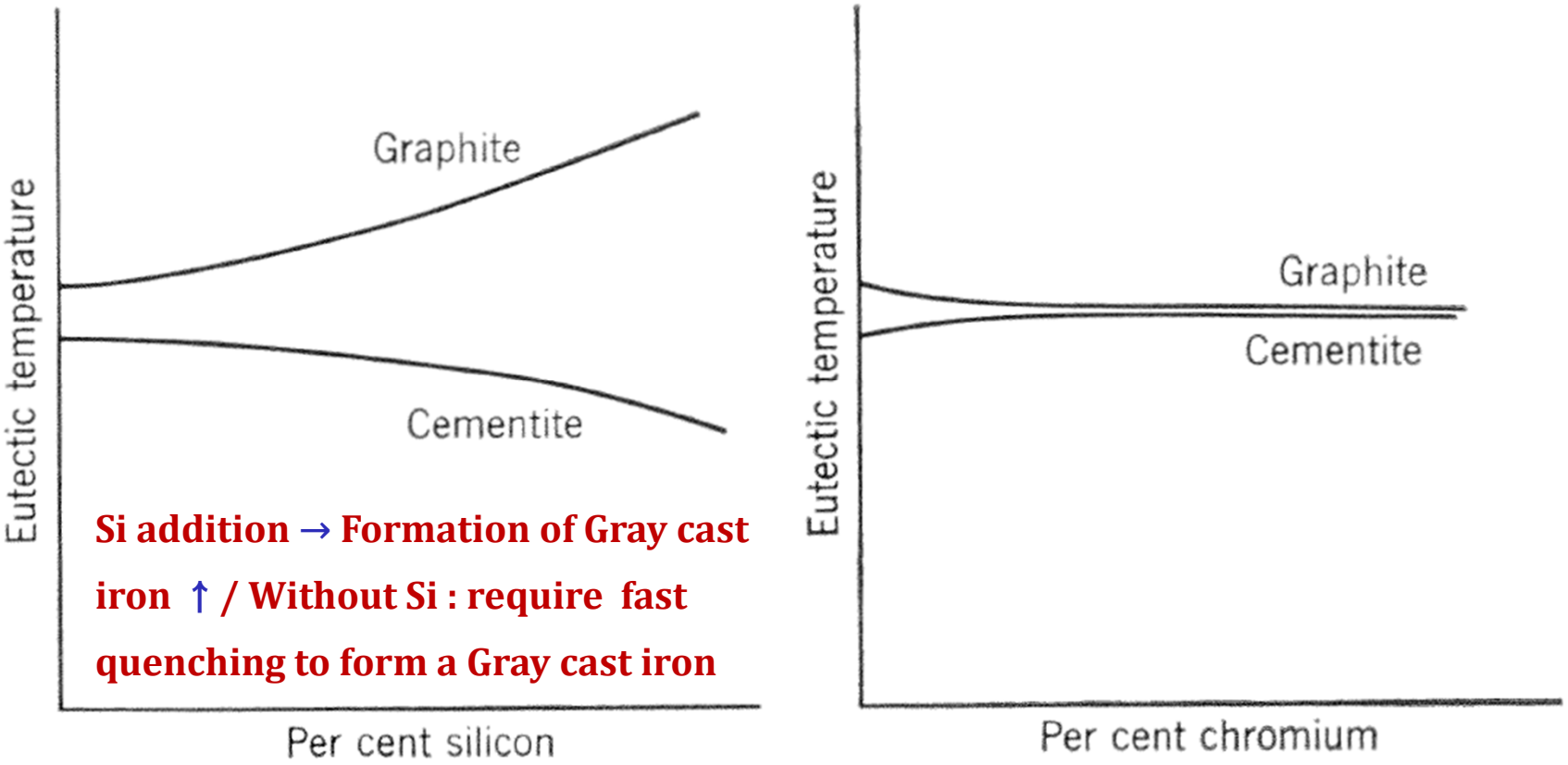

Fig. 6.36. Effect of third component on the eutectic temperatures (schematic). (a) Silicon type, (b) chromium type.

* Graphite morphology

2D: separated flake shape

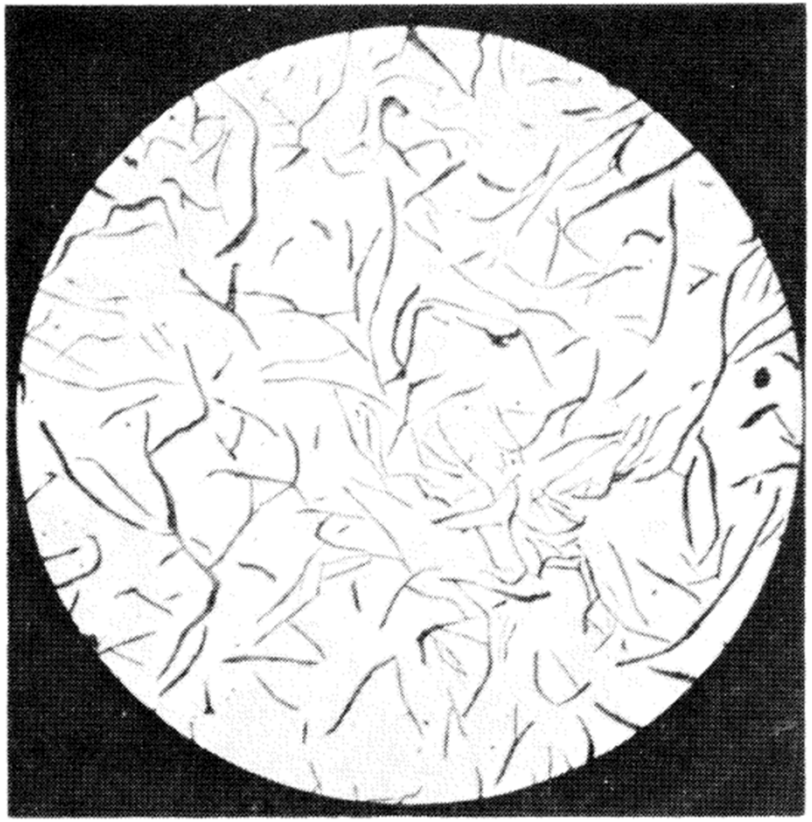

(a)

Fig. 6.37. Graphite in cast iron. (a) Nodular,

3D: Continuous flake shape after dissolving out the iron

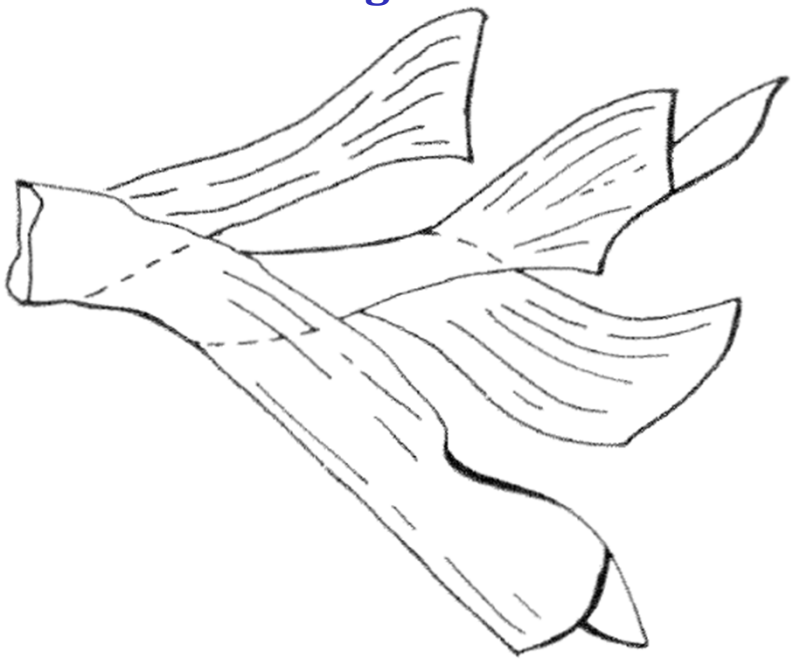

Fig. 6.38. Continuous graphite flake (schematic).

- Spheroidal graphite: Similar to the Si shape control method used for Al-Si for improving mechanical properties, a small amount of Cerium was added to gray cast iron

Continuous flake → formation of discrete spherulet

* Spherulitic graphite morphology

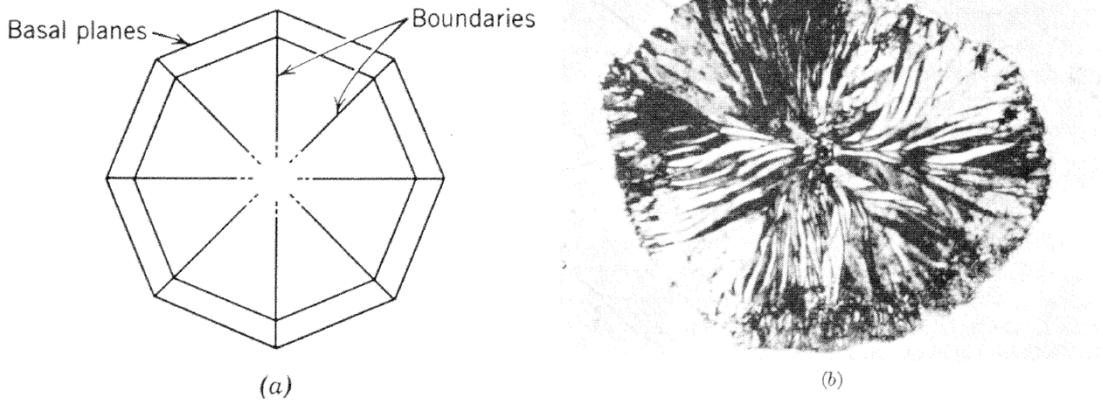

Fig. 6.39. Spherulet of graphite. (a) Schematic, (b) photomicrograph.

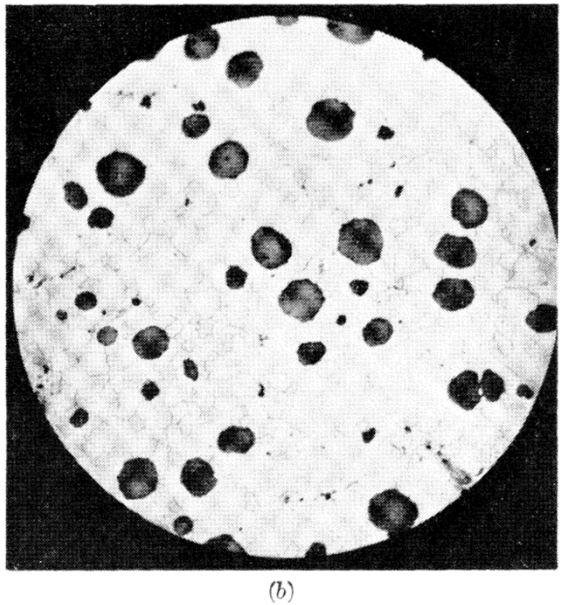

Fig. 6.37. Graphite in cast iron. (b) spherioidal.

- Orientation: everywhere such that the basal plane of the structure (which is the low E surface) faces the melt.→ highly polyhedral structure
- Probably most stable form, energetically (combine a low surface area → spherical shape)
- appears during long-term heat treatment of cast iron (malleableizing) : most stable configuration will be approached.
- Development of Spherulitic form = very low contents of sulfur in Iron melt/ Addition of spherodizing agent (Ce or Mg) → combining with sulfur / Addition of inoculant (Si) → produce graphite rather than cementite

13) Peritectic Solidification

: Occurs when two liquidus lines intersect with a slope of the same direction

*** Eutectic reaction: One liquid is balanced with two solid phases at a fixed composition and temperature**

*** Peritectic reaction $l+\alpha \rightarrow \beta$**

→ complete equilibrium

: Only possible under equilibrium solidification conditions.

→ at peritectic temperature

during cooling, Liquid composition P / α composition S

① $C_0 \rightarrow l+\alpha \rightarrow \beta$

② C_1 or C_2 → Primary α or liquid + β

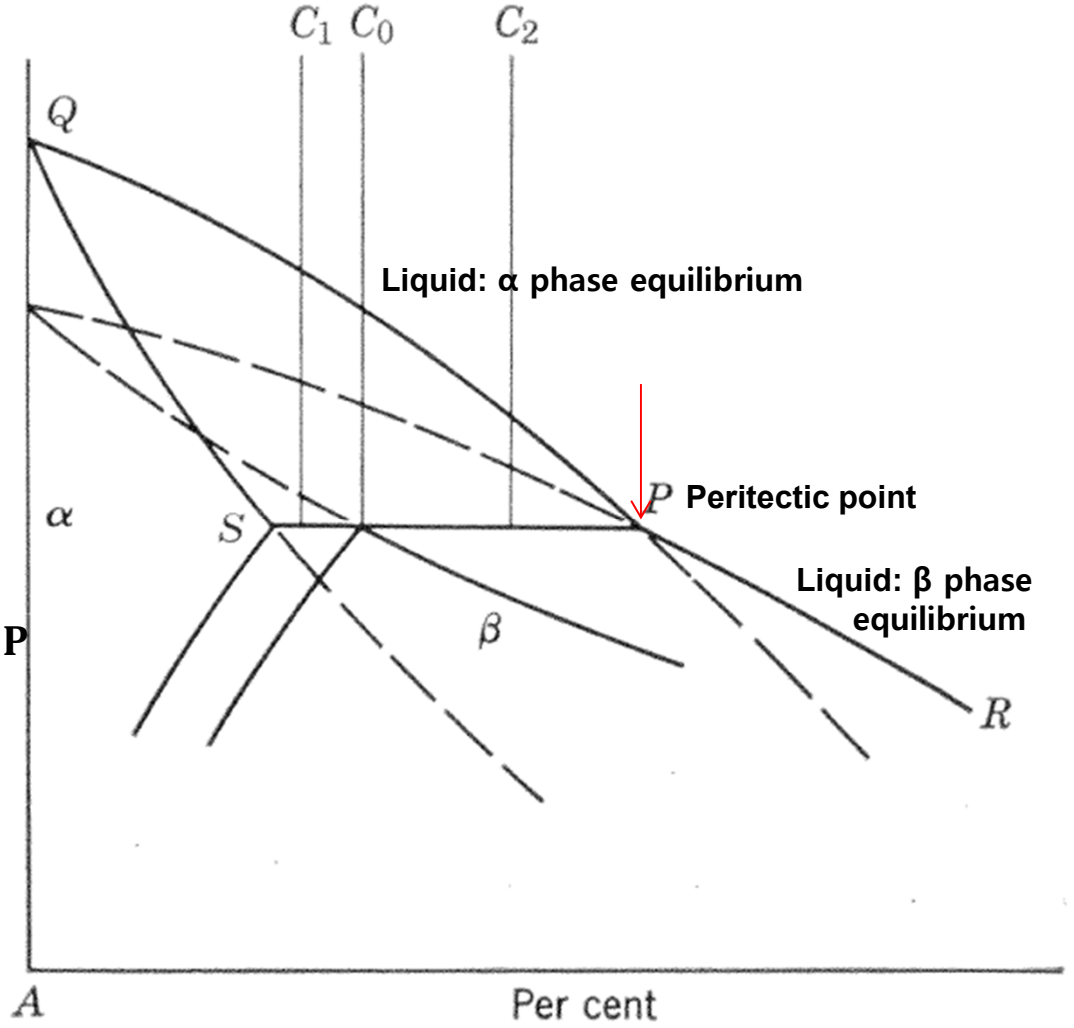

Fig. 6.40. Peritectic system, showing equilibrium phase boundaries —— and nonequilibrium phase boundaries ---.

* L + α → β is a very slow reaction except for the initial state, because liquid and α are separated by β

→ Diffusion must always occur for reaction to continue

→ When β is thickened (diffusion distance increases), the reaction slows down.

* Solidification and microstructure that develop as a result of the peritectic reaction

→ Unlike eutectic, peritectic does not grow into lamellar structure.

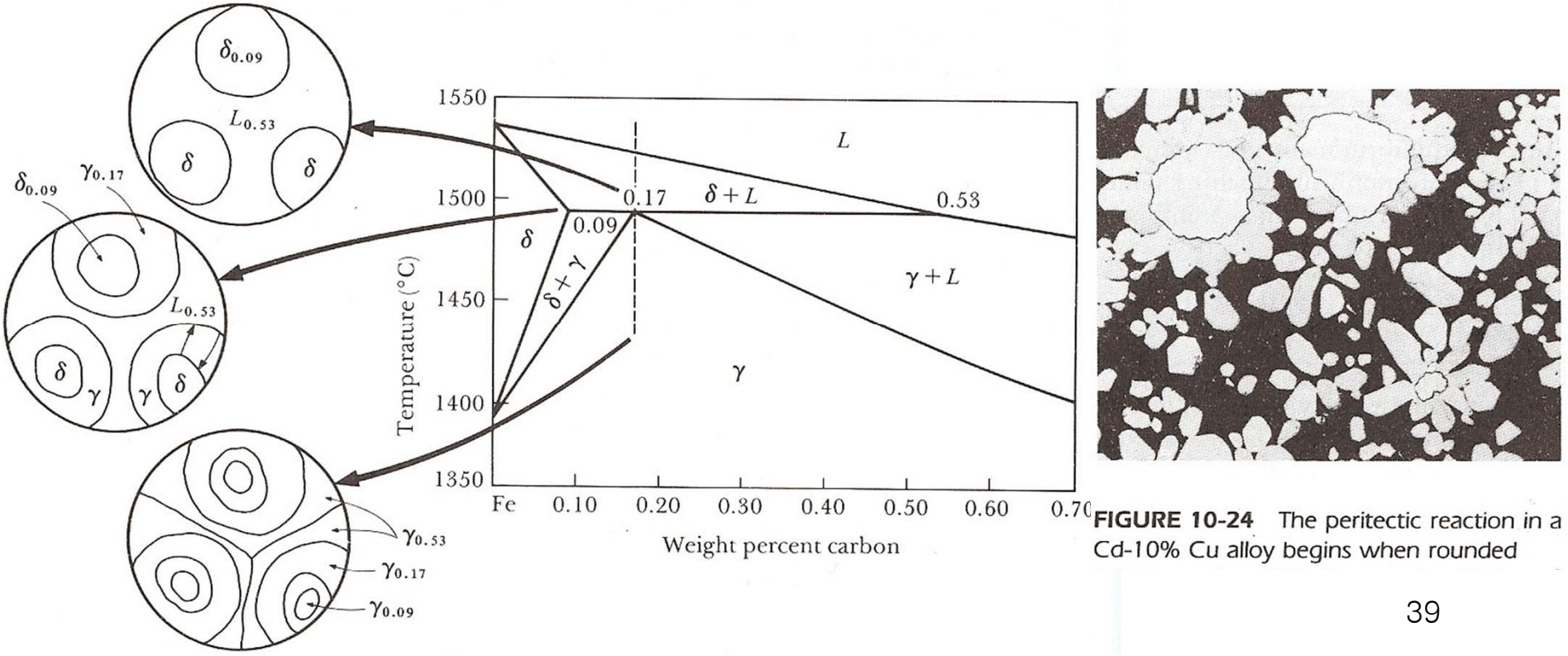

FIGURE 10-24 The peritectic reaction in a Cd-10% Cu alloy begins when rounded

* L + α → β is a very slow reaction except for the initial state, because liquid and α are separated by β

* Uhlmann and Chadwick: Ag-Zn peritectic experiment

→ Peritectic melt of composition M_1 :

→ below T_3, β matrix + massive α dendrites

→ Dendrite α phase remaining at wide composition range and growth speed

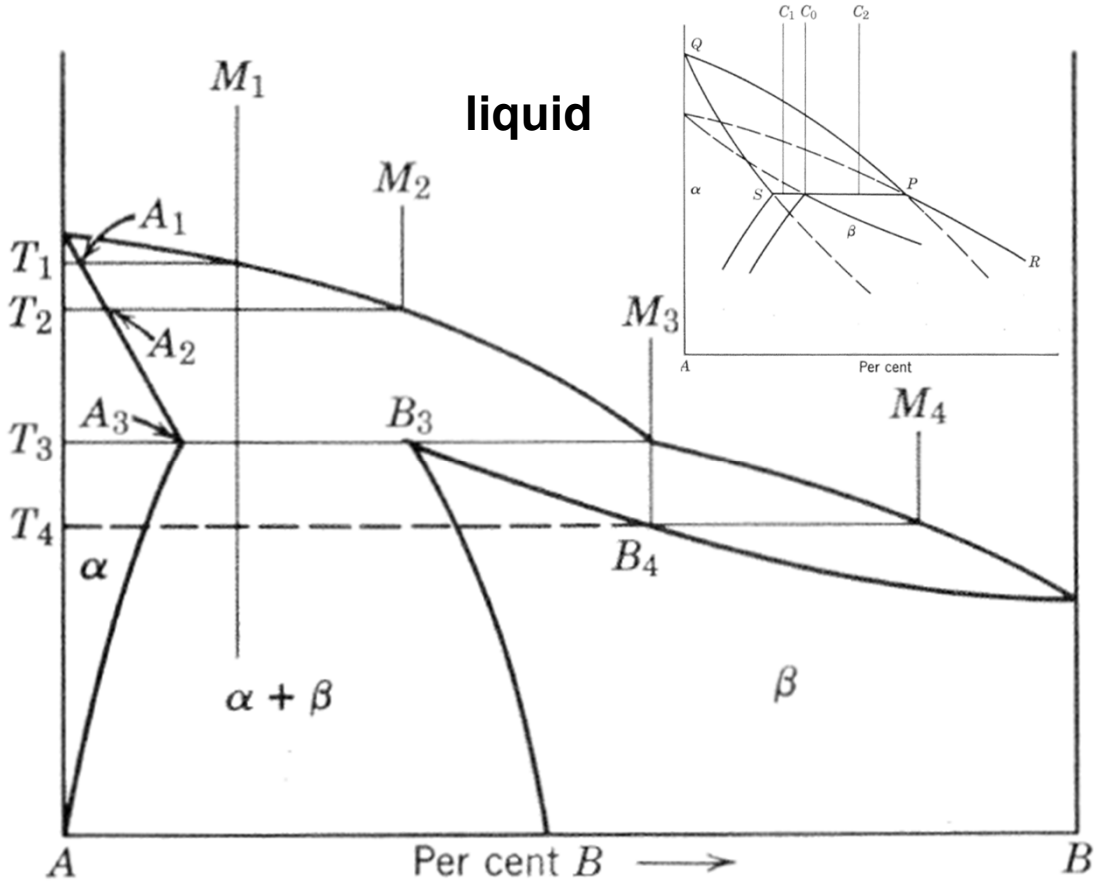

Fig. 6.41. Peritectic system.

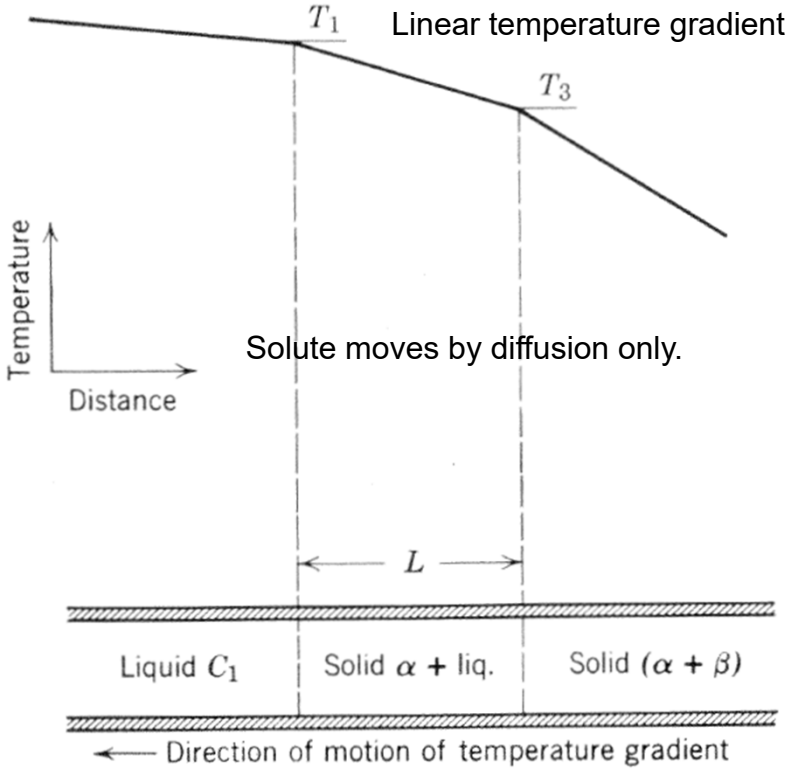

Fig. 6.42. Solidification of a peritectic in a temperature gradient.

*** L + α → β is a very slow reaction except for the initial state, because liquid and α are separated by β**

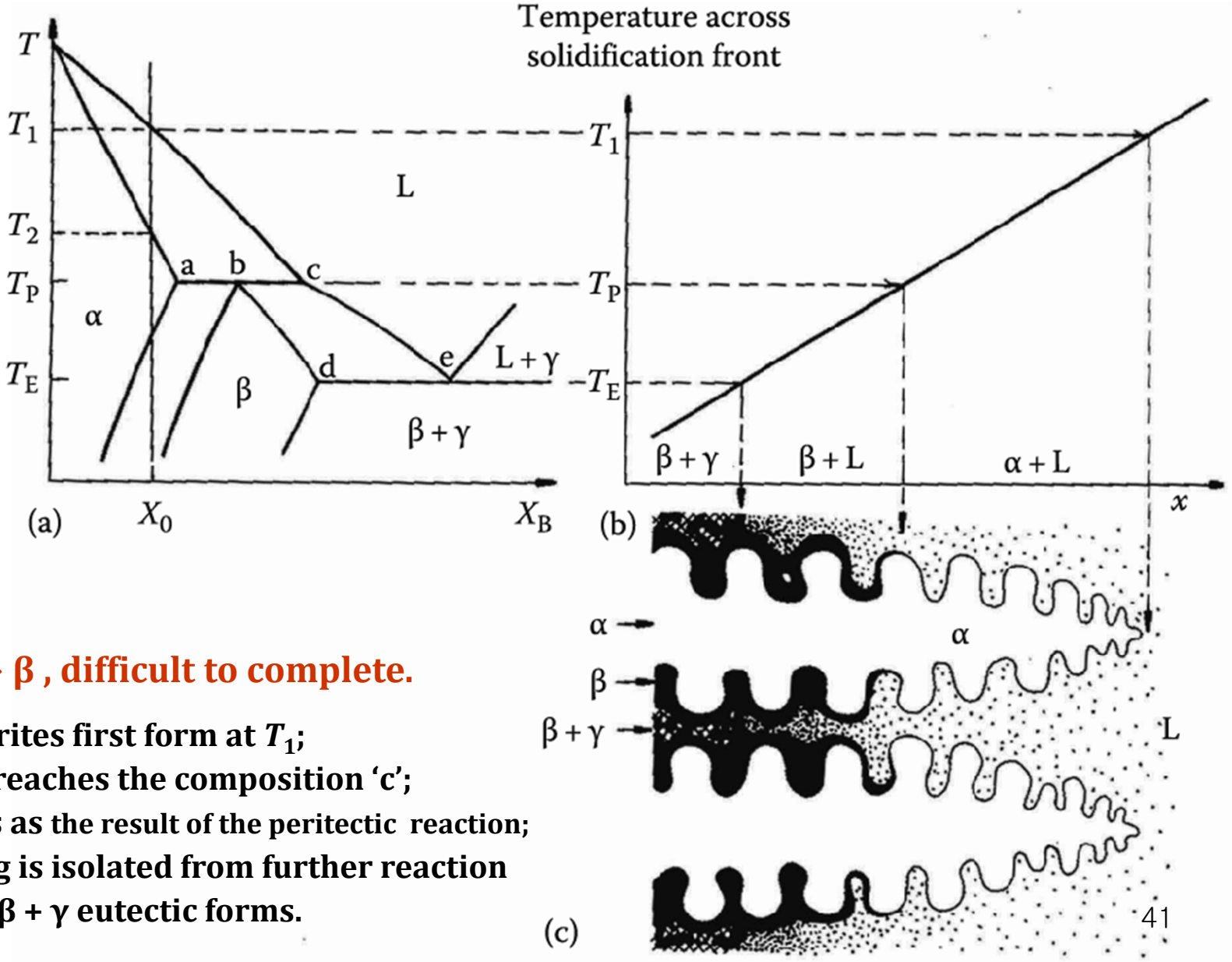

- **L + α → β , difficult to complete.**

- **α dendrites first form at T_1;**
  Liquid reaches the composition 'c';
  β forms as the result of the peritectic reaction;
  α coring is isolated from further reaction
  finally β + γ eutectic forms.

6.4. Solidification in the presence of a solid phase

- If liquid metals contain particles of solid in suspension; their distribution in the resulting solid influence dislocation content (page 58) or directly the mechanical properties. → relevant to consider the interaction btw an advancing S-L interface and solid particles in the liquid.

- **Three factors that may influence the final location of a particle**

(1) If "density" of particle is different from that of liquid: particle ~ float or sink

- Particle behavior dominated by its buoyancy (positive or negative)

: depends on density difference and the size and shape of the particle

Ex) A particle (sufficiently small) will remain in suspension indefinately as a result of its Brownian motion even if its density is substantially different from that of the liquid. The actual size for effective Brownian motion depends on the density difference, but in general is of the order of 0.1 μm.

*** Rate (B) of ascent or descent for large particle: by Stokes formula**

① **Sphere,**

$$B = \frac{2}{9}\frac{gr^2(D_1 - D_2)}{\eta}$$

r = 1 μm particle/ Density difference, Δd=2 gm/cm^3

→ B = order of 10^{-4} cm/sec

② **For non-spherical shapes, the value of B is smaller because a particle always tends to orient itself so that it offers the max. resistance to its own motion through the liquid.**

(2) Second factor = "Fluid motion"_ generated as the liquid enters the mold

large enough to maintain in suspension particles that would sink or float in a stationary liquid

: persist for a considerable time before it gives way to convection caused by thermal and composition gradient.

(3) Third factor = "Interface speed" : Although there may be some vertical separation due to flotation or sedimentation, and some radial separation resulting from centrifugal forces, the smaller particles may remain suspended with a nearly random distribution.

→ ∴ The final distribution in the solid depends on whether a particle is "trapped" in situ by the advancing S-L interface or whether it is pushed ahead as the interface moves forward.

→ Experiments (Uhlmann & Chalmers) : some nonmetallic system

1) Fast rate of advancing interface (>critical velocity, CV) : particles are "trapped".

(ex) MgO particle in Orthoterphenyl: critical velocity_about 0.5 um/sec

2) Although the CV varies from 0 to 2.5 μm/sec depending on the type of matrix and particle, no definitive composition and crystallographic effects have been identified.

3) (surprising feature) Critical velocity is independent of particle size change.

→ This CV (up to 2.5 μm / sec or 1 cm / hr) is very slow compared to most practical solidification or crystal growing processes and it is very unlikely that dispersed particles can change the solidification process if they have a similar CV in metal and semiconductor.

* Solidification of a liquid in a porous solid

: Little attention has been paid to the solidification of a liquid metal that is contained in interconnected channels in a porous solid that is chemically inert to the solidifiying liquid.

(ex) Nonmetallic system: Freezing of water in Soil → Induce "frost heaving load"

- These forces arise not because water expands on freezing, but because a water layer persists between ice and solid particles. As ice is formed, more water is drawn into the region of contact to replace what has frozen. This water in turn stars to freeze, causing more water to be "sucked" in, and forcing the existing ice away from the soil particle.

→ Preference, energetically, for the existence of a liquid layer btw the two solids

→ *A liquid metal contained in a porous matrix may have a similar surface E relationship*, in which case very large forces could be exerted, tending to disrupt the matrix.

7. Macroscopic Heat Flow and Fluid Flow

7.1. General considerations

*** Products made by solidification process should fulfill two major requirements.**

(1) Geometrical consideration

: external shape _satisfactory
& internal voids_within permissible limits of size, shape, and location

(2) Structural consideration

: whether the desired property is achieved _determined by its structure

Before considering in detail the interaction of the various factors that control the structure and the geometry, however, it is necessary to review the problems associated with ①the flow of metal into a mold and ②the extraction of heat from the metal.

→ These two problems are by no means independent of each other, because loss of heat by the metal while it is flowing into a mold is often a limiting process.

7. Macroscopic Heat Flow and Fluid Flow

7.2. Fluid Flow

*** The ability of a molten metal to flow =**

(1) poured from a container in which it was melted into a mold in which it is to solidify.

: effect of the macroscopic geometry of the casting (Chapter 7)

(2) Relative motion of different parts of the liquid can occur while it is solidifying.

: its implications in relation to the structure of the solidified metal (Chapter 8)

1) Viscosity of liquid metal

liquid metal : Flow rate depends on the force = shear rate is proportional to the shear stress

ex) Flow rate of a liquid through a tube depends on the pressure difference btw the ends of the tube (ΔP), on its length (l), and on the radius of the tube (r).

The quantity flowing per unit time, Q

$$Q = \frac{\pi r^4}{8\mu} \cdot \frac{P_1 - P_2}{l}$$

μ = viscosity

→ The formula given above applies only in cases in which the flow is of the "stream-line" or laminar type, which occurs at relatively slow rates of flow.

Fragility

- **Fragility ~ ability of the liquid to withstand changes in medium range order with temp.**
  ~ extensively use to figure out liquid dynamics and glass properties corresponding to "frozen" liquid state

< Classification of glass >

***Strong network glass* : Arrhenius behavior**

$$\eta = \eta_0 \exp[\frac{E_a}{RT}]$$

***Fragile network glass* : Vogel-Fulcher relation**

$$\eta = \eta_0 \exp[\frac{B}{T - T_0}]$$

< Quantification of Fragility >

$$m = \left.\frac{d \log \eta(T)}{d(T_{g,n}/T)}\right|_{T=T_{g,n}} = \left.\frac{d \log \tau(T)}{d(T_g/T)}\right|_{T=T_g}$$

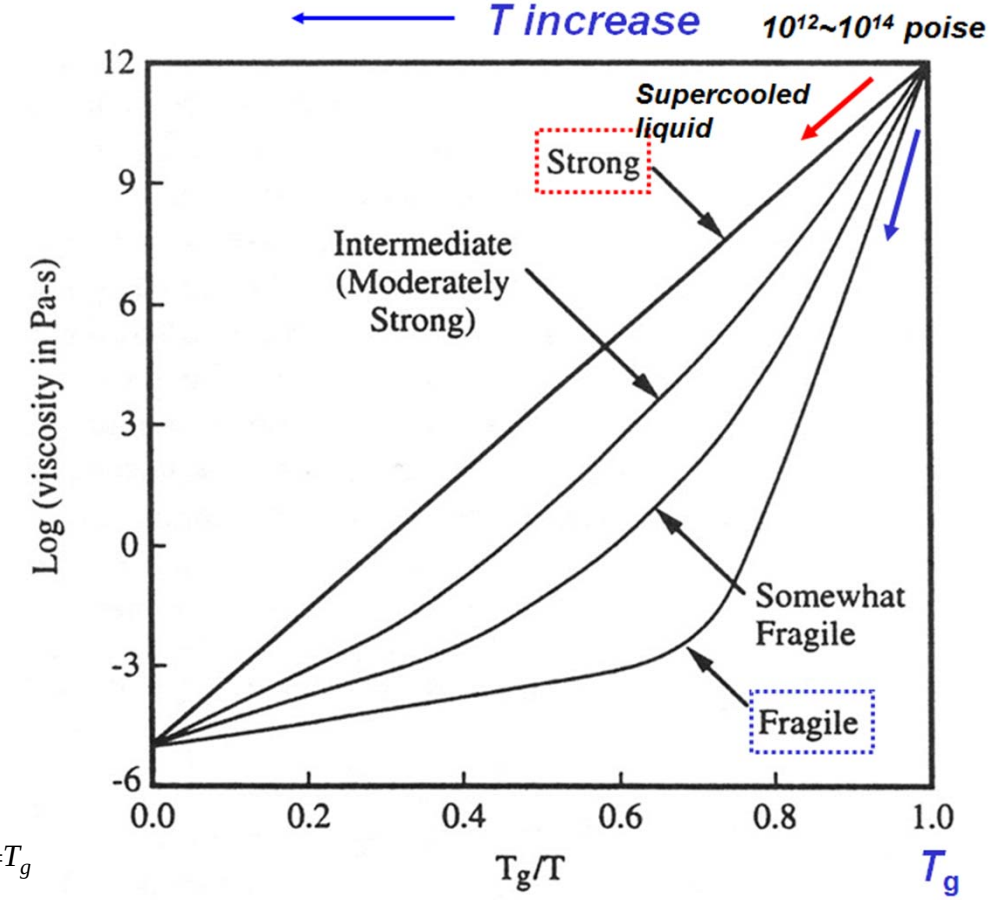

Slope of the logarithm of viscosity, η (or structural relaxation time, τ) at T_g

Mold Filling

Bernouli's Equation:

$$p/w + Z + q^2/2g = \text{constant}$$

(p= pressure w = specific weight q = velocity
g = gravity z = elevation)

Reynold's Number:

$$Re = \gamma v l / \mu$$

γ = density , v = velocity,
μ = viscosity, l = linear dimension

- **Short filling times**
- **Potential Turbulence**

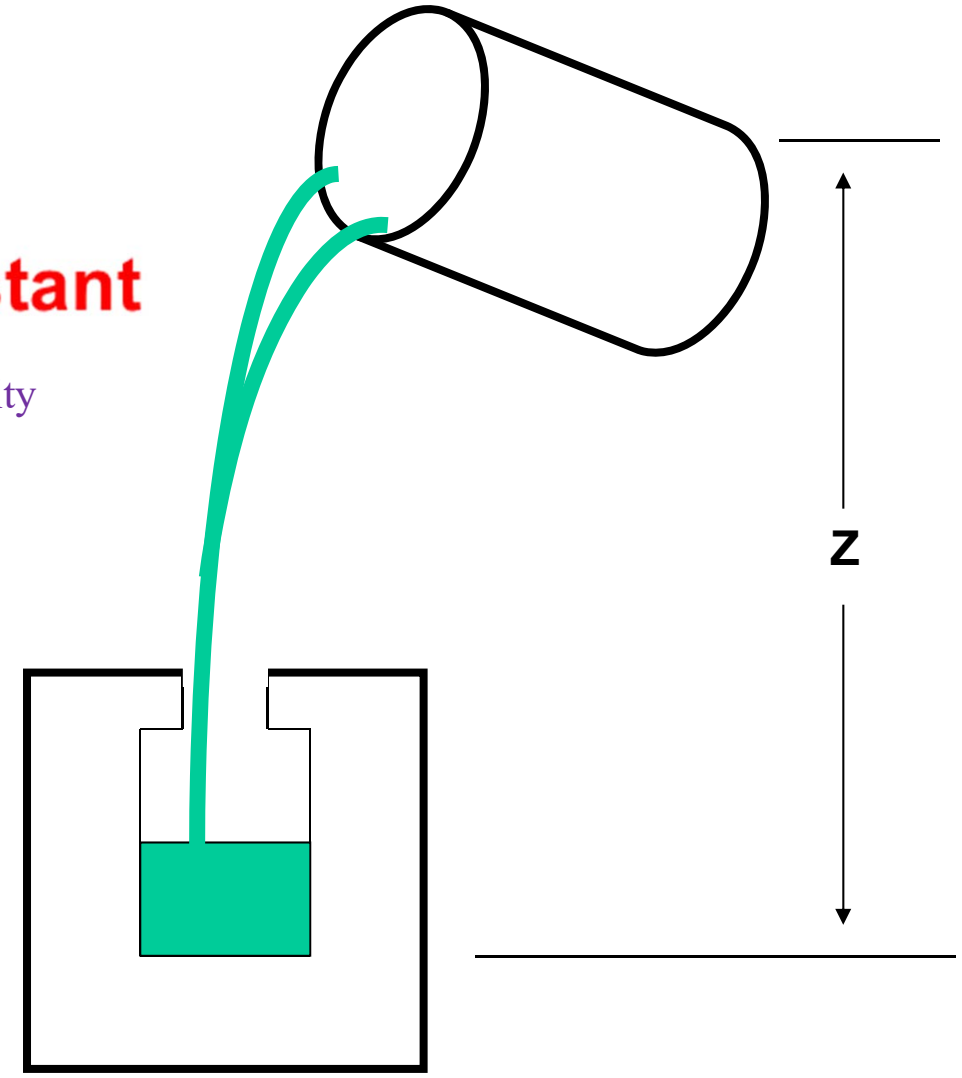

*Bernoulli theorem: Applicable for dynamic behavior of fluid_Fluid Mechanics

By assuming that fluid motion is governed only by pressure and gravity forces, applying Newton's second law, $F = ma$, leads us to the Bernoulli Equation.

For a flowing liquid,

$$p/w + Z + q^2/2g = \text{constant}$$ **along a streamline**

The pressure due to head of liquid

(p= pressure w = specific weight q = velocity g = gravity z = elevation)

In a steady flow, the sum of all forms of energy in a fluid along a streamline is same at all points on that streamline: "principle of conservation of energy"

A streamline is the path of one particle of water. Therefore, at any two points along a streamline, the Bernoulli equation can be applied and, using a set of engineering assumptions, unknown flows and pressures can easily be solved for.

(a) At any two points on a streamline:

$$p_1/w + Z_1 + q_1^2/2g = p_2/w + Z_2 + q_2^2/2g$$

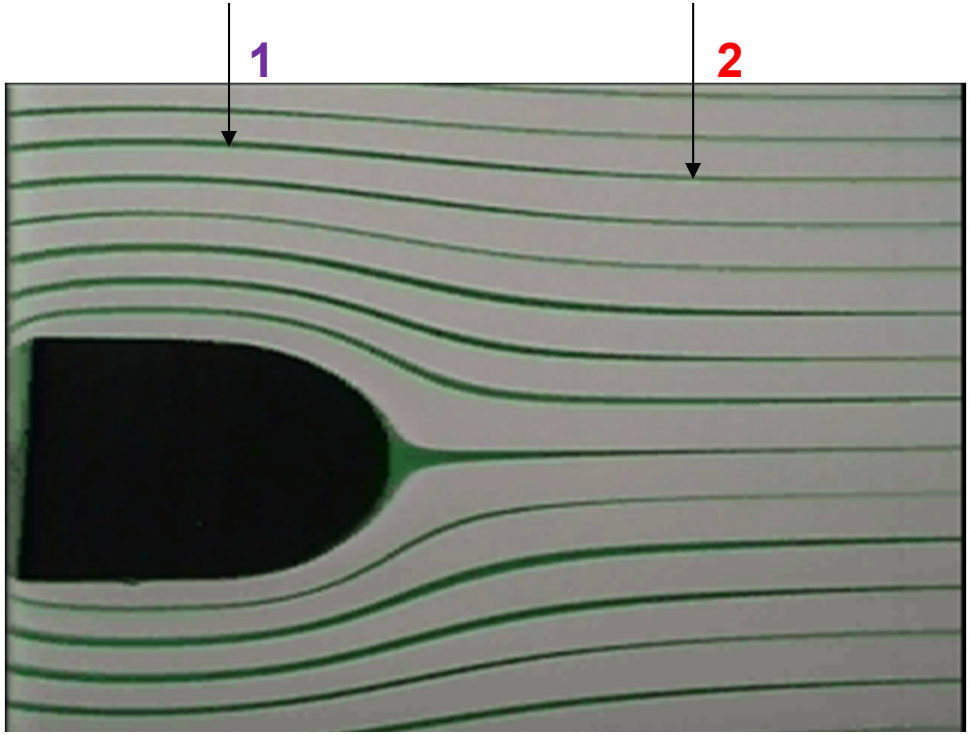

(b) If the fluid velocity, q, of the liquid increases, the pressure of the liquid decreases due to the effect of the passing tube. → ∴ In the case of liquid metals flowing through a complicated mold, the pressure decreases due to the influence of air bubbles entering the liquid phase from the mold wall and flowing together. These air bubbles cause internal void formation in casting.

Mold Filling

Bernouli's Equation (incompressible flow):

$$p/w + Z + q^2/2g = \text{constant}$$

(p= pressure w = specific weight q = velocity
g = gravity z = elevation)

principle of conservation of energy

Reynold's Number:

$$\mathrm{Re} = \gamma v l / \mu$$

γ = density , v = velocity,
μ = viscosity, l = linear dimension

- **Short filling times**
- **Potential Turbulence**

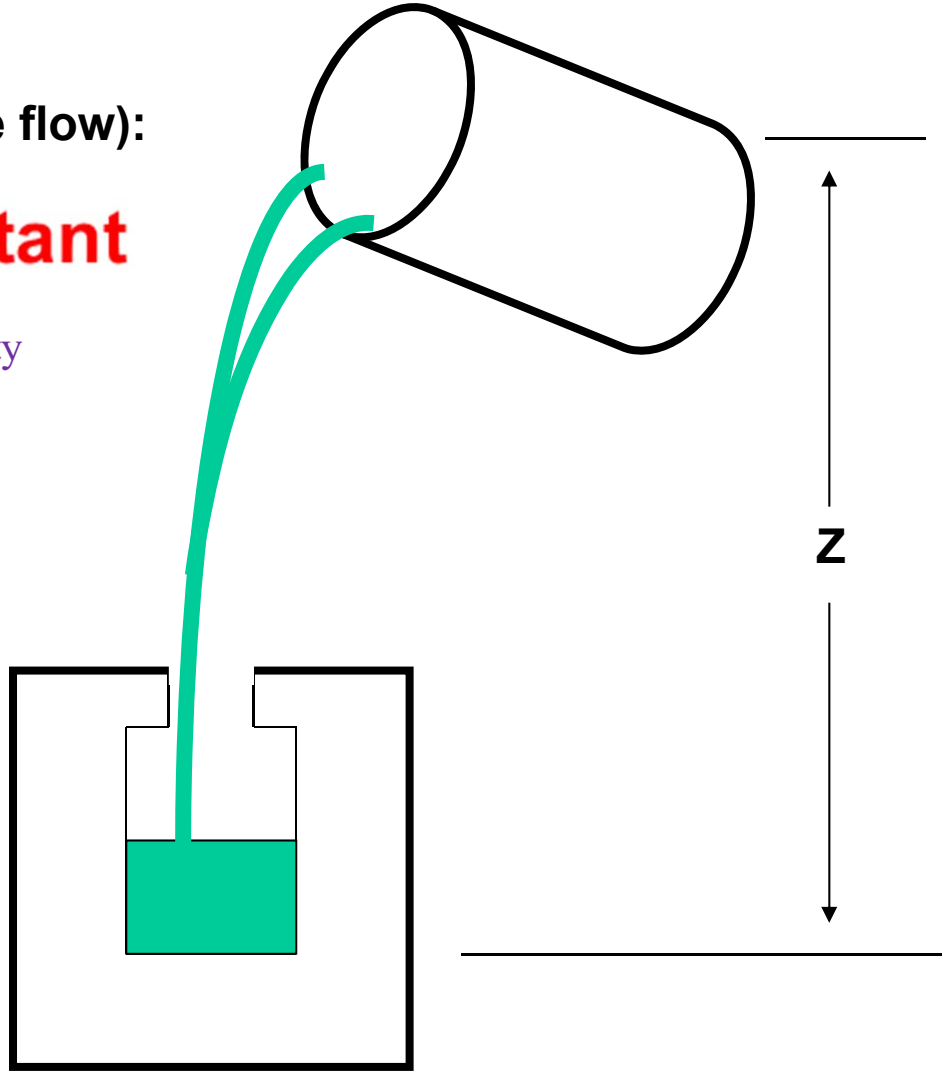

→ To compare "rates of flow" in this case,

Reynolds' number = $\gamma v l / \mu$

γ = density , v = velocity,
μ = viscosity, l = linear dimension

* If the value of Reynolds' number is high (>1400) for a tube leading out of a containing vessel, the flow becomes turbulent and Q drops below the value that would be calculated from the above formula. → Derive the **Kinematic viscosity, μ / γ** from the above equation : Used for calculation of flow rate when pressure difference is caused by flowing liquid → For solidification it is considered more important.

Table 7.1 Values of viscosity and kinematic viscosity of some liquid metals at T_m

Metal	Viscosity (poise)	Kinematic Viscosity (cm^2/sec)
Mercury	0.021	0.0012
Lead	0.028	0.0025
Tin	0.020	0.00231
Copper	0.038	0.0047
Iron	0.040	0.0050
Water (comparison)	0.010	0.010

→ Liquid metals, when they are completely liquid, flow rather more easily than water, and that their viscosity is seldom, if ever, a limiting factor in the process of filling a mold, even through a rather narrow channel.

* Fluidity: The ability of being fluid or free-flowing_distinguished from viscosity

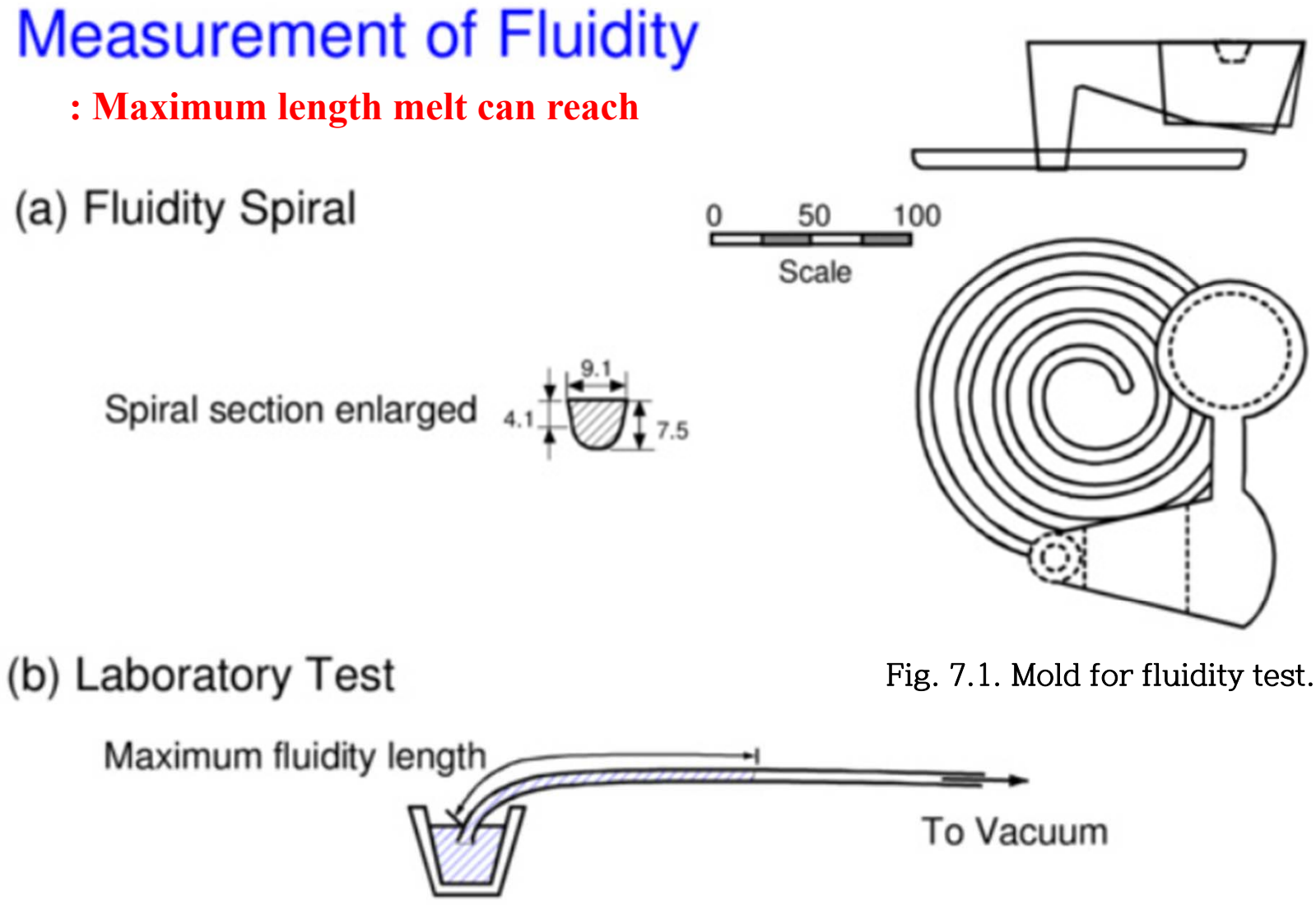

Fig. 7.1. Mold for fluidity test.

New Design of Fluidity Test piece

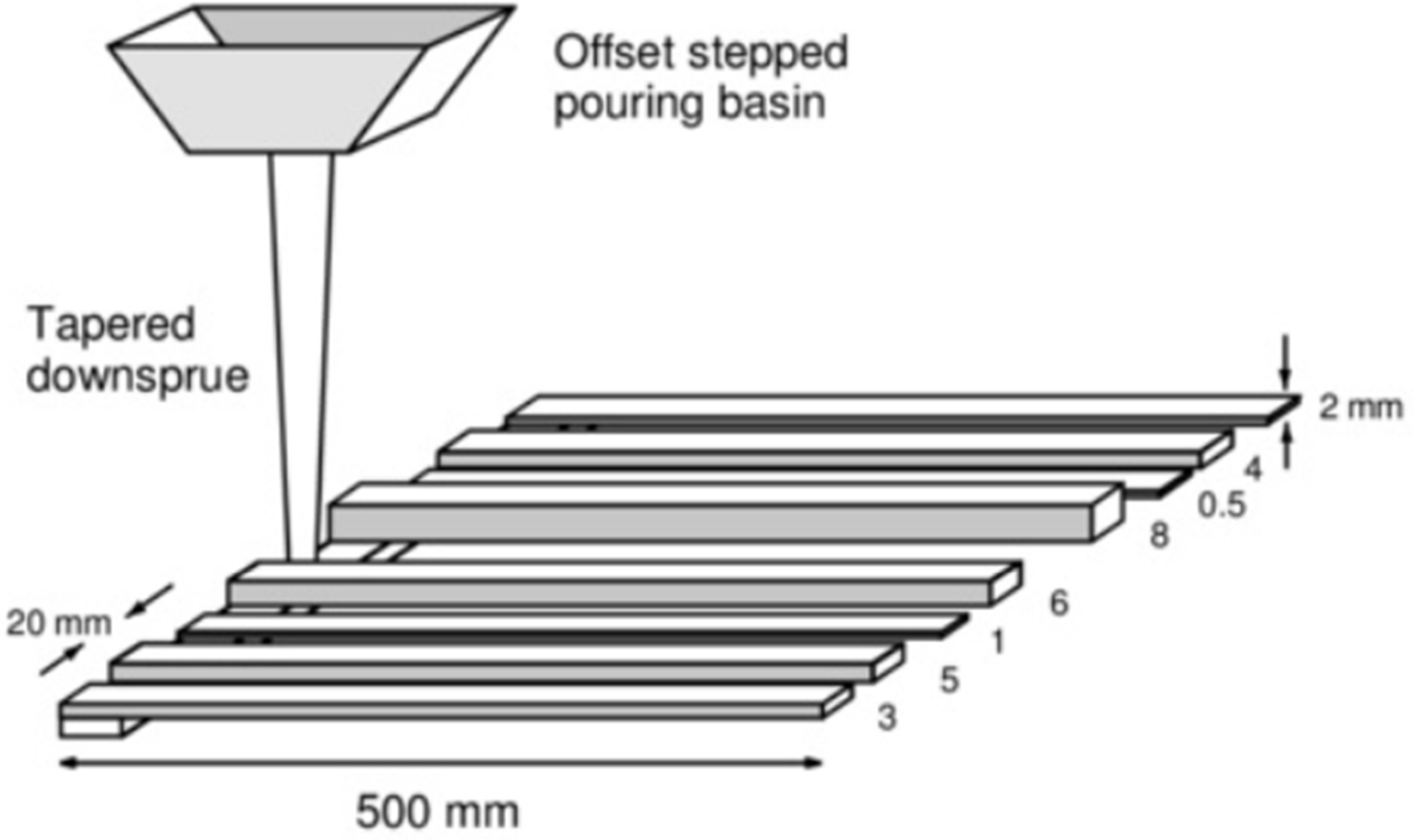

Solidification Rate

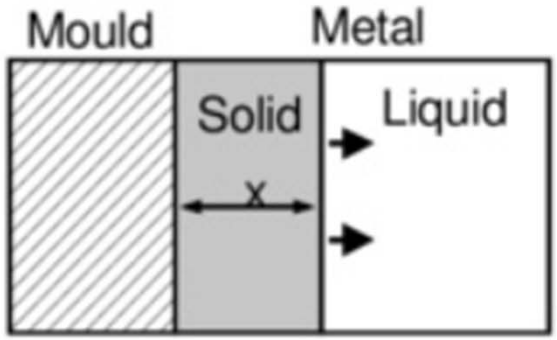

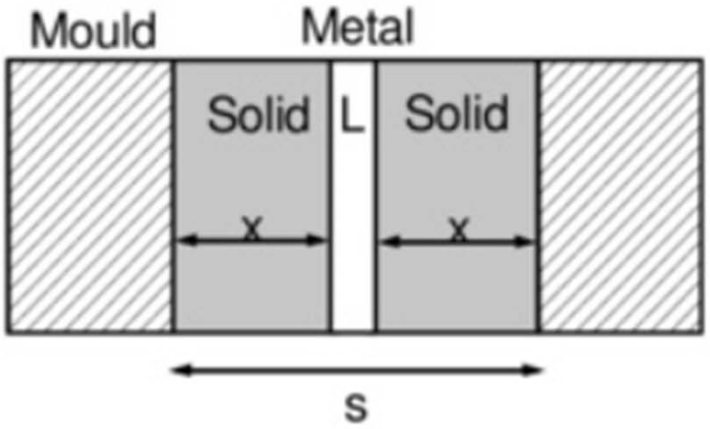

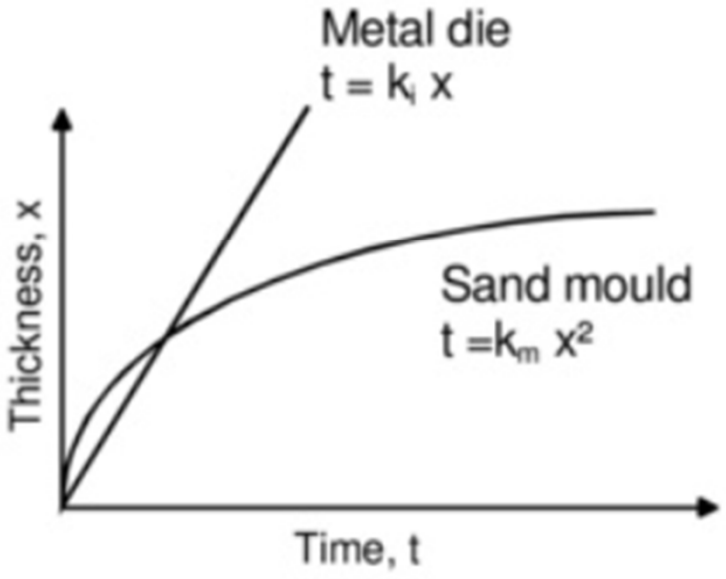

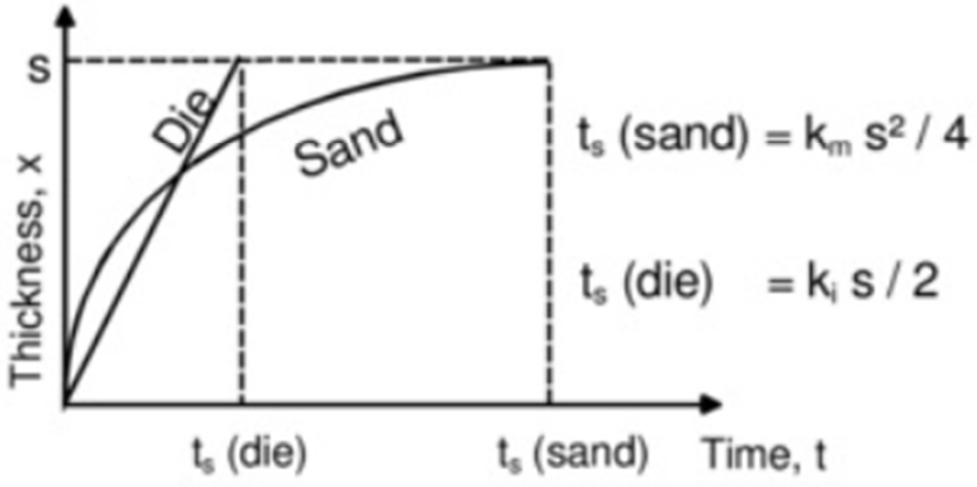

① **Effect of composition**

Fluidity of short Freezing Range Alloys

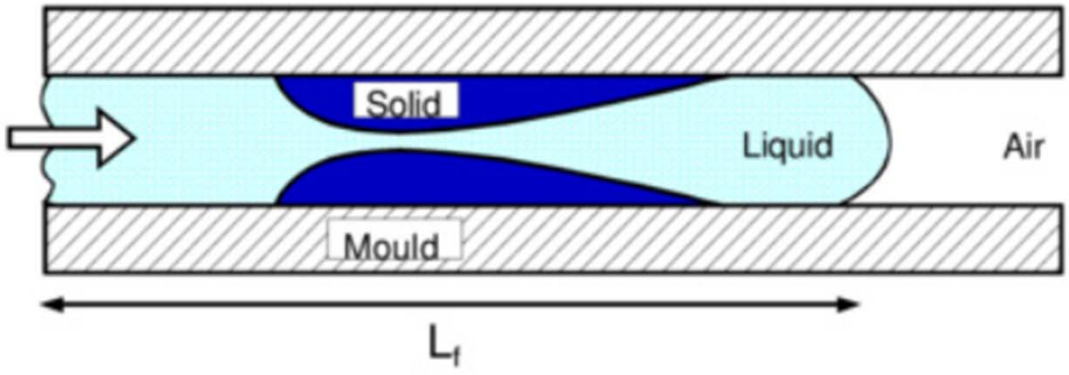

Fluidity Distance $L_f = V\, t_s$ where V = flow velocity
t_s = solidification time

	Sand Mould	Metal Die
t_s	$k_m\, s^2 / 4$	$k_i\, s / 2$
L_f	$V\, k_m\, s^2 / 4$	$V\, k_i\, s / 2$

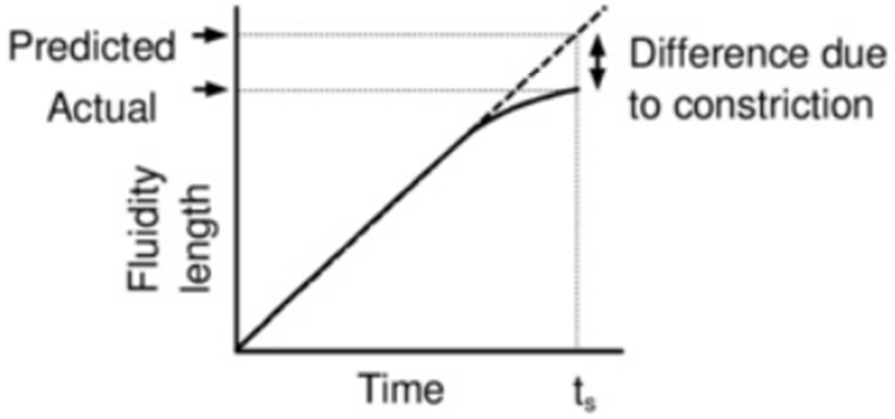

Fluidity of Long Freezing Range Alloys

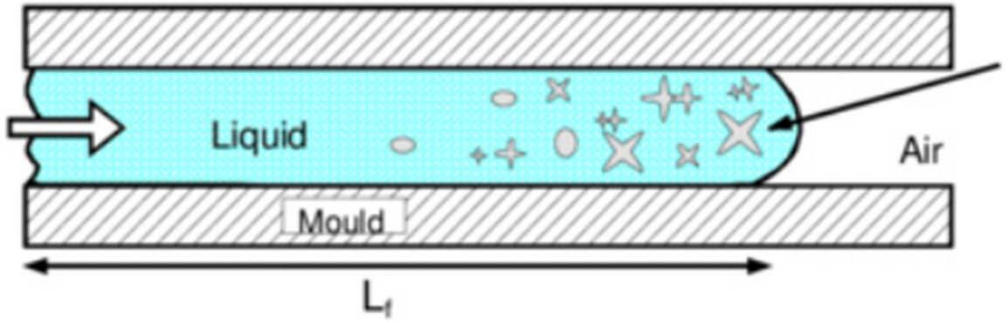

Flow stops when 25 - 50% solid is present,
i.e. when x = S/8 to S/4

	Sand Mould	Metal Die
	$t = k_m x^2$	$t = k_i x$
25% solid	$t = k_m S^2 / 64$	$t = k_i S / 8$
50% solid	$t = k_m S^2 / 16$	$t = k_i S / 4$
Therefore	$L_f = V k_m S^2 / 64$ to $V k_m S^2 / 16$	$V k_i S / 8$ to $V k_i S^2 / 4$
Remember that for short freezing range alloys:	$L_f = V k_m S^2 / 4$	$V k_i S / 2$

Therefore $\frac{\text{Short freezing range}}{\text{long freezing range}}$: 4 - 16 2 - 4

Mapping the Fluidity of Binary Alloys

Fluidity of Al-Sn alloys

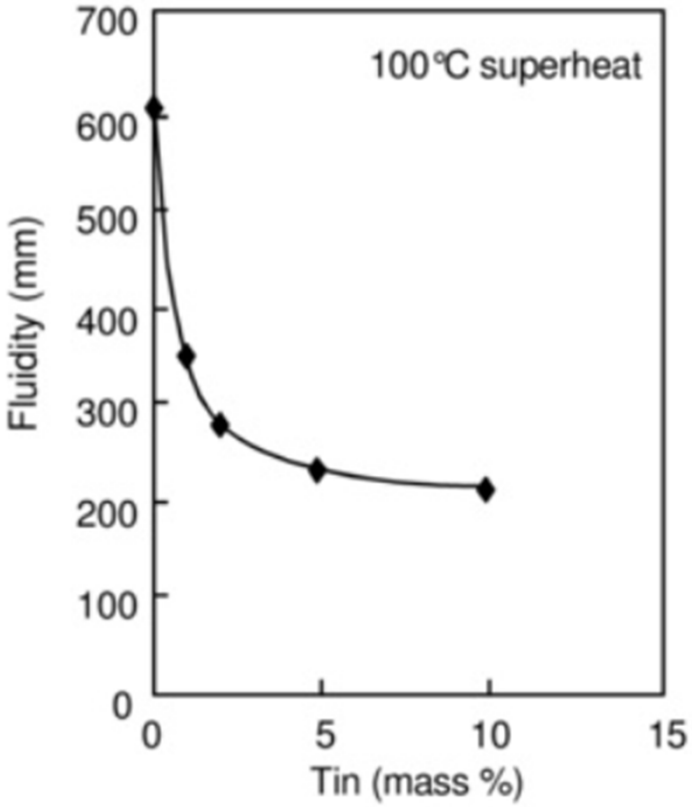

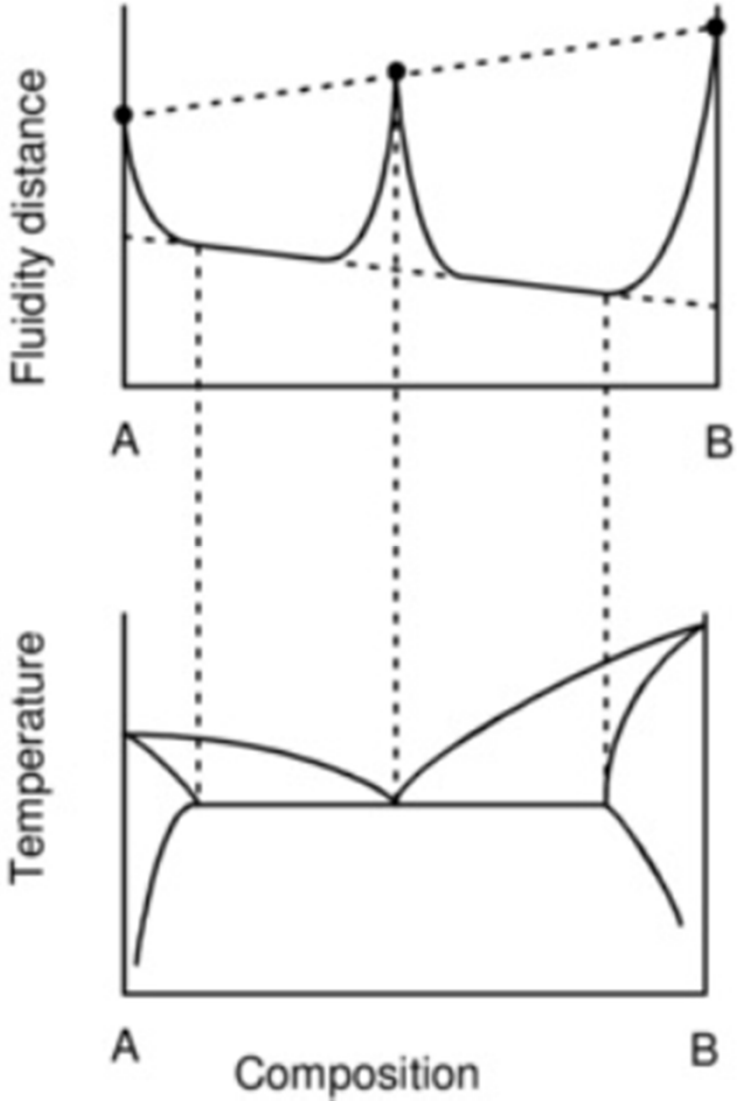

The Fluidity of Al-Si alloys

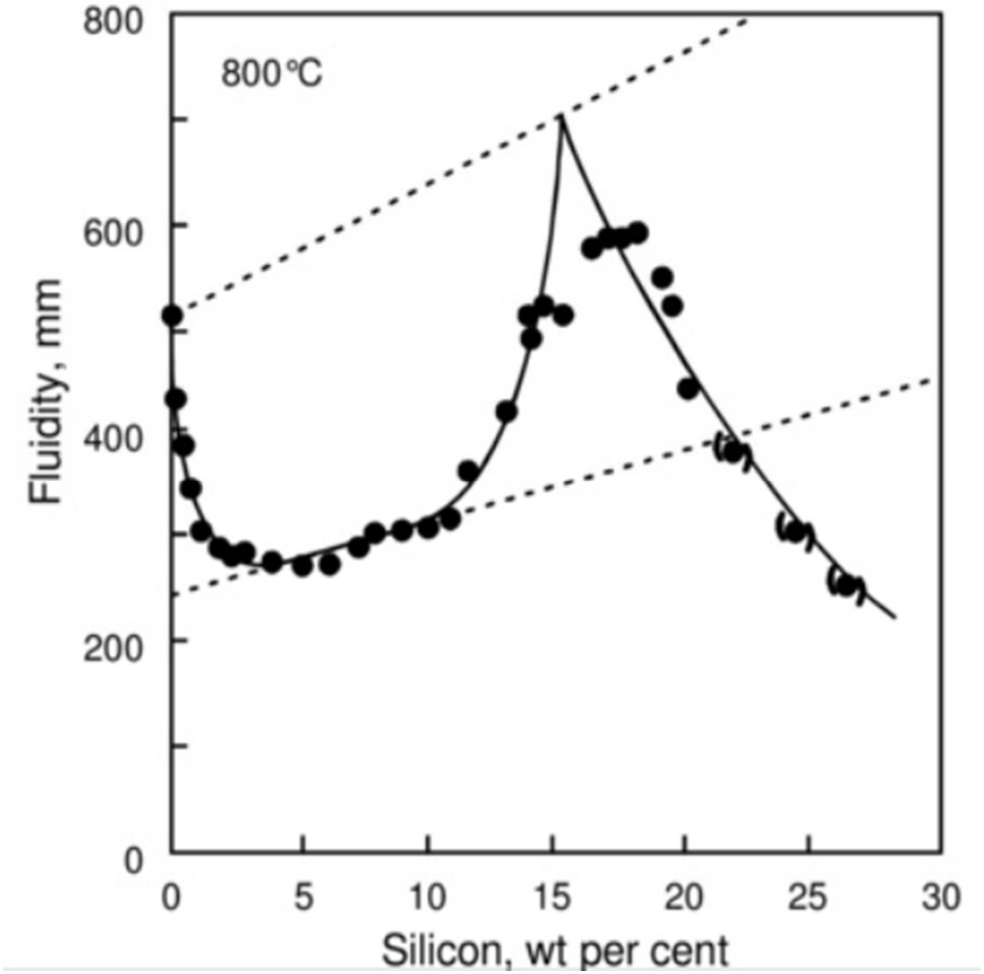

The Fluidity of Al-Zn alloys

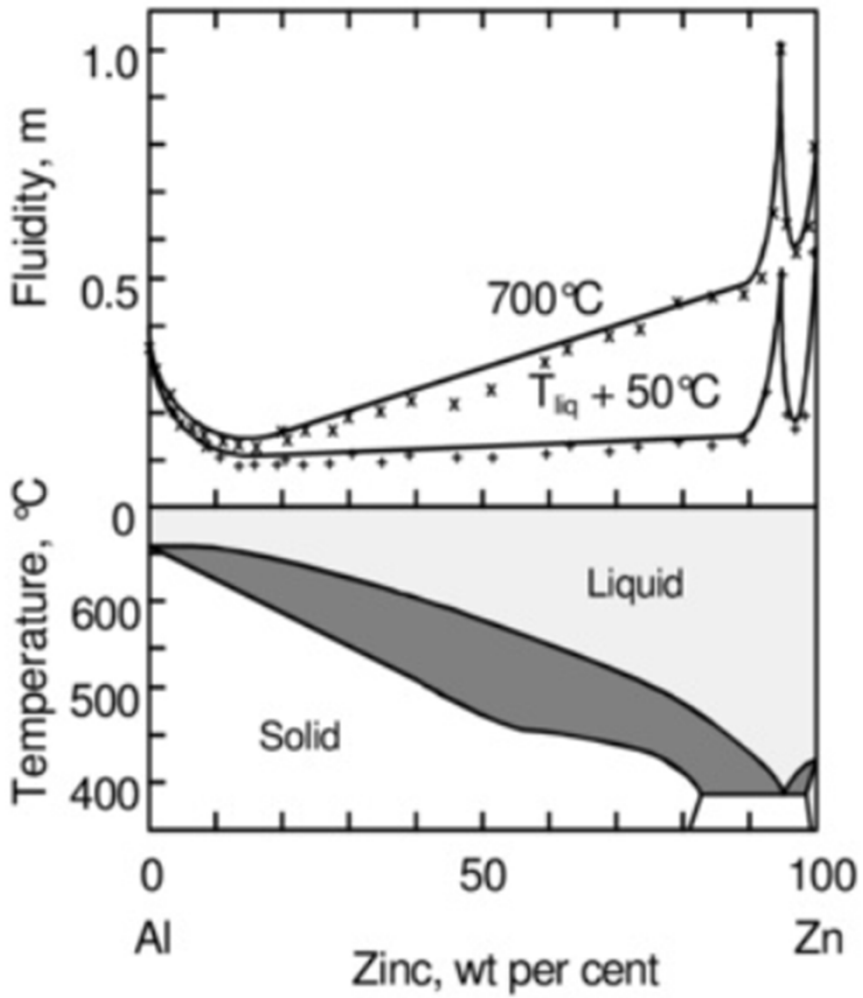

The Fluidity of Al-Cu-Si Alloys

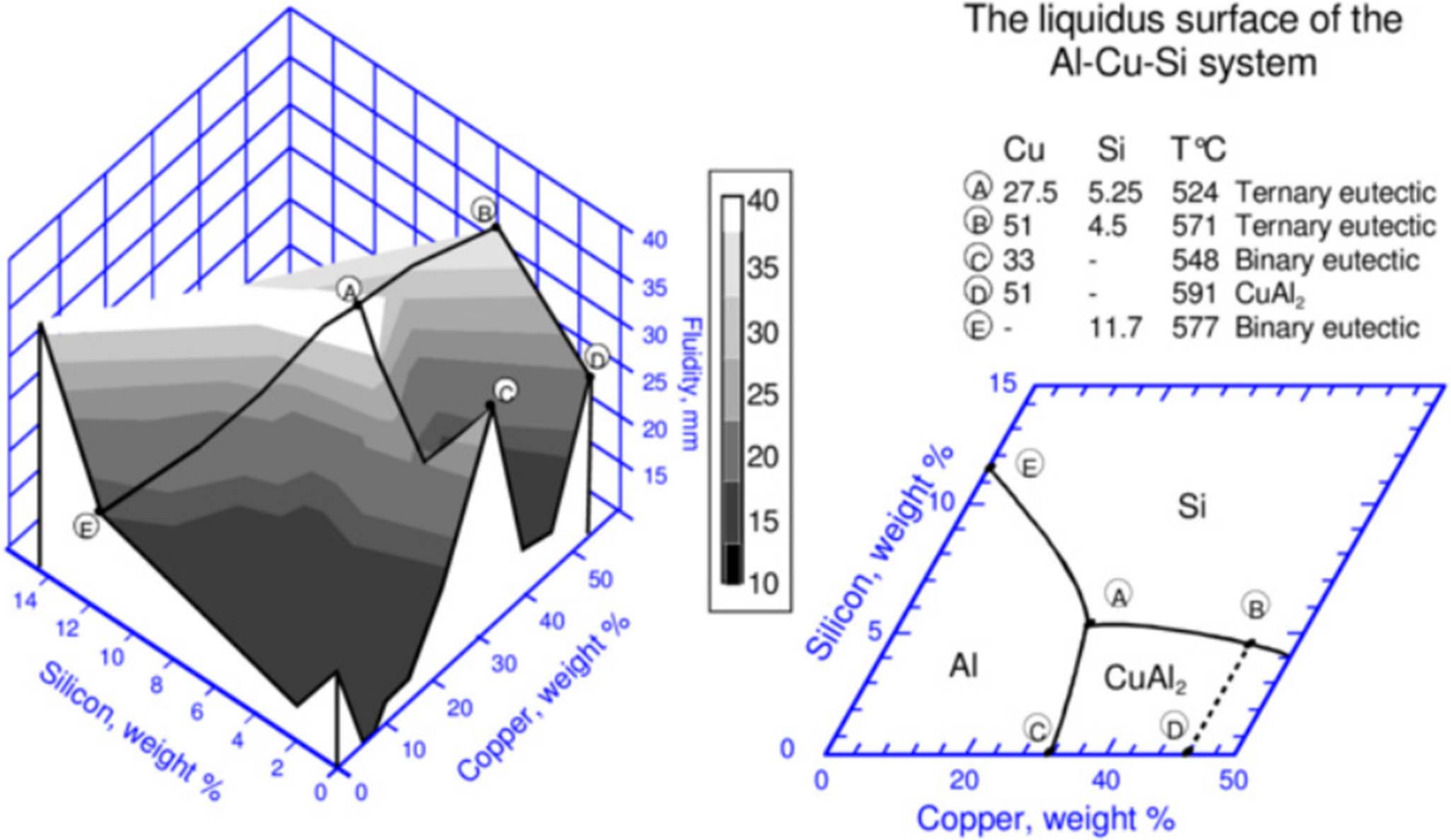

② **Effect of temperature**

The Fluidity of ZA 27 Zinc-Aluminum Alloy

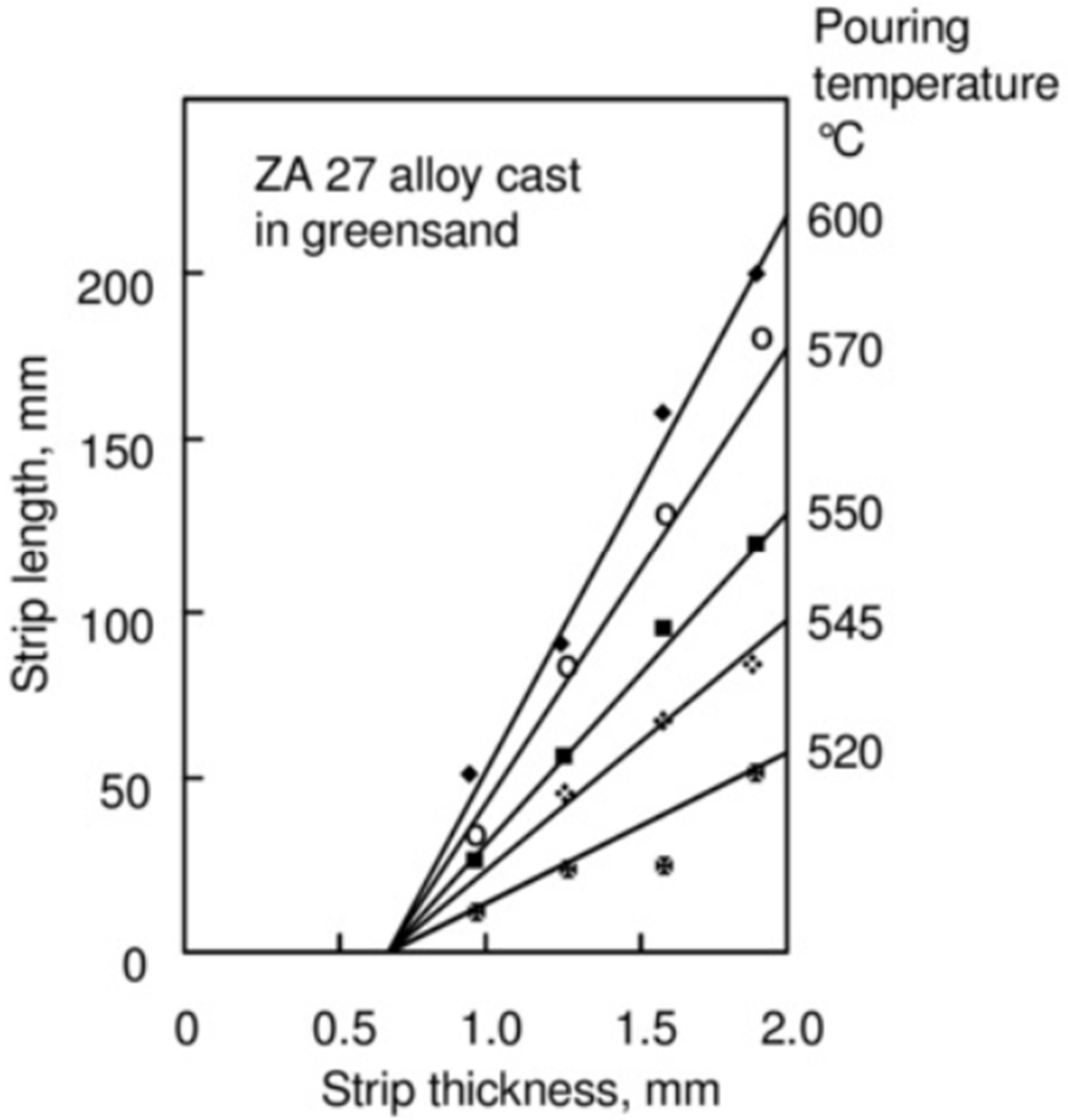

Comparison of Fluidity Measurements

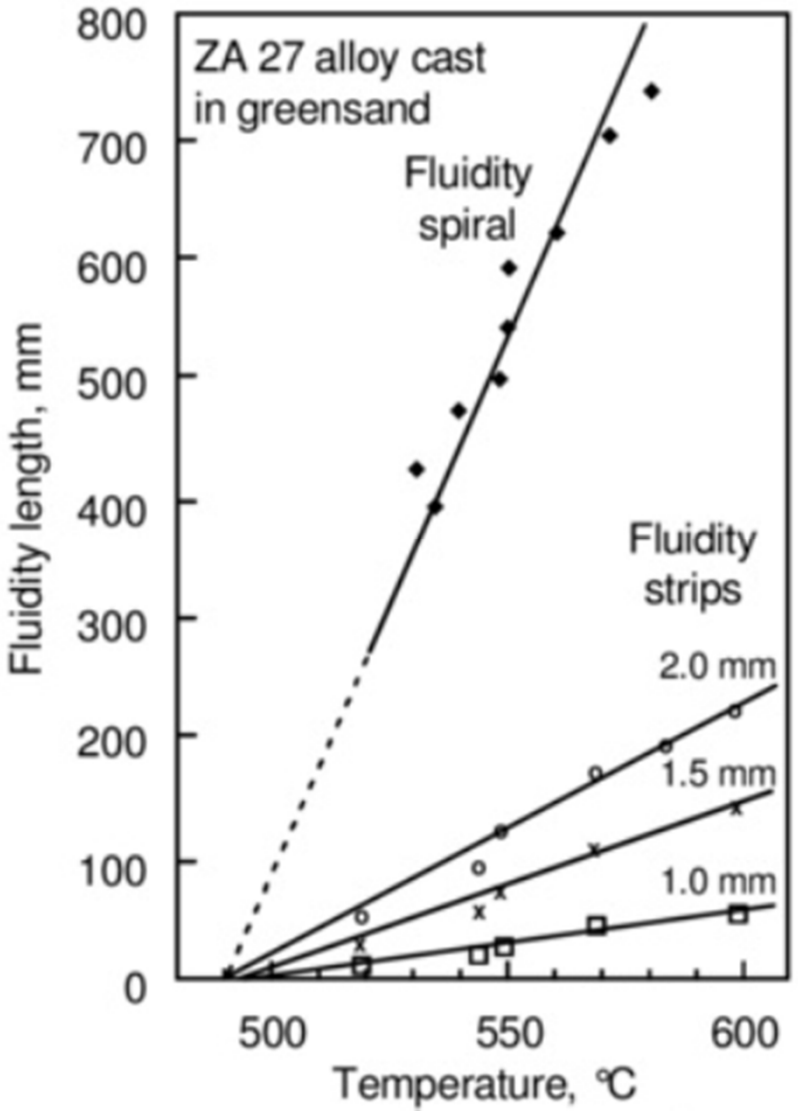

Rationalisation of Fluidity Measurement

- ◆ Spiral lengths / 4.44
- ○ 2.0 effective strip thickness, mm
- × 1.5 strip / 0.572
- □ 1.0 strip / 0.243

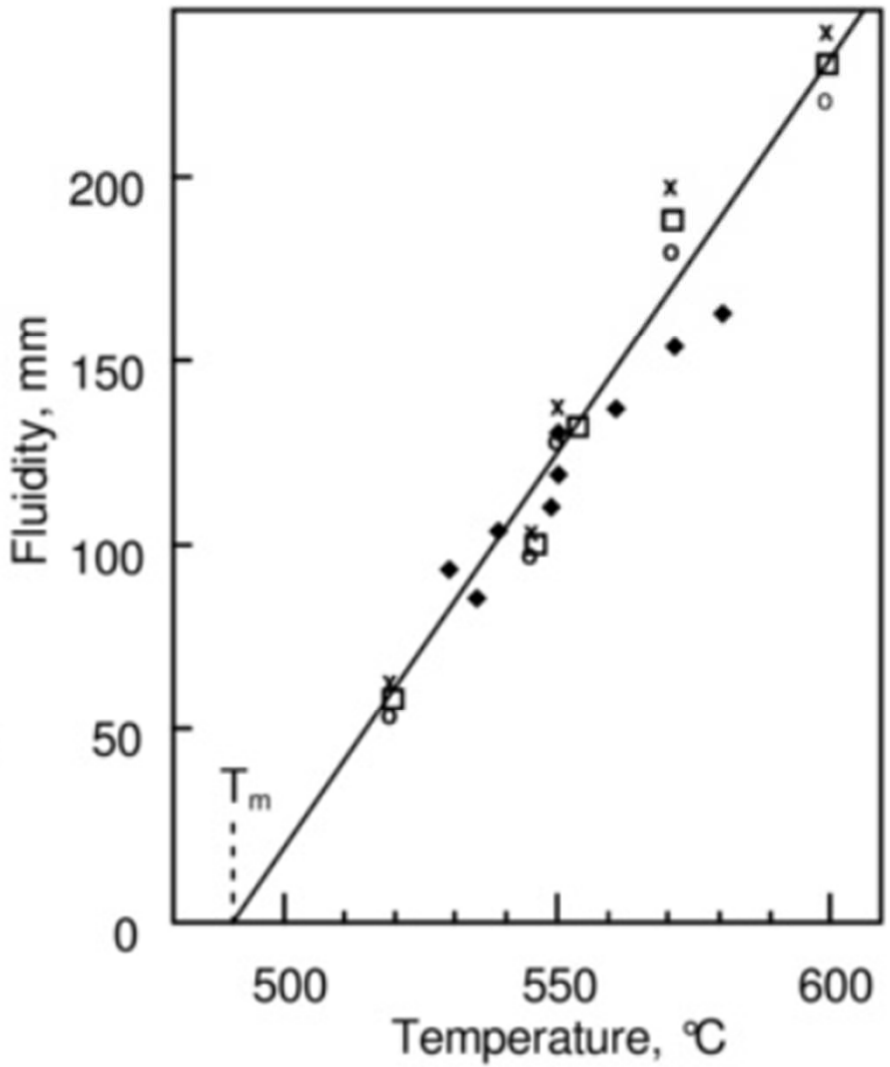

Continuous Fluidity

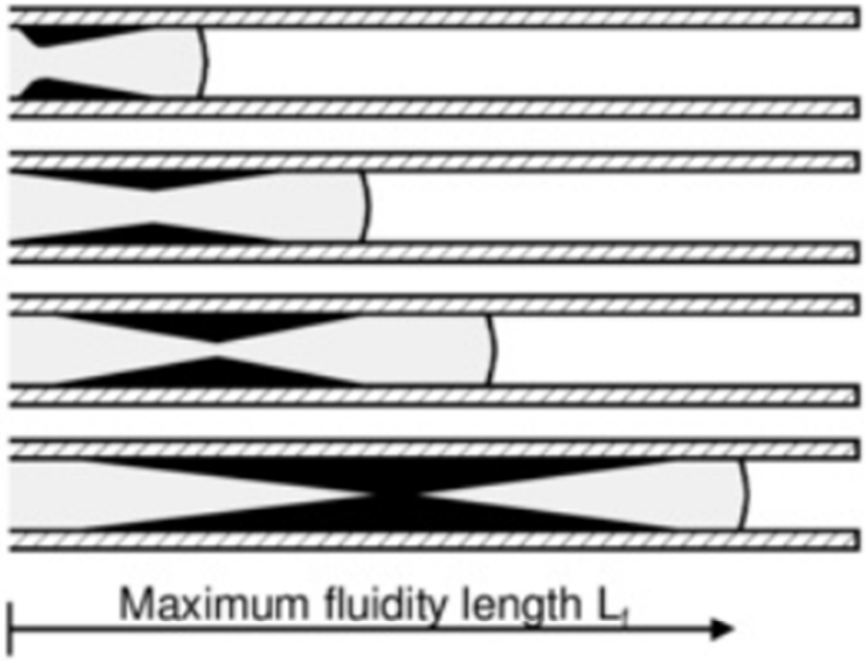

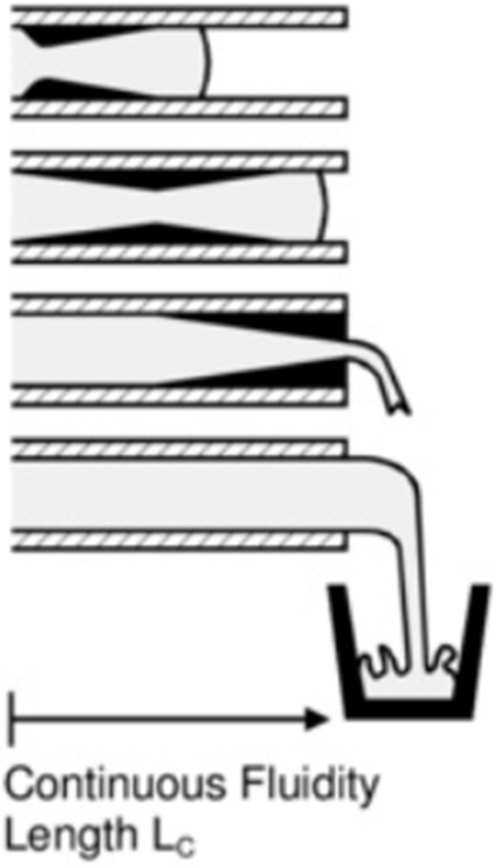

Regimes of continuous, partial and impossible flow

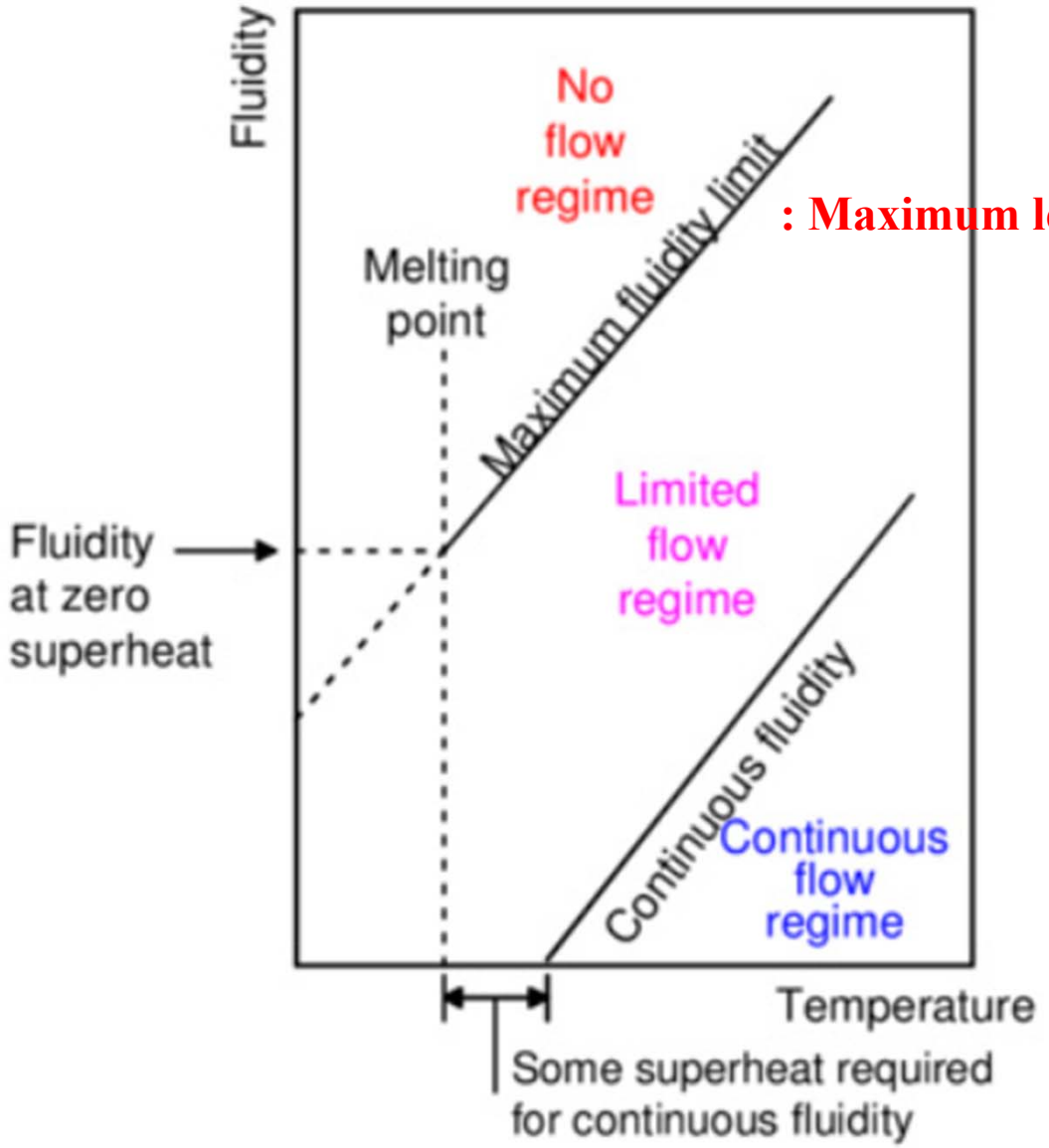

: Maximum length melt can reach

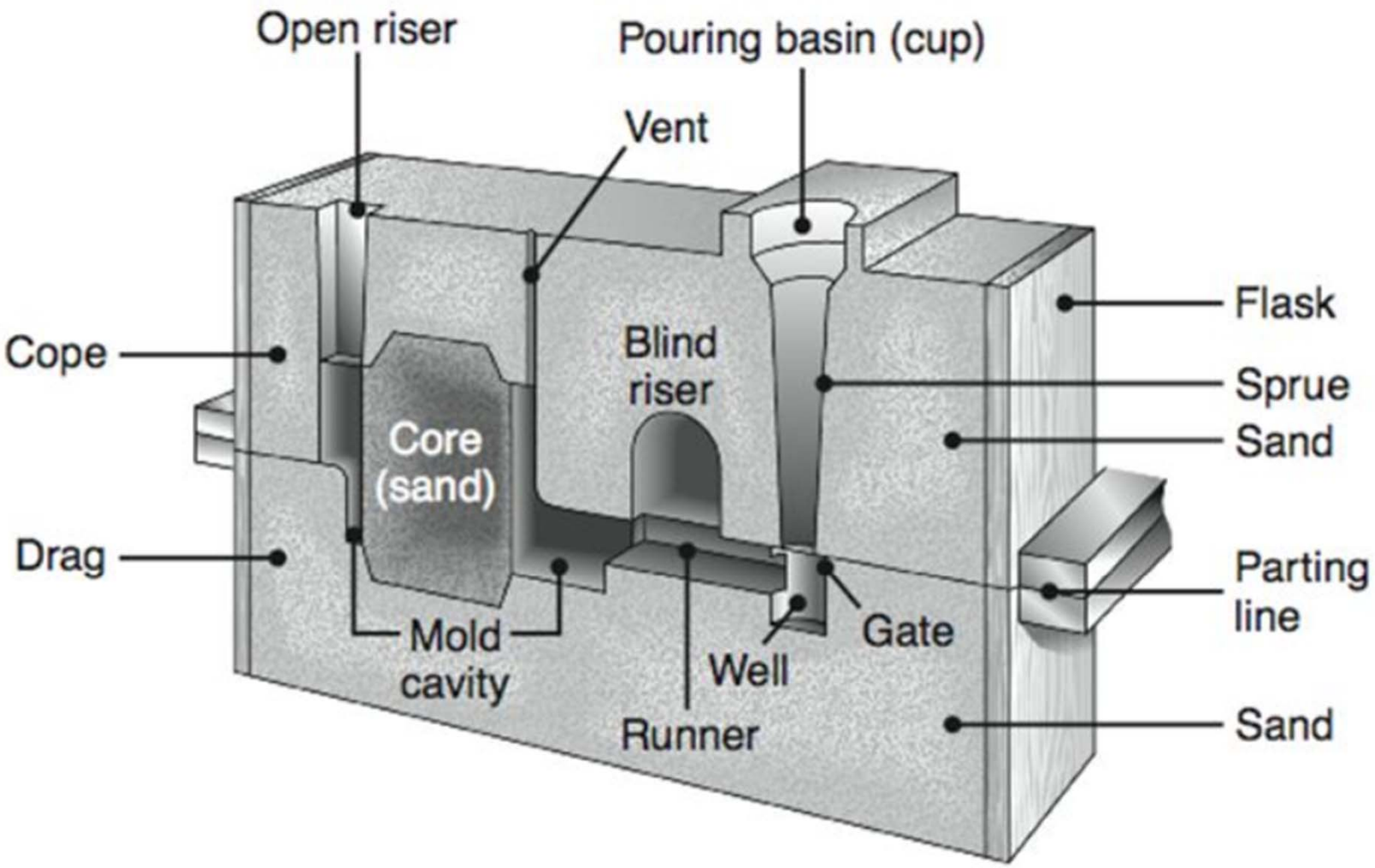

Fluid Flow : Molten metal → Pouring basin → Sprue → Runner → Cavity → Riser

Top versus Bottom Gating

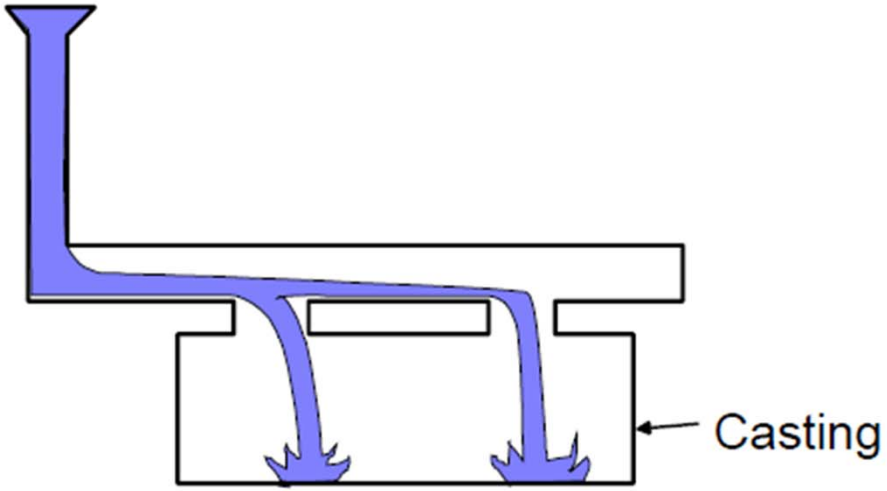

Top gating - causes turbulence

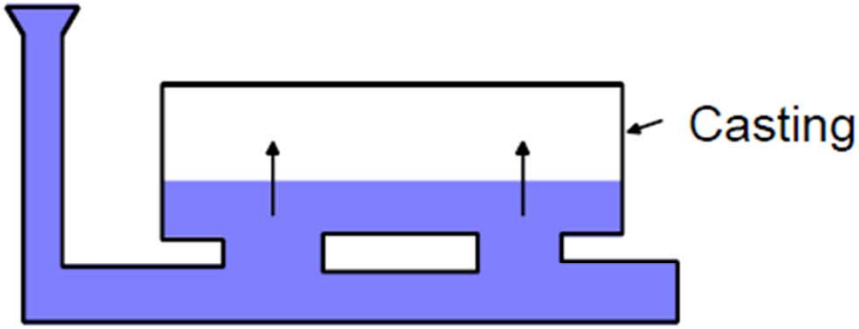

Bottom gating - prevents turbulence

Good Design 1: Pouring Basin

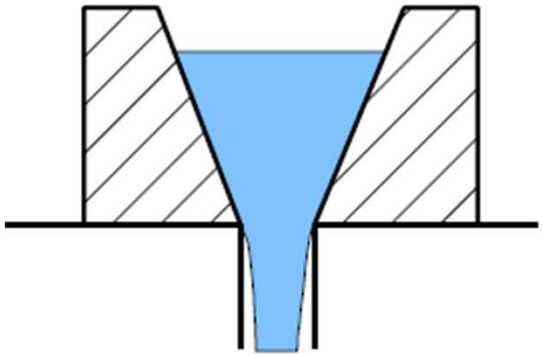

BAD
conical basin

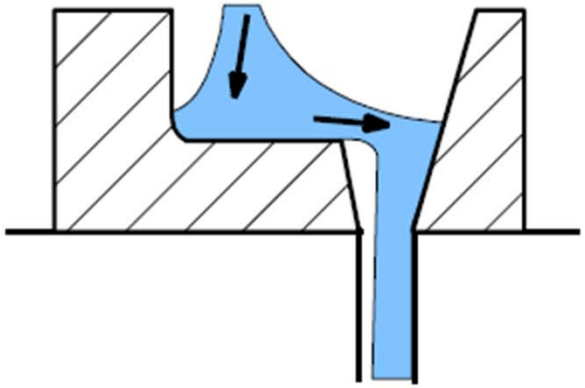

BETTER
offset basin

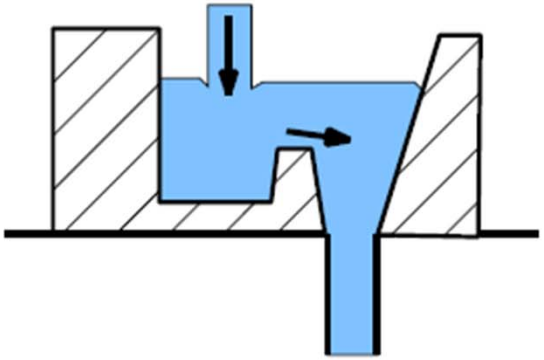

BEST
offset stepped basin

Good Design 2: Tapered Sprue

탕구

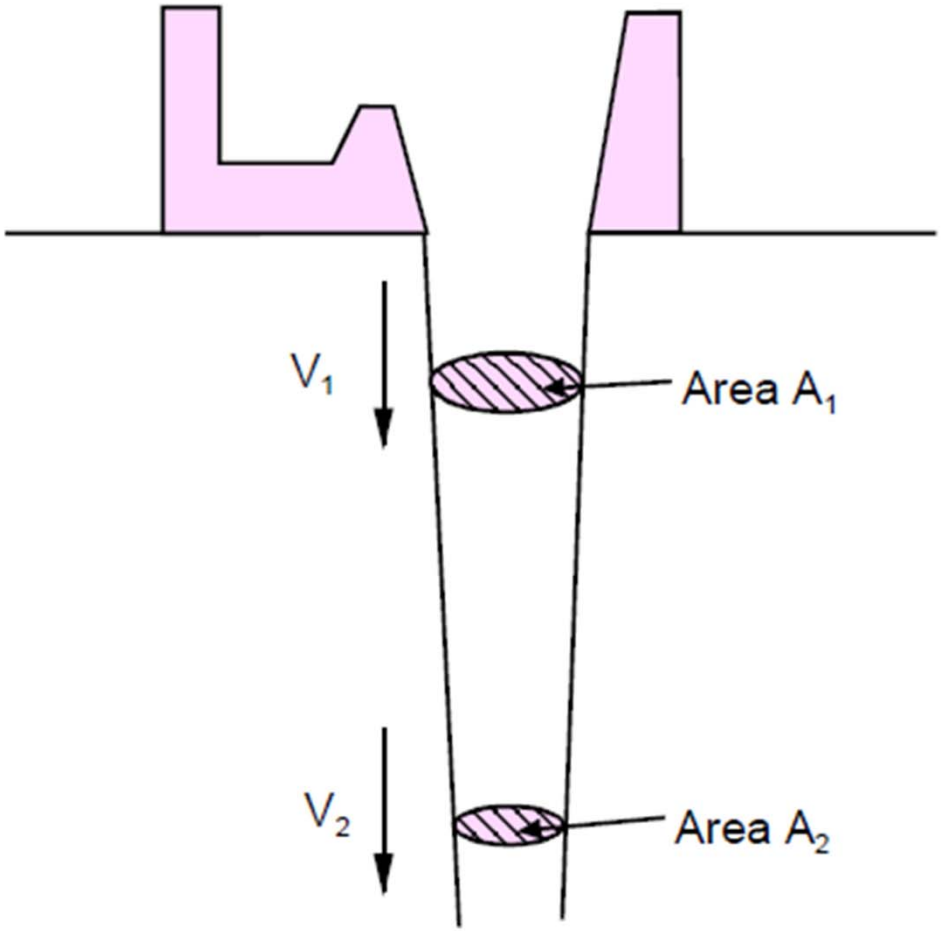

Metal accelerates from V_1 to V_2 due to gravity.

Sprue will remain full of metal if the sprue is tapered so that

$$A_1 \cdot V_1 = A_2 \cdot V_2$$

Good Design 3: Sprue Well

The sprue well helps to:
(i) Declarate metal
(ii) Stop first splash
(iii) Fill runner

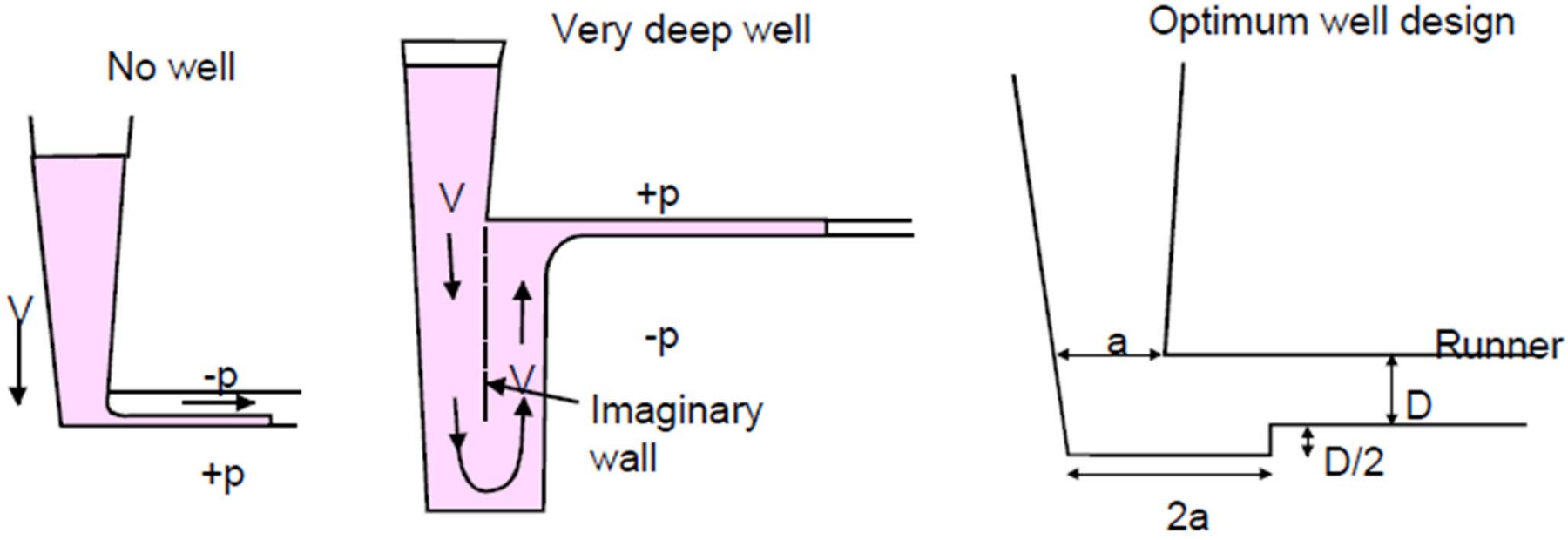

Good Design 4: Runner Bar and Gates

AIMS: (i) to distribute metal to lowest point(s) on a casting
(ii) to reduce metal velocity.

Casting with a single ingate

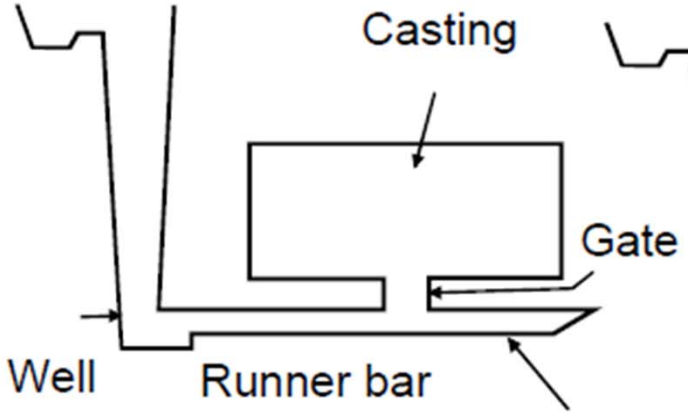

Uneven flow in multigated casting as a result of incorrect runner bar design

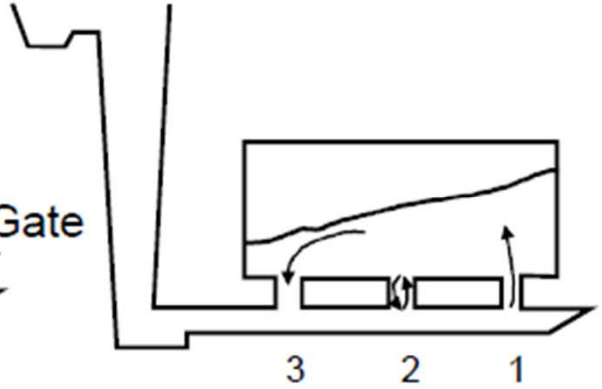

Uniform flow promoted by the use of stepped runner bar

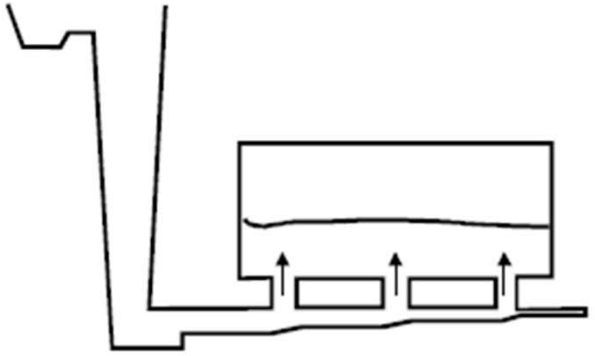

Alternative tapered runner bar

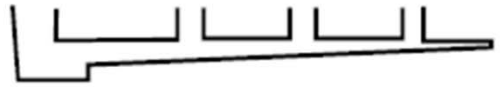

Good Design 4 (Continued): Runner Bar and Gates

Waterfall effects must be avoided so that:

(a) splashing is prevented
(b) the critical velocity is not exceeded
(b) the metal meniscus is never stationary